bioRxiv preprint doi: https://doi.org/10.1101/510768; this version posted May 29, 2019. The copyright holder for this preprint (which was not certified by peer review) is the author/funder. All rights reserved. No reuse allowed without permission.

Published online xx 2019 ***Synthetic Biology (Revision Invited)**, 2019, Vol. xx, No. xx* **1–65**

Optimization of the experimental parameters of the ligase cycling reaction

Niels Schlichting, Felix Reinhardt, Sven Jager, Michael Schmidt, Johannes Kabisch *

Department of Biology, TU Darmstadt, Schnittspahnstraße 12, DE-64287, Germany.

Received xx, 2019; Revised x, 2019; Accepted xx, 2019

ABSTRACT

The ligase cycling reaction (LCR) is a scarless and efficient method to assemble plasmids from fragments of DNA. This assembly method is based on the hybridization of DNA fragments with complementary oligonucleotides, so-called bridging oligos (BOs), and an experimental procedure of thermal denaturation, annealing and ligation. In this study, we explore the effect of molecular crosstalk of BOs and various experimental parameters on the LCR by utilizing a fluorescence-based screening system. The results indicate an impact of the melting temperatures of BOs on the overall success of the LCR assembly. Secondary structure inhibitors, such as DMSO and betaine, are shown to negatively impact the number of correctly assembled plasmids. Adjustments of the annealing, ligation and BO-melting temperature further improved the LCR. The optimized LCR was confirmed by validation experiments. Based on these findings, a step-by-step protocol is offered within this study to ensure a routine for high efficient LCR assemblies.

INTRODUCTION

One of the aims of synthetic biology is to specify, design, build and test genetic circuits, and this goal requires rapid prototyping approaches to facilitate assembly and testing of a wide variety of circuits. To this end, many assembly methods were used in the last decades to build DNA constructs, e.g., Gibson assembly (1), Golden Gate assembly (2, 3), circular polymerase extension cloning (CPEC, 4), biopart assembly standard for idempotent cloning (BASIC, 5) and yeast homologous recombination (YHR, 6). Some of these methods require specific modifications of the DNA parts such as overhangs or restriction sites, which hamper the reusability, while other methods leave scars. Additionally, DNA part standardization approaches, e. g. the BioBrick-system, result in sequence redundancies which have a negative impact on assembly efficiencies (7).

By contrast, the ligase cycling reaction (LCR) fulfills the prerequisites for automated assemblies and uses phosphorylated DNA parts (8, 9, 10, 11). The assembly order is determined by single-stranded oligonucleotides building a bridge (so-called bridging oligonucleotides, BOs) between adjacent parts. Bridging oligos are typically designed based on general rules provided by the literature (8, 9). One important parameter for the LCR-assembly is the melting temperature (T_m) of the BOs at around 70 °C for each half to facilitate optimal hybridization of template and oligonucleotide for given cycling parameters. Closely related is the free energy ΔG, which is assumed as the more important quantity for oligonucleotide-based biological experiments (12, 13). In the LCR, its impact is counteracted by using dimethyl sulfoxide (DMSO) and betaine to increase ΔG and thus to reduce secondary structures (8, 9). Nevertheless, the roles of ΔG-related crosstalk and the potential of ΔG-optimized BOs in the LCR have not been investigated so far.

The literature offers several tools regarding LCR optimization. Nowak et al. (14) provides a tool for the assembly of DNA that codes for a protein, where they return both the DNA fragments as well as the BOs to minimize unwanted effects. The tool considers codon mutations, as long as they encode the same amino acid, and is intended to be applied for LCR-based gene synthesis. Bode et al. (15) offers similar functionality. Another web-application includes the design of primers and performs T_m and ΔG cross-checks for the oligonucleotide sequences against themselves, their DNA probes and whole genomes (13) but is not applied for the LCR. Robinson et al. (16) use a BO-design-tool with an adjustable target melting temperature but without optimizing the crosstalk. An experimental perspective is given by de Kok et al. (8), where a design-of-experiment approach and multivariate data analysis were used to assess the impact of a wide range of parameters including the concentrations of the secondary structure inhibitors DMSO and betaine. The following study starts with these baseline-conditions. The LCR is investigated with the scope on the impact of the choice of BOs, their intramolecular and intermolecular crosstalk and the context of the experimental temperatures. For this, a toy-model plasmid and fluorescence-based readout is utilized (graphical abstract: Figure 1) to detect and validate the influence of all parameters and to generate new rules for an optimized LCR-assembly. Finally, the new LCR-conditions are used to assemble two additional plasmids to verify the findings.

*To whom correspondence should be addressed. Tel: +49 6151 1622044; Email: johannes@kabisch-lab.de

© 2019 The Author(s)

This is an Open Access article distributed under the terms of the Creative Commons Attribution Non-Commercial License (http://creativecommons.org/licenses/by-nc/2.0/uk/) which permits unrestricted non-commercial use, distribution, and reproduction in any medium, provided the original work is properly cited.

bioRxiv preprint doi: https://doi.org/10.1101/510768; this version posted May 29, 2019. The copyright holder for this preprint (which was not certified by peer review) is the author/funder. All rights reserved. No reuse allowed without permission.

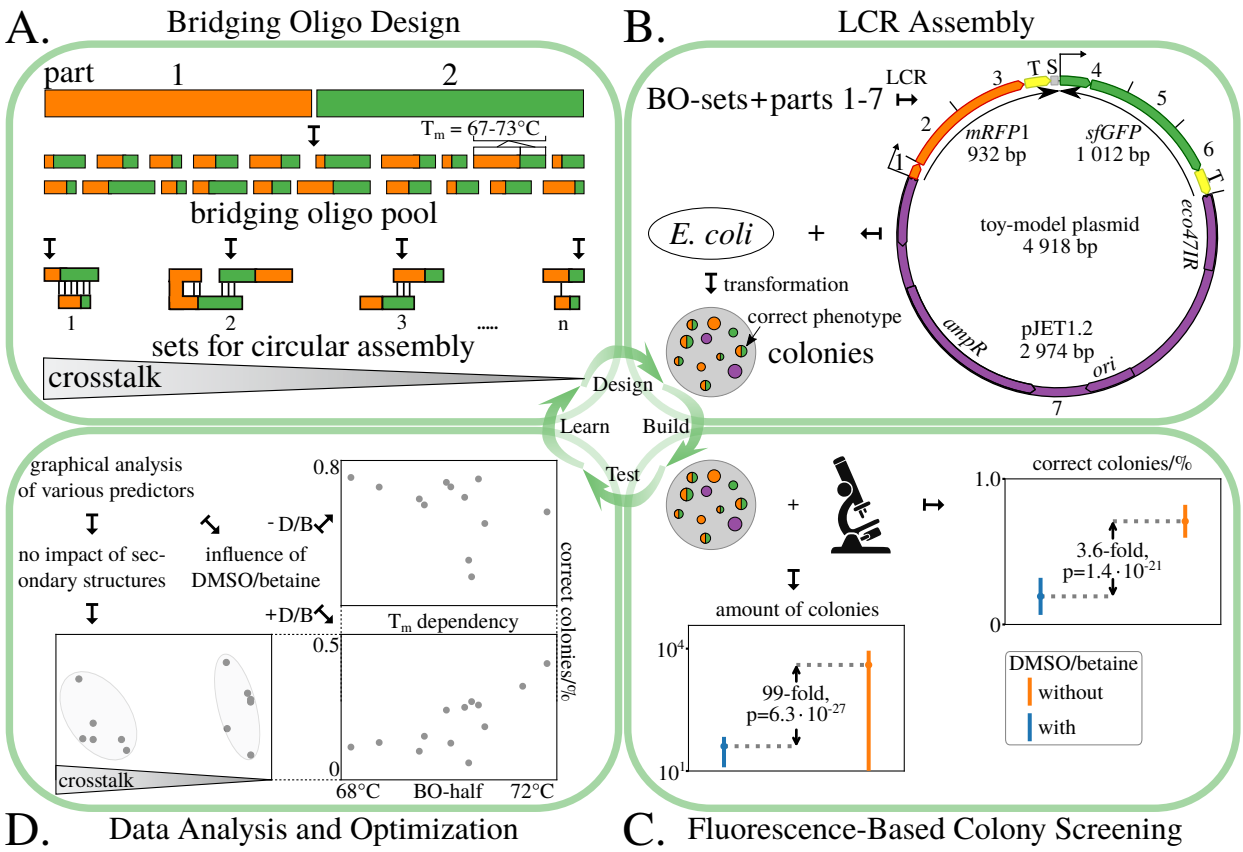

Figure 1. Workflow for the LCR optimization. **A**. Bridging oligo-sets (BO-sets) were designed using general design rules with the focus on ΔG-related BO-crosstalk while maintaining a T_m of $70 \pm 3\,^{\circ}\mathrm{C}$. **B**. In total, 25 sets were designed, including one manually designed set using the software `Primer3`, and utilized for the LCR-assembly of a toy-model plasmid. The plasmid consists of seven parts with lengths in the range of 79 bp to 2974 bp and a total length of 4918 bp. It contains two genes for fluorescent proteins, *mRFP1* and *sfGFP*, and a vector. Both fluorescent protein genes were split into three subparts (*mRFP1*: parts 1-3, *sfGFP*: parts 4-6). The same terminator *BBa_B0015* (T) was used twice to simulate sequence redundancies. A DNA-spacer S (37 bp) was added at the end of part 3 to avoid hybridization of the BO utilized for the ligation of parts 6 and 7. The sequences of all parts are shown in Table 1. **C**. The toy-model plasmid enables a fast and reliable fluorescence-based readout to observe the LCR efficiency and the total amount of colonies to investigate various LCR conditions. Based on this method, a significant negative impact by using the baseline LCR conditions ($8\,\%\mathrm{v/v}$ DMSO, $0.45\,\mathrm{M}$ betaine) was revealed for the seven-part toy-plasmid. The p-values were derived from a Kolmogorov-Smirnov test between the two sets of data shown in Supplementary Figures 4 and 5. **D**. With the focus on all BO-sets, no ΔG-related impact was detected in the baseline and DMSO/betaine-free LCR conditions. Further graphical analysis of the BO-sets revealed an association of the average BO-T_m, the efficiency and total amount of colonies. Finally, the optimizations were applied on another split of the toy-plasmid (three-part design: 1. *mRFP1*, 2. *sfGFP*, 3. vector) and two validation plasmids (Supplementary Figure 18 and 19). *ampR*: gene for ampicillin resistance, $\pm$*D/B*: with or without DMSO and betaine, *eco47IR*: gene for a restriction enzyme (reduction of religations of the vector), *mRFP1*: monomeric red fluorescent protein 1, *ori*: origin of replication, *sfGFP*: superfolder green fluorescent protein, T_m: melting temperature.

MATERIALS AND METHODS

Toy-model plasmid for the optimization experiments

All LCRs for the optimizations were performed with a toy-model plasmid made of seven fragments (Figure 1B), with a total length of 4918 bp. This plasmid consists of six inserts and the plasmid cloning vector CloneJet pJET1.2/blunt (2974 bp; Thermo Fisher Scientific, Massachusetts, USA). For the inserts, two genes of fluorescent proteins, *sfGFP*, *mRFP1*, were ordered at Addgene (www.addgene.org: pYTK001, pYTK090; 17) and split into three subparts each to increase size heterogeneity, so that the plasmid fragment length ranges from 79 bp to 2974 bp. Additionally, the same terminator *BBa_B0015* was used in both fluorescent protein genes to further increase assembly complexity. A spacer sequence "S" of 37 bp was added to prevent the ligation of part 3 with part 7 (Figure 1B). For all *in silico* cloning, the software `Geneious` was utilized (v. 11.0.5, http://www.geneious.com, 18). A GenBank-file of the toy-model plasmid is available in the supplement and at www.gitlab.com/kabischlab.de/lcr-publication-synthetic-biology.

Part amplification

Primers for the amplification (Eurofins Genomics, Ebersberg, Germany) were phosphorylated by the T4-polynucleotidekinase/-buffer (New England Biolabs, Ipswich, USA) prior to amplification *via* PCR (Q5® High-Fidelity Polymerase, New England Biolabs, Ipswich, USA). Forward and reverse primers were phosphorylated separately in 50 µL total volume with 4 µM primer, 4 mM ATP and 10 U of T4-PNK for 1 h at 37 °C and 20 min at 65 °C for the denaturation. The low primer concentration was chosen because it is beneficial for the enzymatic phosphorylation. The 79 bp promoter of *mRFP1* (part 1, Figure 1B) was ordered as forward and reverse strand (lyophilized, salt-free). Both strands were phosphorylated separately as described

bioRxiv preprint doi: https://doi.org/10.1101/510768; this version posted May 29, 2019. The copyright holder for this preprint (which was not certified by peer review) is the author/funder. All rights reserved. No reuse allowed without permission.

for the amplification primers, followed by an annealing procedure to obtain double-stranded DNA (3 min at 95 °C and 70 cycles of 20 s with an incremental decrease of 1 °C). The backbone-part pJET1.2/blunt was PCR-amplified using a template containing a lacZ coding sequence (pJET1.2/blunt-*lacZ*). Choosing primers which omit *lacZ* during PCR allows to screen for plasmid-carryover through blue-white screening. The *lacZ* does not exist in the final sequence of the toy-model plasmid. Afterwards, all PCR products were DpnI-digested (60 min at 37 °C; inactivation: 20 min at 80 °C), purified (column-based NEB Monarch® PCR & DNA Cleanup Kit; New England Biolabs, Ipswich, USA) and the DNA quantity/quality was measured by photometry (Spectrophotometer UV5Nano, Mettler Toledo, Columbus, USA). Afterwards, the phosphorylated primers and DNA parts were stored at −20 °C. The sequences of the amplification primers are shown in Supplementary Table 2. The sequences of the toy-model parts are shown in Supplementary Table 1.

Bridging oligo design

Bridging oligos were predicted according to the rules given in de Kok et al. (8): they were all orientated in forward direction and designed at specific concentrations of 10 mM Mg^{2+}, 50 mM Na^{+}, 3 nM plasmid parts, 30 nM BOs and 0 mM dNTPs. `Geneious` asks for a concentration of dNTPs but they are not utilized in the LCR. Though, the concentration has to be adjusted to 0 mM. All BOs were ordered lyophilized from Eurofins Genomics (Ebersberg, Germany) as salt-free custom DNA oligonucleotides. Quality was checked by Eurofins Genomics *via* matrix-assisted laser desorption ionization-time of flight (MALDI-TOF) or capillary electrophoresis (CE).

One BO-set was designed manually with the melting temperature tool of `Primer3` (19), which is distributed with the software suite `Geneious`. For the T_m calculation and salt correction, the nearest-neighbor algorithm and the corresponding salt correction by SantaLucia (20) were utilized to design a BO-set with melting temperatures of 70 °C for each half-BO. `Primer3` only accepts a single DNA concentration, despite the experiment using different concentrations of parts and BOs. As prompted by `Geneious`, only the BO concentration of 30 nM was inputted. This manual set is denoted by an "M".

To investigate the crosstalk of BOs, additional sets were designed by minimizing or maximizing ΔG-dependent crosstalk between oligonucleotides while maintaining a T_m between 67 °C and 73 °C. Crosstalk is based on secondary structure and among others defined as the sum of all minimum free energies (MFEs) when cofolding each oligonucleotide of a BO-set with each oligonucleotide in that set and with itself. As a reference temperature for the crosstalk calculations, the annealing temperature of the multi-step LCR protocol was used (55 °C, 8). As with the manual set, the SantaLucia parameters were utilized for the T_m calculations. Additionally, the DNA part concentration was adjusted to 3 nM to match the experiment. The impact of DMSO and betaine were not considered for the calculations of the MFEs. Sets with minimized crosstalk are denoted by "L" for low crosstalk and sets with maximized crosstalk by a "H" for high crosstalk. All BO-sets, sequences and melting temperatures are provided in Supplementary Table 3 and are available at www.gitlab.com/kabischlab.de/lcr-publication-synthetic-biology. Further details on the BO design are given in the supplement (21, 22, 23, 24, 25, 26, 27).

Ligase cycling reaction

For the assembly, the purified PCR products were mixed with supplements with the following concentrations: 1×-Ampligase® ligase buffer, 0.5 mM NAD^{+}, 3 nM of toy-plasmid parts 1-6, 0.45 M betaine and 8 %v/v DMSO. In contrast to de Kok et al. (8), the concentration of the vector pJET1.2/blunt (part 7) was reduced to 0.3 nM to achieve fewer religations of the vector. Positive effects of increasing the molar insert-to-vector ratio were already described for other cloning methods (28, 29) and were confirmed in preliminary LCRs (data not shown). LCRs using these experimental concentrations, i.e. the manually designed BOs and the cycling conditions described in the next paragraph, are referred to as baseline-conditions. A 10×-Ampligase® reaction buffer was self-made with the concentrations described by the manufacturer of the Ampligase® (Lucigen, Wisconsin, USA). NAD^{+} was supplied separately by using a self-prepared 10 mM stock solution. Bridging oligo sets were premixed in nuclease-free water with 1.5 µM of each BO, heated up for 10 min at 70 °C and cooled down on ice before adding them to the split master-mixes. Subsequently 7.5 U of Ampligase® (Lucigen, Wisconsin, USA) was added. After mixing by inverting and centrifugation, each LCR was split typically in three ($n=3$) reactions with a cycling-volume of 3 µL. LCR-quintuplets ($n=5$) were used to investigate the impacts of crosstalk and utilizing or omitting DMSO/betaine, which are presented in Figure 2, 5 and 12. After the cycling, all LCRs were cooled down on ice to recondense evaporated liquid in the PCR-tubes, and centrifuged.

For the cycling, a DNA Engine Tetrad®2 thermal cycler, 96-well Alpha™ Unit cycling block and low-profile PCR stripes (Bio-Rad Laboratories GmbH, Muenchen, Germany) were utilized. The speed of ramping used for all LCRs was 3 °C s^{-1}. The cycling was initiated by a denaturation step at 94 °C for 2 min, followed by 25 cycles at 94 °C for 10 s, 55 °C for 30 s and 66 °C for 1 min. In contrast to the published protocols (8, 9), 25 cycles instead of 50 cycles were used due to the low total LCR volume of 3 µL. Afterwards, either 30 µL electro-competent or chemically-competent NEB® 10-β *E. coli* cells (New England Biolabs, Ipswich, USA) were transformed as described in the following paragraph.

Electroporations were performed serially for each single LCR. For this, each LCR condition was transformed in a non-batch-wise manner to reduce workflow-derived influences, so that, e.g., each condition was transformed once before proceeding with the second replicates. 1. cells were mixed from a master-aliquot for each experiment with one LCR-replicate of one LCR condition, 2. suspension was transferred to a cuvette, 3. an electric pulse was applied (2.5 kV), 4. 450 µL SOC-medium were added, 5. the cell-suspension was transferred to a tube, 6. the tube was put for 1 h in a thermal cycler for recovery and 7. finally the suspension was plated on agar plates. After the recovery, an appropriate volume of the transformation mix was plated on Lysogeny Broth (Miller) plates containing 1 %m/v agar and 100 µg mL^{-1} ampicillin to

bioRxiv preprint doi: https://doi.org/10.1101/510768; this version posted May 29, 2019. The copyright holder for this preprint (which was not certified by peer review) is the author/funder. All rights reserved. No reuse allowed without permission.

get a total amount in the range of 10-200 CFUs per plate. The plates were grown for 15 h at 37 °C.

For chemical transformations, the experiments were performed in a parallel manner: 1. cells were mixed from a master-aliquot for each experiment with all replicates of all LCRs in a 96-well PCR-plate using a multi-channel pipette, 2. the suspensions were incubated on ice for 30 min, 3. the heat-shock of 30 sec was applied in a PCR-cycler by using 96-well PCR-plates, 4. the suspensions were placed on ice for 10 min, 5. 170 µL SOC-medium were added to all LCR-cell-mixes followed by recovery of 1 h and plating as described for the electroporations.

Colony screening and plasmid sequencing

By transforming the LCRs into *E. coli*, the toy-model plasmid enables a fluorescence-based discrimination of correct (red and green-fluorescent CFUs) and misligated plasmids (red or green or non-fluorescent CFUs). To investigate the LCR assembly, the efficiencies of all LCRs were determined by observing the phenotype of ampicillin-resistant CFUs *via* fluorescence microscopy (microscope: Axio Vert.A1, Carl Zeiss Microscopy GmbH, Jena, Germany, 50×-magnification; LEDs for sfGFP/mRFP1: 470/540−580 nm). To calculate the LCR efficiency, the phenotypes of all CFUs per LCR were screened. For plates with more than 100 CFUs, 100 colonies were screened randomly by first picking the spot of interest macroscopically followed by the observation with the microscope. The efficiency was obtained by dividing the number of correct CFUs by the total number of microscopically observed CFUs. The phenotypes of the CFUs were determined by visual observation only. An example image of all phenotypes is shown in 3.

The amount of CFUs per 3 µL was obtained from the total CFUs per plate and the used plating volume and dilution.

To validate this fluorescence-based system, plasmids from 120 CFUs with different phenotypes were isolated with the Monarch® Plasmid Miniprep Kit (New England Biolabs, Ipswich, USA) and analyzed *via* Sanger-sequencing (Eurofins Genomics, Ebersberg, Germany) to correlate them with the genotypes.

Graphical analysis

Unless specified otherwise, T_m calculations in the following sections were performed with the thermodynamic parameters and salt correction by SantaLucia (20) and the divalent salt conversion by von Ahsen et al. (30). The shown T_ms are of half-BOs. Each half-BO is complementary to the DNA part that it is designed to attach to. A BO is the direct concatenation of two half-BOs. Dangling ends and coaxial stacking were not included in the calculation. Error bars are the standard deviation with Bessel's correction. The average T_m of a BO-set is obtained from all half-BOs of the set.

Validation experiments

For the validation experiments two additional plasmids-constructs were split in three and seven parts (Supplementary Figures 18 and 19) and were assembled using the baseline and two optimized conditions (Table 1) derived by the results of the toy-model plasmid. Both plasmids and splits are similar in size range in comparison to the toy-model plasmid with *sfGFP* and *mRFP1*. GenBank-files of the validation plasmids are available in the supplement and at www.gitlab.com/kabischlab.de/lcr-publication-synthetic-biology. In the validation plasmids the *lacZ* and two or one antibiotic resistance genes were split into subparts (Supplementary Figures 18 and 19). This enables a blue-white screening of correct assembled plasmids (blue colonies) and misassembled ones (white) by plating them on agar with the antibiotics and X-Gal/IPTG. For both plasmids, 3 µL per LCR were transformed in 30 µL NEB® 10-β *E. coli* cells.

For the validation plasmid 1, the transformed cells was transferred to LB agar plates with 100 µg mL^{-1} spectinomycin after one hour of recovery followed by an overnight incubation for 16 h at 37 °C. 40 CFUs were transferred to agar plates containing spectinomycin, 50 µg mL^{-1} kanamycin, 40 µg mL^{-1} X-Gal and 200 nM IPTG by using sterile tooth picks to identify colonies with correct assembled and misassembled plasmids. After 16 h, all transferred colonies were checked for a blue/white phenotype and empty spots were regarded as kanamycin sensitive. Blue colonies represented correct assembled plasmids. White colonies and empty spots were treated as misassembled plasmids. To calculate the efficiency for each LCR the amount of blue colonies was divided by the amount of transferred CFUs. Ten plasmids of blue, spectinomycin and kanamycin resistant colonies were sequenced *via* Sanger sequencing. Further, four plasmids of white, spectinomycin and kanamycin resistant colonies were analyzed.

For the validation plasmid 2, the transformed cells were transferred to LB agar plates containing 100 µg mL^{-1} spectinomycin, 40 µg mL^{-1} X-Gal and 200 nM IPTG. After the incubation of 16 h at 37 °C, all colonies per plate were checked for a blue/white phenotype. For the calculation of each LCR efficiency, the amount of blue colonies were divided by the sum of blue and white colonies. As described for the validation plasmid 1, Sanger sequencing of plasmids from ten colonies with the correct phenotype "blue" and plasmids from four colonies with the wrong phenotype "white" was used to validate the results.

RESULTS AND DISCUSSION

Toy-Model plasmid offers robust system to investigate LCR assemblies

To simulate a challenging SynBio-construct for the investigations of the LCR, a toy-model plasmid was designed (Figure 1B). This plasmid consists of seven parts of varying size (79 bp to 2974 bp) and the same BioBrick terminator sequence *BBa_B0015* in both fluorescent protein genes. To investigate the LCR different bridging oligo sets, experimental parameters, a toy-model plasmid and fluorescence-based analysis were used. For the analysis and optimization, ∼100 CFUs/LCR (if available) were screened *via* visual observation by using fluorescence microscopy to calculate the efficiency of each assembly reaction. The four observable phenotypes "non-fluorescent", "green fluorescent", "red fluorescent" and "green + red fluorescent" are demonstrated in Supplementary Figure 3. The amount of CFUs per 3 µL LCR was determined by macroscopic

bioRxiv preprint doi: https://doi.org/10.1101/510768; this version posted May 29, 2019. The copyright holder for this preprint (which was not certified by peer review) is the author/funder. All rights reserved. No reuse allowed without permission.

counting of all colonies per agar plate and extrapolation by using the dilution-factor. In total, 61 different experimental conditions were tested and more than 15000 colonies were screened by fluorescence-microscopy to obtain the assembly efficiencies. In contrast to the vector concentration of 3 nM in the literature (8, 9), the concentration was decreased to 0.3 nM to counteract religations.

No fluorescent CFUs were obtained in the control reactions without the ligase (Supplementary Figure 5). Additionally, blue-white screening of about 1000 non-fluorescent CFUs revealed no carry-over of the template used for the amplification of the vector pJET1.2/blunt. A carry-over of the templates pYTK001 or pYTK090 used for the amplification of *sfGFP* and *mRFP1* was not possible due to a change of the antibiotic resistance marker gene.

To validate the fluorescence-based readout, the observed phenotypes of 120 CFUs with different phenotypes were correlated with the corresponding plasmids *via* Sanger sequencing. The analyzed plasmids from 60 CFUs with a bicolored fluorescence (red and green) contained all seven DNA parts in the correct order/orientation when compared with the *in silico* sequence of the toy-plasmid. Sequencing results of 60 plasmids with a different phenotype (20 plasmids from only green fluorescent CFUs, 20 plasmids from only red fluorescent CFUs and 20 plasmids from non-fluorescent CFUs) indicated that they lacked at least one *sfGFP*-subpart or *mRFP1*-subpart (still red or green) or were religated vector (no fluorescence). The latter phenotype was also observed for plasmids with missing subparts of both fluorescent protein genes in preliminary experiments. Point-mutations in the LCR products were regarded as errors introduced by amplification primers, PCRs or *E. coli* and were not treated as LCR-misassemblies since they occurred outside of the ligation areas.

In our experiments, the misassembled plasmids from green fluorescent colonies lacked at least one subpart of the *mRFP1*. Interestingly, about 10 bp to 100 bp of both ends of the missing subparts were still existent. For the 20 analyzed CFUs with only the red fluorescent phenotype, the plasmids lacked the spacer sequence at the 3'-end of the *mRFP1* and the entire *sfGFP*. This suggests that *E. coli* can recognize the 129 bp *BBa_B0015* terminator that is used for both *sfGFP* and *mRFP1* and delete it by *recA*-independent recombination (31, 32). Thus repetitive sequences in the LCR assembly cause misassemblies. Related to this, the BO that spans parts 6 and 7 can partly hybridize with the terminator in part 3 and may negatively influence the ligation. This suggests that duplicates at the end of DNA parts negatively influence LCR efficiency.

Another issue is related to the heterogeneous LCR-mixture, which contains the desired DNA fragments, debris of these fragments from PCRs, amplification primers and PCR templates (even if they are digested and purified). *E. coli* may circularize any linear DNA in the mixture. The subsequent transformation of *E. coli* enables a ring closure by endogenous mechanisms and the growth of CFUs containing the religated vector or plasmids with missing parts. This was observed in the control reaction without ligase in Supplementary Figure 5. Thus the carry-over of DNA in combination with the ability of *E. coli* to ligate linear DNA contributes both to the amount of misassembled plasmids and correct plasmids.

In summary, the fluorescence-based screening of colonies employed here is a valid and fast (manually: $\sim 500\,\mathrm{CFUs\,h^{-1}}$) method to determine the assembly efficiencies and to investigate the influence of changing parameters in the LCR. A correlation of the phenotype and genotype is a useful tool without the need for next generation sequencing and offers an objective true-false readout by microscopy (as utilized for these studies) or photometric analysis of images (using e.g. `OpenCFU`, 33; `CellProfiler`, 34).

Influence of DMSO, betaine and the T_m of bridging oligos on LCR assemblies

Thirteen different BO-sets, with sequences given in Supplementary Table 4, were used to assemble the toy-model plasmid made of seven fragments. Two separate experiments were performed with different conditions. The baseline LCR used 8 %v/v DMSO and 0.45 M betaine, whereas the crosstalk-increased LCR did not use any DMSO or betaine (Figure 2).

On average, the LCRs with both detergents revealed 3.6× lower efficiencies and 99× fewer total CFUs per 3 µL in comparison to assemblies without DMSO and betaine ($p < 0.001$, Figure 1C; raw data in Supplementary Figure 4). Further confirmation of these results can be seen in Supplementary Figures 12 and 14 in more consistent experiments using the same batches of DNA parts and competent cells. Graphical analysis of various predictors revealed no ΔG-related effects for assembling the toy-plasmid for both experimental setups (Figure 2, Supplementary Figure 6A+B; more predictors in Supplementary Figures 7, 8, 9 and 10). Guanine or cytosine at the 3'-end of BOs were not found to affect the LCR. Notably, the conditions without DMSO and betaine resulted in less red fluorescent phenotypes for all utilized bridging oligo sets (Supplementary Figure 4). Apparently, this phenotype is mainly related to *recA*-independent deletion by *E. coli*. Probably, the omission of both detergents is beneficial for assemblies with repetitive sequences.

For LCRs with DMSO and betaine, BO-related differences were detected, e.g., the LCR using BO-set L1 was less efficient than using H1 (Supplementary Figure 5A). Further analysis of the used BO-sets revealed an impact of the melting temperature despite the T_ms of all sets being similar ranging from 68 °C to 72 °C (Supplementary Figure 6C). The set with a BO-T_m of 68 °C had an efficiency of 10% whereas the set with a BO-T_m of 72 °C showed an efficiency of 50%. This suggests that a melting temperature higher than 72 °C may result in even better assemblies for LCRs with DMSO and betaine. This is confirmed by recalculating the melting temperatures of the set of sequences designed to have a T_m of 70 °C by de Kok et al. (8), who used the SantaLucia parameters with the salt correction by Owczarzy et al. (35). We have found the average T_m of these half-BOs to be 72.2 °C when calculated using these parameters. When using the SantaLucia parameters and SantaLucia salt correction as has been done so far in this study, the T_m is found at 74.8 °C. The impact of different salt corrections is illustrated in Supplementary Figure 11. Overall, for LCRs with 8 %v/v DMSO and 0.45 M betaine, a BO target temperature above 70 °C was found to be beneficial.

bioRxiv preprint doi: https://doi.org/10.1101/510768; this version posted May 29, 2019. The copyright holder for this preprint (which was not certified by peer review) is the author/funder. All rights reserved. No reuse allowed without permission.

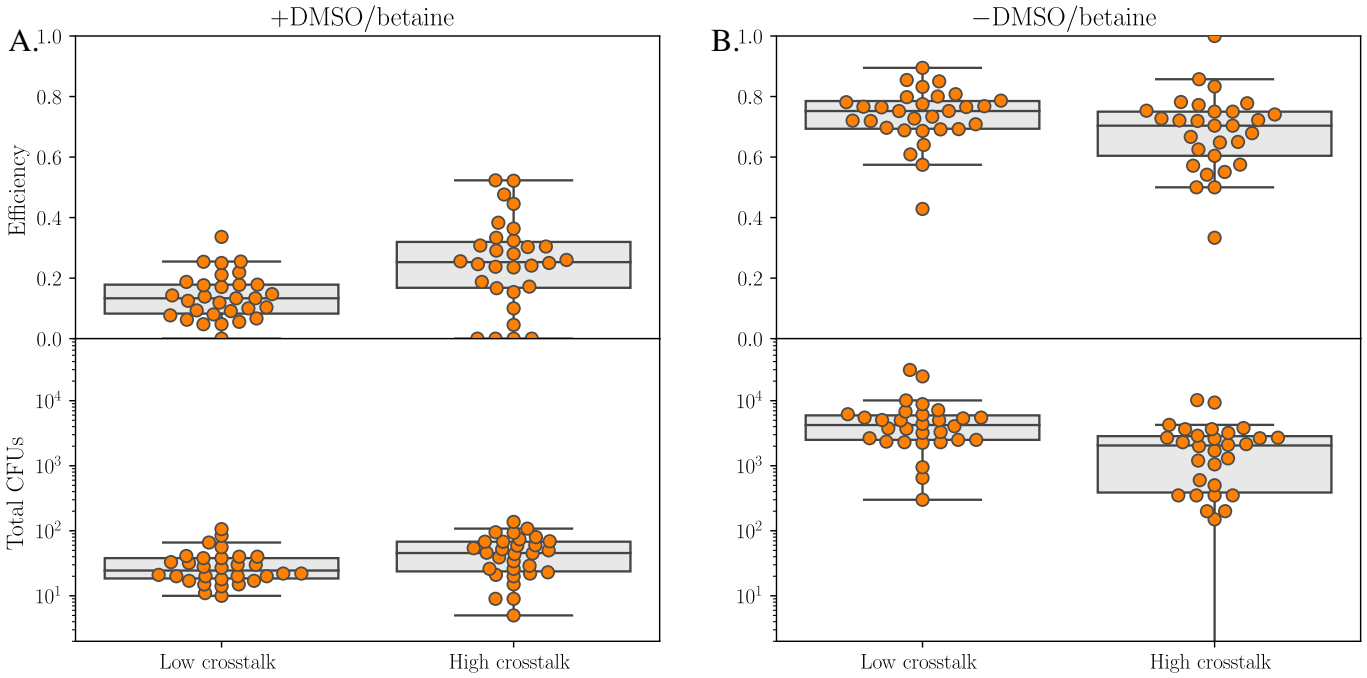

Figure 2. Overview of the seven-part LCR of the toy-model plasmid by utilizing six bridging oligo-sets (BO-sets) with low crosstalk and six BO-sets with high crosstalk. Each BO-set was used five times to assemble the toy-model plasmid (Figure 1B) by using the baseline-conditions with 8 %v/v DMSO/0.45 M betaine and without both detergents. For all LCRs, 3 µL were transformed by electroporation in 30 µL NEB® 10-β *E. coli* cells. For more detailed results of each BO-set refer to Supplementary Figures 4 and 5. **A.** The baseline-conditions with DMSO and betaine resulted in low efficiencies and low amounts of colonies. No correlation between crosstalk and BO performance was found. **B.** LCRs without DMSO and betaine resulted in more colonies and higher efficiencies in comparison to the baseline-conditions. The sequences of all BO-sets are shown in Supplementary Table 3. BO: bridging oligo, CFU: colony forming unit, DMSO: dimethyl sulfoxide.

Investigation of the `Primer3` source code used for the design of the manual BO-set and comparison with SantaLucia (20) revealed that the code expects both concentrations to be identical and to sum up to the input amount. Thus the prompted BO concentration of 30 nM corresponds to part and BO concentrations of 15 nM. Due to this, the manual BO-set had an average T_m of 71.5 °C (Supplementary Figure 6) when evaluated in full accordance with the SantaLucia formula instead of the targeted 70 °C.

An alternative approach to obtain higher assembly efficiencies without rising costs due to synthesizing longer oligonucleotides is to omit DMSO and betaine. This omission also aids automated liquid handling approaches because both detergents have unfavorable properties like extreme viscosities, hygroscopic characteristics and acting as surfactants. These new experimental conditions greatly improved both the efficiency and total number of CFUs (Supplementary Figure 5). Consistent with the results of the LCRs with DMSO/betaine, the melting temperature is the most influencing parameter. As a result of the omission of DMSO and betaine, BO-sets with lower T_ms became favorable, yielding the greatest total amount of colonies at high efficiency (Supplementary Figure 6D). This behavior is also observed by comparing the total CFUs derived by utilizing the BO-sets L2, H1 and the manual one (Supplementary Figure 12). Similar to this seven-part toy-plasmid, another LCR-design with a T_m-independent BO-design (20 bp for each BO-half) was published by Roth et al. (10) where six parts in a range of 79 bp to 2061 bp were assembled with high efficiencies. The *Taq*-ligase and a two-step LCR-protocol with annealing and ligation at the same temperature of 60 °C were utilized. This supports our findings that the omission of DMSO and betaine and to increase the annealing temperature can be helpful for ligation-based DNA assemblies.

An explanation for low efficiencies in the baseline LCR is related to the large difference between the annealing temperature of 55 °C and ligation temperature of 66 °C in combination with the utilization of DMSO and betaine. Both detergents reduce the energies required for strand separations (36, 37). Together with the experimental temperatures, this may result in an extensive reduction of template for the ligase by separating already hybridized BO/probe double strands. Bridging oligo-sets with lower T_ms are theoretically more affected than sets with higher melting temperatures and should benefit from decreasing the temperature interval. Related to this, a reduction of the ligation temperature is expected to be advantageous. This was validated by using three BO-sets with different melting temperatures (Supplementary Figure 13) despite the ligation temperature of 60 °C being lower than the optimum temperature of the ligase (according to the manufacturer: 70 °C). Increasing the annealing temperature, which would also decrease the interval, was assumed to be disadvantageous due to accelerated BO/template-separation and was not investigated.

Several mechanisms are suspected to cause the total CFU decrease in LCRs with DMSO/betaine. First, lower LCR efficiencies result in fewer fully assembled

bioRxiv preprint doi: https://doi.org/10.1101/510768; this version posted May 29, 2019. The copyright holder for this preprint (which was not certified by peer review) is the author/funder. All rights reserved. No reuse allowed without permission.

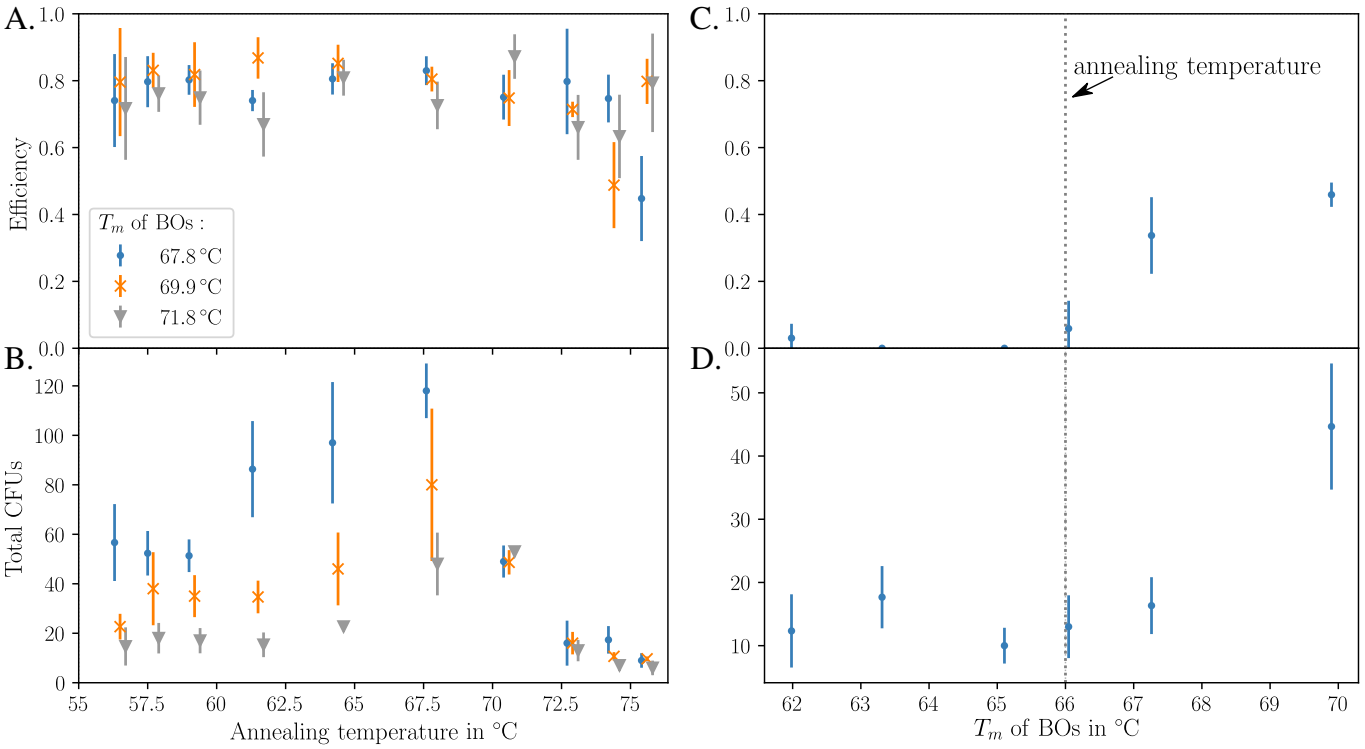

Figure 3. Adjustment of the annealing temperature and melting temperature of bridging oligo halves of DMSO/betaine-free LCR. The LCRs were performed as triplicates using the same DNA parts and chemically competent cells. The standard deviation for each LCR is indicated by error bars. **A.** For a better visibility the bars of the results were shifted with an offset of the annealing temperatures shown on the x-axis. Optimization of the annealing temperature of the seven-part plasmid *via* gradient-LCR. The temperature range for the annealing was 56.5 °C to 75.6 °C. Three BO-sets with different melting temperatures were used (67.8 °C, 69.9 °C and 71.8 °C). For the three BO-sets the LCR-efficiency was at a similar level. It started decreasing at an annealing temperature of more than 70.6 °C. **B.** As already observed, the total amount of colonies increased with a lower BO-T_m. Overall, the LCRs using these BO-sets resulted in a maximum of colonies in a range of ∼66-71 °C with 2× more colonies (also shown in Supplementary Figure 15). The BO-set sequences of the three sets are shown in Supplementary Table 4. **C+D.** Based on the optimization shown in A+B, the annealing temperature of 66 °C was used to investigate the influence of BO-halves with lower T_ms of 62.0 °C to 67.3 °C. As a reference, the BO-set "71.8 °C" from A+B was used. Further decrease of the BO-T_m did not improve the LCR at the optimized annealing temperature of 66 °C. In comparison to A+D, the LCR with the BO-set "69.9 °C" was less efficient due to loss of function by additional repeated freeze-thaw cycles of the DNA parts and BOs. The sequences of the BO-sets "62.0 °C" to "67.3 °C" are shown in Supplementary Table 5. BO: bridging oligo, CFU: colony forming unit, DMSO: dimethyl sulfoxide, T_m: melting temperature of a BO-half.

plasmids and fewer colonies. The effects of DMSO and betaine were also investigated separately to prove these results (Supplementary Figure 14). Second, DMSO/betaine negatively influence the electroporation process. This can also be seen in Supplementary Figure 14, where an LCR without DMSO/betaine was mixed with both detergents before the electroporation and 3-4× fewer CFUs were obtained in comparison to DMSO/betaine-free controls. In contrast to the literature (8, 9), a lower volume-ratio of LCR and cells was used for the transformations (1:10; 2× higher concentration of DMSO/betaine). These conditions are not toxic for the *E. coli* strain NEB® 10-β because chemical transformations of the same strain with the plasmid pUC19 revealed no negative effects of utilizing a combination of DMSO and betaine (Supplementary Figure 17). A negative impact of DMSO and a positive impact of betaine was observed. A strain-dependent influence of DMSO in chemical transformations was described in (38) and such an influence is also plausible for betaine and a combination of both reagents. To counteract the CFU-reducing effects of detergents, a 30 min dialysis using *aq. dest.* and a nitrocellulose-membrane after the LCR was found to increase the amount of colonies (data not shown).

The omission of DMSO/betaine was beneficial for the assembly of the seven-part split of the toy-model plasmid. To investigate optimal experimental temperatures for the new conditions without DMSO and betaine, the interaction of the annealing, ligation and BO-melting temperatures need to be considered.

Increased annealing temperature is beneficial for LCRs without DMSO and betaine

To optimize the LCR without DMSO/betaine, several experiments were performed. Supplementary Figure 6D shows that the BO-sets with low T_ms yield the most correct CFUs, which suggests that the BOs may bind too strongly to unwanted sites and be unavailable for ligation. To counteract this, the optimal annealing temperature was determined by performing a gradient-LCR, i.e. LCRs at different cycling conditions. For this, three new BO-sets were composed from the existing pool of BOs used in LCRs shown in Supplementary Figure 5 to obtain sets with average melting temperatures of 67.8 °C, 69.9 °C and 71.8 °C

bioRxiv preprint doi: https://doi.org/10.1101/510768; this version posted May 29, 2019. The copyright holder for this preprint (which was not certified by peer review) is the author/funder. All rights reserved. No reuse allowed without permission.

(sequences in Supplementary Table 4). In an annealing temperature range of 56.5 °C to 75.6 °C these sets were analyzed by chemically transforming the corresponding LCRs in chemically competent NEB® 10-β *E. coli*. This resulted in roughly 100× lower transformation efficiency in comparison to the electrocompetent cells utilized in previous experiments.

For all sets, the efficiency was similar throughout the entire temperature range (Figure 3A). Consistent with previous results, the total amount of CFUs increased with lower BO-T_ms (comparing the results shown in Supplementary Figure 6H and Figure 3B). Furthermore, all sets have a global CFU maximum in the annealing temperature range of ∼66-71 °C. This range contains the ligase optimum of 70 °C, which suggests positive effects of prolonging the total ligation time to 1.5 min (30 s annealing at 66-68 °C, 1 min ligation at 66 °C) in comparison to the baseline-condition of 30 s annealing at 55 °C and 1 min ligation at 66 °C.

In total, increasing the annealing temperature from 55 °C to 66 °C improved the CFU yield of every BO-set by a factor of two without a loss of efficiency. The BO-set "67.8 °C" performed better than the other sets. Supplementary Figure 16 shows that at the optimum annealing temperature of 67.8 °C, the BO-set "67.8 °C" also showed slightly greater efficiency than the other sets.

Lower BO melting temperatures may have additional benefits for LCR assemblies without DMSO and betaine. To validate this, new BO-sets with lower melting temperatures of 62 °C to 67.3 °C were designed and applied for ligations at 66 °C (Figure 3C+D, sequences in Supplementary Table 5). Surprisingly, a drop-off in efficiency and CFUs was observed for BO-sets with equal or lower melting temperatures than 66 °C. In comparison to the results shown in Figure 3A the efficiency of the 69.9 °C-set is 30% lower. This result is most likely related to a loss of function by additional freeze-thaw cycles or contamination of the DNA parts, BO-sets and/or supplements. Negative impacts of repeated freeze-thaw cycles on the DNA parts and BOs were already mentioned for the LCR (16) and for single-stranded oligonucleotides (39). Nevertheless, the total amount of CFUs was further optimized by using BOs with a T_m of 67.8 °C for each half and by increasing the annealing temperature in the range of the ligase optimum without decreasing the efficiency. Together with previous optimizations by performing the LCR without DMSO and betaine the assembly of the seven-part was highly improved. For the following experiments, we defined an improved LCR-protocol (Table 1).

New LCR protocol improves the assembly of two different toy-model plasmid splits

In order validate the positive effects of omitting DMSO/betaine and to use a higher annealing temperature of 66 °C in DMSO/betaine free conditions, the sequence of the seven-part plasmid was used for a three-part split consisting of *mRFP1* as part 1, *sfGFP* as part 2 and pJET1.2/blunt as part 3. The BOs for this assembly were newly ordered and new aliquots of all LCR supplements were utilized. This plasmid was assembled by using the baseline and improved LCR conditions (Table 1). For the baseline condition, the LCR was performed using the manual BO-set with a T_m of 71.4 °C for each half, 8 %v/v DMSO, 0.45 M betaine and the annealing at 55 °C. For the improved LCR condition, the BO-set had a T_m of 67.8 °C for each half (set was already used for the gradient-LCR in Figure 3), no DMSO/betaine were used and the annealing was at 66 °C. The sequences of both BO-sets are shown in Supplementary Table 10. In general, the three-part plasmid was built by the two different LCR-protocols with no differences in the total plasmid size (4918 bp), sequence and BOs in comparison to the seven-part version. Further, the seven-part split was also assembled by using both protocols.

For both splits of the toy-model, the omission of DMSO and betaine was beneficial (plasmid "TP" in Figure 4 and Table 1) although the differences are lower in comparison to the optimization experiments. The low efficiencies of the seven-part split without DMSO/betaine in comparison to the high efficiencies obtained in the LCRs shown in Figure 2 are likely related to the repeated freeze-thaw cycles of the DNA parts. Further, the three-part LCR split was transformed in chemically and electrocompetent cells (Supplementary Figure 20). The results indicate that the LCR efficiencies are independent of the transformation method. Interestingly, the amount of colonies are similar for the chemical transformation and electroporation although the pUC19-transformation efficiency of the electrocompetent cells was ∼100× higher. We assume that the negative effects of DMSO/betaine in the electroporation and the higher transformation efficiency (Supplementary Figure 14) compensate each other. For the LCRs without DMSO and betaine the amount of CFUs was higher when the electroporation was used.

Validation of the improved protocol

To further verify the improved LCR protocol, we designed two validation plasmids based on the reporter genes *lacZ* and one or two antibiotic resistance genes (Supplementary Figures 18 and 19). For both plasmids a three-part and seven-part split were designed and three protocols were applied: the baseline, improved and a third protocol using BO-sets with a higher target melting temperature of 74.8 °C. According to the results shown in Supplementary Figures 6C and 11A, BOs with a higher T_m may improve the efficiency.

As shown by the optimizations for the toy-model plasmid, the improved LCR protocol is beneficial for the assembly of both splits of the validation plasmids "VP1" and "VP2" (Figure 4 and Table 1). Due to high efficiencies when the baseline protocol was applied, the effect of an increased efficiency by the improved protocol was only seen for the seven-part split of the toy-model plasmid "TP" and validation plasmid "VP1". Nevertheless, the optimized protocol without DMSO/betaine increased the total amount of CFUs in comparison to the baseline protocol. According to the results of the third protocol, higher BO melting temperatures improved the LCR with DMSO and betaine but with a low impact (Supplementary Figure 21 and 22). In addition, longer BOs are used in this protocol which are typically more expensive. For automated assemblies the usage of DMSO and betaine would also be disadvantageous.

For both seven-part splits, Sanger sequencing of ten plasmids from CFUs with the correct phenotypes "blue" and resistance to the antibiotic(s) was performed for each validation plasmid. No false-positives were revealed. Control

bioRxiv preprint doi: https://doi.org/10.1101/510768; this version posted May 29, 2019. The copyright holder for this preprint (which was not certified by peer review) is the author/funder. All rights reserved. No reuse allowed without permission.

Table 1. Summary of the LCRs for the validation experiments using the toy-model plasmid and the validation plasmids 1 and 2 (Figure 1B, Supplementary Figure 18 and 19). Each plasmid was split into three and seven parts which were assembled by using the baseline and improved LCR protocol (Table 1). The LCRs were transformed in chemically competent cells by a heat-shock. For results indicated by an *, the LCRs were transformed by electroporation due to low or no colonies when chemical transformation was used. BO: bridging oligo, CFU: colony forming unit, DMSO: dimethyl sulfoxide, T_m: melting temperature of a BO-half using the calculation of SantaLucia (20).

Factor	Unit	LCR protocol			Toy-model plasmid (TP)		Validation plasmid 1 (VP1)		Validation plasmid 2 (VP2)	
		Baseline	75 °C	Improved	Protocol	3 parts	7 parts	3 parts	7 parts	3 parts	7 parts
DMSO	%v/v	8	8	/				Efficiency (%)			
Betaine	M	0.45	0.45	/	Baseline	37±6	0±0*	88±4	17±29*	98±2	93±12
Annealing temperature	°C	55.0	55.0	66.0	Improved	47±6	17±7*	96±1	98±3*	95±0	93±3
Target T_m for each	°C	70.0	74.8	67.8				Total CFUs (per 3 µL LCR)			
bridging oligo half					Baseline	250±46	6±3*	125±8	1±1*	365±63	12±2
					Improved	559±33	30±14*	493±19	323±70*	2023±331	189±26

reactions without BOs and Ampligase® were performed for all splits and revealed no colonies. Additionally, four plasmids from colonies with the wrong phenotype "white" were analyzed for each validation plasmid. For the validation plasmid 1, the sequences had point-mutations in the 80 bp part of the *lacZ*. This part was ordered as oligonucleotides. This suggests that the mutations are due to the oligonucleotide synthesis. For the validation plasmid 2, three out of four plasmids had a point-mutation in the same *lacZ* part mentioned for the validation plasmid 1. One plasmid lacked the *lacZ*-parts 1 and 2 (parts 4 and 5 of the seven-part split shown in Supplementary Figure 18). Nevertheless, the validation experiments support the improved LCR protocol because the false-negative rate only affects the efficiencies and not the total amount of CFUs.

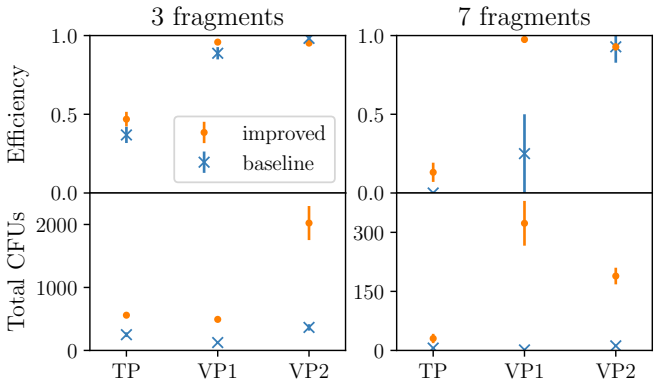

Figure 4. Comparison of the baseline and the improved LCR protocol for assembling the toy-model plasmid ("TP") and the validation plasmids 1 ("VP1") and 2 ("VP2"). The improved protocol increased the total amount of (correct) colonies for all assemblies. The efficiencies were also improved, although the LCRs of the three-part splits were similar for both protocols. LCRs were performed as triplicates and were transformed by chemical transformation. For the seven-part split LCRs of the toy-model plasmid "TP" and validation plasmid "VP1" the LCRs were transformed by electroporation due to low or no colonies when chemical transformation was used. CFU: colony forming unit.

Besides general factors like the genetic context, total plasmid size, amount of parts, purification grade and freeze-thaw-cycles, the successful optimization of the LCR depends on BOs with melting temperatures which fit the kinetic conditions in the reaction. According to this study, the assembly of two splits of three plasmids showed a negative impact when DMSO and betaine are supplied (Figures 2 and 4) although it is considered to be beneficial in the literature (8).

CONCLUSION

To our knowledge, the presented assembly of a plasmid with *sfGFP* and *mRFP1* is the first documented experimental LCR-design that includes a direct and fast readout to investigate the influence of various plasmid designs and experimental conditions. The utilized toy-model plasmid in combination with the fluorescence-based analysis enables a robust and easy-to-adapt *in vivo* system to get valuable insights into the LCR and is also adaptable for investigations of other assembly techniques.

Based on this workflow, the impact of intramolecular and intermolecular crosstalk between BOs is assumed to be negligible for the assembly of a seven-part toy-plasmid, whereas a strong interdependence in regards to the addition of DMSO/betaine, the BO-T_m, the annealing temperature and ligation temperature was observed. Those findings were validated by assembling two validation plasmids by comparing the baseline conditions with an improved LCR protocol without DMSO/betaine, a target T_m of 67.8 °C for each BO-half and an annealing temperature of 66 °C. Related to this, it is of crucial importance to be consistent in the choice of the algorithms for the T_m calculation. Sets with a melting temperature of 67.8 °C when using the formula of SantaLucia (20) are recommended. A melting temperature of 65.2 °C is recommended when using the algorithms of SantaLucia (20) and the salt correction of Owczarzy et al. (35). Using guanine or cytosine at the 3'-end of the BOs was not found to be beneficial.

In total, we used a new toy-model plasmid to investigate an improved LCR protocol without DMSO/betaine and successfully applied it for the assembly of two validation plasmids. We conclude that our improved LCR protocol will help to achieve more efficient assemblies and to enable a simpler way for automated LCR assemblies by omitting DMSO/betaine and adjustments of the thermal conditions. To ensure reproducible conditions we provide a step-by-step LCR-protocol. You can download it from the digital supplement. We also offer a beta-version of a `Geneious`-plugin to design LCR-constructs and bridging oligos with the

bioRxiv preprint doi: https://doi.org/10.1101/510768; this version posted May 29, 2019. The copyright holder for this preprint (which was not certified by peer review) is the author/funder. All rights reserved. No reuse allowed without permission.

improved parameters at www.gitlab.com/kabischlab.de/lcr-publication-synthetic-biology. In the future, we will provide a web-application and a stand-alone tool for the automated design of LCR-constructs and bridging oligos. To accelerate the screening process flow cytometry could applied to use this validated method for future applications to e.g., investigate more rules for the LCR or other assembly methods. Another interesting approach would include the combination of *in vitro* studies using cell-free systems (40) and the toy-model plasmid.

ACKNOWLEDGEMENTS

We thank Carolin Dombrowsky for her technical support to perform the transformations of *E. coli* and the fluorescence-based screening. The authors also acknowledge the scientific discussions and advices with members of the LOEWE CompuGene-group. We further thank Brigitte Held and Dunja Sehn for their organizational support and Alexander Rapp for providing the fluorescence microscope and technical assistance.

FUNDING

Hessen State Ministry of Higher Education, Research and the Arts (HMWK) *via* the LOEWE CompuGene project (to N.S., F.R., S.J., J.K.) and financial support of M.S. by the Deutsche Forschungsgemeinschaft within the GRK 1657, project 1A.

Conflict of interest statement. None declared.

SUPPLEMENTARY DATA

Supplementary data in a pdf file. A step-by-step LCR protocol with the improved conditions is also provided.
All GenBank-files, bridging oligos sequences and the `Geneious`-plugin for the design of bridging oligos are available at www.gitlab.com/kabischlab.de/lcr-publication-synthetic-biology. The GenBank-files also contain the manually designed bridging oligos, amplification primers and sequencing primers.

REFERENCES

1. Gibson,D.G., Young,L., Chuang,R.Y., Venter,J.C., Hutchison,C.A., and Smith,H.O. (May, 2009) Enzymatic assembly of DNA molecules up to several hundred kilobases. *Nature Methods,* **6**(5), 343–345.
2. Engler,C., Kandzia,R., and Marillonnet,S. (November, 2008) A one pot, one step, precision cloning method with high throughput capability. *PLoS ONE,* **3**(11), e3647.
3. Engler,C., Gruetzner,R., Kandzia,R., and Marillonnet,S. (May, 2009) Golden gate shuffling: a one-pot DNA shuffling method based on type IIs restriction enzymes. *PLoS ONE,* **4**(5), e5553.
4. Quan,J. and Tian,J. (July, 2009) Circular polymerase extension cloning of complex gene libraries and pathways. *PLoS ONE,* **4**(7), e6441.
5. Storch,M., Casini,A., Mackrow,B., Fleming,T., Trewhitt,H., Ellis,T., and Baldwin,G.S. (July, 2015) BASIC: A new biopart assembly standard for idempotent cloning provides accurate, single-tier DNA assembly for synthetic biology. *ACS Synthetic Biology,* **4**(7), 781–787.
6. Ma,H., Kunes,S., Schatz,P.J., and Botstein,D. (1987) Plasmid construction by homologous recombination in yeast. *Gene,* **58**(2), 201–216.
7. Torella,J.P., Lienert,F., Boehm,C.R., Chen,J.H., Way,J.C., and Silver,P.A. (August, 2014) Unique nucleotide sequenceguided assembly of repetitive DNA parts for synthetic biology applications. *Nature Protocols,* **9**(9), 2075–2089.
8. de Kok,S., Stanton,L.H., Slaby,T., Durot,M., Holmes,V.F., Patel,K.G., Platt,D., Shapland,E.B., Serber,Z., Dean,J., Newman,J.D., and Chandran,S.S. (February, 2014) Rapid and reliable DNA assembly *via* ligase cycling reaction. *ACS Synthetic Biology,* **3**(2), 97–106.
9. Chandran,S. (2017) Rapid assembly of DNA via ligase cycling Reaction (LCR). In Hughes,R.A., (ed.), *Synthetic DNA*, Vol. 1472, pp. 105–110 Springer New York New York, NY.
10. Roth,T.L., Milenkovic,L., and Scott,M.P. (September, 2014) A rapid and simple method for DNA engineering using cycled ligation assembly. *PLOS ONE,* **9**(9), e107329.
11. Pachuk,C.J., Samuel,M., Zurawski,J.A., Snyder,L., Phillips,P., and Satishchandran,C. (February, 2000) Chain reaction cloning: a one-step method for directional ligation of multiple DNA fragments. *Gene,* **243**(1-2), 19–25.
12. SantaLucia,J. (2007) Physical principles and visual-OMP software for optimal PCR design. In Walker,J.M. and Yuryev,A., (eds.), *PCR Primer Design*, Vol. 402, pp. 3–33 Humana Press Totowa, NJ.
13. Hendling,M., Pabinger,S., Peters,K., Wolff,N., Conzemius,R., and Barii,I. (July, 2018) Oli2go: an automated multiplex oligonucleotide design tool. *Nucleic Acids Research,* **46**(W1), W252–W256.
14. Nowak,R.M., Wojtowicz-Krawiec,A., and Plucienniczak,A. (2015) DNASynth: a computer program for assembly of artificial gene parts in decreasing temperature. *BioMed Research International,* **2015**, 1–8.
15. Bode,M., Khor,S., Ye,H., Li,M.H., and Ying,J.Y. (July, 2009) TmPrime: fast, flexible oligonucleotide design software for gene synthesis. *Nucleic Acids Research,* **37**(suppl_2), W214–W221.
16. Robinson,C.J., Dunstan,M.S., Swainston,N., Titchmarsh,J., Takano,E., Scrutton,N.S., and Jervis,A.J. (January, 2018) Chapter Thirteen - Multifragment DNA Assembly of Biochemical Pathways via Automated Ligase Cycling Reaction. In Scrutton,N., (ed.), *Methods in Enzymology*, Vol. 608 of Enzymes in synthetic biology, pp. 369–392 Academic Press.
17. Lee,M.E., DeLoache,W.C., Cervantes,B., and Dueber,J.E. (September, 2015) A highly characterized yeast toolkit for modular, multipart assembly. *ACS Synthetic Biology,* **4**(9), 975–986.
18. Kearse,M., Moir,R., Wilson,A., Stones-Havas,S., Cheung,M., Sturrock,S., Buxton,S., Cooper,A., Markowitz,S., Duran,C., Thierer,T., Ashton,B., Meintjes,P., and Drummond,A. (June, 2012) Geneious basic: an integrated and extendable desktop software platform for the organization and analysis of sequence data. *Bioinformatics,* **28**(12), 1647–1649.
19. Untergasser,A., Cutcutache,I., Koressaar,T., Ye,J., Faircloth,B.C., Remm,M., and Rozen,S.G. (August, 2012) Primer3-new capabilities and interfaces. *Nucleic Acids Research,* **40**(15), e115.
20. SantaLucia,J. (February, 1998) A unified view of polymer, dumbbell, and oligonucleotide DNA nearest-neighbor thermodynamics. *Proceedings of the National Academy of Sciences,* **95**(4), 1460–1465.
21. Zuker,M. and Stiegler,P. (Jan, 1981) Optimal computer folding of large RNA sequences using thermodynamics and auxiliary information. *Nucleic Acids Res.,* **9**(1), 133–148.
22. Bernhart,S.H., Tafer,H., Flamm,C., Stadler,P.F., and Hofacker,I.L. (2006) Partition function and base pairing probabilities of RNA heterodimers. *Algorithms Mol Biol,* p. 2006.
23. McCaskill,J.S. (1990) The equilibrium partition function and base pair binding probabilities for RNA secondary structure. *Biopolymers,* **29**(6-7), 1105–1119.
24. Dimitrov,R.A. and Zuker,M. (2004) Prediction of Hybridization and Melting for Double-Stranded Nucleic Acids. *Biophysical Journal,* **87**(1), 215–226.
25. Lorenz,R., Bernhart,S.H., Höner zu Siederdissen,C., Tafer,H., Flamm,C., Stadler,P.F., and Hofacker,I.L. (Nov, 2011) ViennaRNA Package 2.0. *Algorithms for Molecular Biology,* **6**(1), 26.
26. Galassi,M., Davies,J., Theiler,J., Gough,B., Jungman,G., Booth,M., and Rossi,F. GSL-GNU Scientific Library: Reference manual (01, 2003).
27. Kirkpatrick,S., Gelatt,C.D., and Vecchi,M.P. (1983) Optimization by Simulated Annealing. *Science,* **220**(4598), 671–680.
28. Zhang,Y., Werling,U., and Edelmann,W. (April, 2012) SLiCE: a novel bacterial cell extract-based DNA cloning method. *Nucleic Acids Research,* **40**(8), e55.
29. Jacobus,A.P. and Gross,J. (March, 2015) Optimal cloning of PCR fragments by homologous recombination in *Escherichia coli*. *PLOS ONE,* **10**(3), e0119221.
30. von Ahsen,N., Wittwer,C.T., and Schütz,E. (2001) Oligonucleotide

bioRxiv preprint doi: https://doi.org/10.1101/510768; this version posted May 29, 2019. The copyright holder for this preprint (which was not certified by peer review) is the author/funder. All rights reserved. No reuse allowed without permission.
main — 2019/5/22 — 19:03 — page 11 — #11

melting temperatures under PCR conditions: nearest-neighbor corrections for Mg2+, deoxynucleotide triphosphate, and dimethyl sulfoxide concentrations with comparison to alternative empirical formulas. *Clinical Chemistry,* **47**(11), 1956–1961.
31. Dutra,B.E., Sutera,V.A., and Lovett,S.T. (January, 2007) RecA-independent recombination is efficient but limited by exonucleases. *Proceedings of the National Academy of Sciences,* **104**(1), 216–221.
32. Bzymek,M. and Lovett,S.T. (July, 2001) Instability of repetitive DNA sequences: the role of replication in multiple mechanisms. *Proceedings of the National Academy of Sciences,* **98**(15), 8319–8325.
33. Geissmann,Q. (February, 2013) OpenCFU, a new free and open-source software to count cell colonies and other circular objects. *PLOS ONE,* **8**(2), e54072.
34. Carpenter,A.E., Jones,T.R., Lamprecht,M.R., Clarke,C., Kang,I.H., Friman,O., Guertin,D.A., Chang,J.H., Lindquist,R.A., Moffat,J., Golland,P., and Sabatini,D.M. (October, 2006) CellProfiler: image analysis software for identifying and quantifying cell phenotypes. *Genome Biology,* **7**(10), R100.
35. Owczarzy,R., Moreira,B.G., You,Y., Behlke,M.A., and Walder,J.A. (May, 2008) Predicting stability of DNA duplexes in solutions containing magnesium and monovalent cations. *Biochemistry,* **47**(19), 5336–5353.
36. Escara,J.F. and Hutton,J.R. (July, 1980) Thermal stability and renaturation of DNA in dimethyl sulfoxide solutions: acceleration of the renaturation rate. *Biopolymers,* **19**(7), 1315–1327.
37. Henke,W., Herdel,K., Jung,K., Schnorr,D., and Loening,S.A. (October, 1997) Betaine improves the PCR amplification of GC-rich DNA sequences. *Nucleic Acids Research,* **25**(19), 3957–3958.
38. Hanahan,D. (June, 1983) Studies on transformation of *Escherichia coli* with plasmids. *Journal of Molecular Biology,* **166**(4), 557–580.
39. Davis,D.L., O'Brie,E.P., and Bentzley,C.M. (October, 2000) Analysis of the degradation of oligonucleotide strands during the freezing/thawing processes using MALDI-MS. *Analytical Chemistry,* **72**(20), 5092–5096.
40. Shin,J. and Noireaux,V. (January, 2012) An *E. coli* cell-free expression toolbox: application to synthetic gene circuits and artificial cells. *ACS Synthetic Biology,* **1**(1), 29–41.
41. Wenzel,M. and Altenbuchner,J. (2015) Development of a markerless gene deletion system for *Bacillus subtilis* based on the mannose phosphoenolpyruvate-dependent phosphotransferase system. *Microbiology (Reading, England),* **161**(10), 1942–1949.
42. Cermak,T., Doyle,E.L., Christian,M., Wang,L., Zhang,Y., Schmidt,C., Baller,J.A., Somia,N.V., Bogdanove,A.J., and Voytas,D.F. (July, 2011) Efficient design and assembly of custom TALEN and other TAL effector-based constructs for DNA targeting. *Nucleic Acids Research,* **39**(12), e82.
43. Silbersack,J., Juergen,B., Hecker,M., Schneidinger,B., Schmuck,R., and Schweder,T. (December, 2006) An acetoin-regulated expression system of *Bacillus subtilis*. *Applied Microbiology and Biotechnology,* **73**(4), 895–903.

bioRxiv preprint doi: https://doi.org/10.1101/510768; this version posted May 29, 2019. The copyright holder for this preprint (which was not certified by peer review) is the author/funder. All rights reserved. No reuse allowed without permission.

SUPPLEMENT

Bridging oligo optimization details

Crosstalk-optimized sets of bridging oligonucleotides (BOs) were obtained by quantifying the crosstalk with a score derived from secondary structure and then sampling with simulated annealing from the search space.

Search space

The oligo search space is restricted because each half-oligo (henceforth called primer) must be complementary to the end of a DNA part and the melting temperature between them must be slightly above the experimental ligation temperature. While perfect complementarity is technically not required because thermodynamic data exists for mismatches, melting temperature calculations are too inaccurate for such an approach. *In silico*, changing the set of thermodynamic parameters often has a bigger impact on the melting temperature than inserting a mismatch, and so sensible design of non-complementary oligos is not feasible.

The oligo candidates were created by concatenating two primers, each of which is complementary to one end of one DNA part. For each end of each DNA part, a list of primers was created by taking substrings of varying lengths, where one end of the substring had to coincide with an end of the part. Taking the complementary was not necessary because the experiments contained double-stranded DNA. Each such primer had to satisfy the conditions that its melting temperature to the part is in the range $67°\mathrm{C} \leq T_m \leq 73°\mathrm{C}$. The list of BOs for a pair of DNA parts was obtained by taking the Cartesian product of the set of primers for the 3' end of one part with the set of primers of the 5' end of the next part, and finally concatenating the individual elements of the product. This yielded a list q_i of all possible BOs for every bridging site $1 \leq i \leq N$, which were used for the subsequent calculations.

Scoring

The score to be minimized was defined in terms of the Hamiltonian $H(\vec{\sigma})$ with $\vec{\sigma} = (\sigma_1,...,\sigma_i,...,\sigma_N)$ and $\sigma_i \in \{q_1,...,q_M\}$ being the BO at site i. We implemented three different choices for $H(\vec{\sigma})$, all of which are closely related to secondary structure and the minimum free energy (MFE). Throughout, we have used the dna_mathews2004.par file that ships with the `ViennaRNA`-package (25).

1. Sum of the MFEs of pairwise BO-binding. For this, the Hamiltonian takes the form

$$H_{\mathrm{MFE}}(\vec{\sigma}) = -\sum_{i=1}^{N} h_i(\sigma_i) - \sum_{1 \leq i < j \leq N} J_{ij}(\sigma_i,\sigma_j), \qquad \textbf{(1)}$$

with $h_i(\sigma_i)$ being the MFE of cofolding between two σ_i and $J_{ij}(\sigma_i,\sigma_j)$ being the MFE of cofolding between σ_i and σ_j. The cofolding MFE of every pairwise BO combination is obtained with an implementation of the Zuker algorithm (21). This Hamiltonian choice makes intuitively sense because higher MFEs correspond to less interaction between oligos.

2. Consideration of melting temperature T_m between pairwise BO-binding. The Hamiltonian H_{T_m} takes the same form as in (**1**) with $h_i(\sigma_i)$ now being the negative T_m between two σ_i and $J_{ij}(\sigma_i,\sigma_j)$ being the negative T_m of cofolding between σ_i and σ_j. This negative sign takes into account that the (positive) T_m of a pairwise BO-binding should be as low as possible.
The melting temperatures are computed by an MFE calculation with a modified traceback scheme. Instead of a secondary structure, the traceback returns entropy change ΔS and enthalpy change ΔH. The melting temperature follows as

$$T_m = \frac{\Delta H}{\Delta S + R\ln(C_T/4)} \qquad \textbf{(2)}$$

with the gas constant R and the BO concentration C_T.

3. Consideration of unbound (free) BO concentrations. For the calculation of free BO concentrations we use a similar approach as described in Bernhart et al. (22), where the authors were able to calculate the concentrations of bound and unbound RNA-strands by obtaining equilibrium constants from the McCaskill algorithm (23) and subsequently solving a quadratic equation system. Within their calculations, they considered a two-species model. Here, we adapt their code to an arbitrary number of species.
According to the literature (22, 24), the mass action equilibrium defines the concentration for two cofolded BOs $[\sigma_i,\sigma_j]$ as

$$\forall\, i,j\colon\ [\sigma_i,\sigma_j] = K(\sigma_i,\sigma_j)[\sigma_i][\sigma_j], \qquad \textbf{(3)}$$

where $[\sigma_i],[\sigma_j]$ are the monomer concentrations. The equilibrium constant $K(\sigma_i,\sigma_j) = Z(\sigma_i,\sigma_j)/(Z(\sigma_i)\cdot Z(\sigma_j))$ is defined by the partition function of the bound state $Z(\sigma_i,\sigma_j)$ and the free states $Z(\sigma_i), Z(\sigma_j)$. The partition functions represent the thermodynamic configurations of the corresponding state (bound or unbound) and are obtained from the `ViennaRNA`-package. In analogy to Bernhart et al. (22), we introduce the total particle concentration $[\hat{\sigma}_i]$ for a BO as

$$\forall\, 1 \leq i \leq N\colon\ [\hat{\sigma}_i] := [\sigma_i] + 2[\sigma_i,\sigma_i] + \sum_{\substack{1 \leq j \leq N \\ j \neq i}} [\sigma_i,\sigma_j]. \qquad \textbf{(4)}$$

For a specific sequence $\vec{\sigma}$, eqs. (**3**) and (**4**) yield the following quadratic system of equations due to mass conservation (22):

$$\forall\, 1 \leq i \leq N\colon\ [\hat{\sigma}_i] = [\sigma_i] + 2K(\sigma_i,\sigma_i)[\sigma_i]^2 + \sum_{\substack{1 \leq j \leq N \\ j \neq i}} K(\sigma_i,\sigma_j)[\sigma_i][\sigma_j]. \qquad \textbf{(5)}$$

bioRxiv preprint doi: https://doi.org/10.1101/510768; this version posted May 29, 2019. The copyright holder for this preprint (which was not certified by peer review) is the author/funder. All rights reserved. No reuse allowed without permission.

The Jacobian follows as

$$J_{ij} = \begin{cases} 1 + 4K(\sigma_i,\sigma_i)[\sigma_i] + \sum_{\substack{1 \le j \le N \\ j \neq i}} K(\sigma_i,\sigma_j)[\sigma_j] & \text{if } i = j \\ K(\sigma_i,\sigma_j)[\sigma_i] & \text{else.} \end{cases} \quad (6)$$

In eqs. (5), $K(\sigma_i,\sigma_j)$ and $[\hat{\sigma}_i]$ are calculated or part of the user input, so the system of equations can be solved for $[\sigma_i]$ to obtain the equilibrium concentrations $[\sigma_i^{eq}]$. Within our implementation, we use the root finder of the `GNU Scientific Library` (26). Finally, we define our Hamiltonian by

$$H_{\text{conc}}(\vec{\sigma}) = -\min([\sigma_1^{eq}],...,[\sigma_N^{eq}]). \quad (7)$$

This Hamiltonian choice ensures a sufficient amount of the BO with the minimum equilibrium concentration.

Sampling

We used the simulated annealing algorithm (27), where we define

$$P(\vec{\sigma},\tau) = \frac{\exp[-H(\vec{\sigma})/\tau]}{Z(\tau)}, \quad Z(\tau) = \sum_{\{\vec{\sigma}\}} \exp[-H(\vec{\sigma})/\tau] \quad (8)$$

with the artificial temperature τ. A single mutation step consists of randomly picking $i \in \{1,...,N\}$ and $\sigma_i^{\text{new}} \in \{1,...,q_i\}$ and changing $\sigma_i \to \sigma_i^{\text{new}}$.

For each Hamiltonian, three runs of simulated annealing were performed to obtain three sets with minimized crosstalk. Out of these three, the two sets with the greatest edit distance to each other were selected. The same procedure with opposite-sign Hamiltonians was done for a optimization towards the worst case. In total, we obtained six sets with minimized crosstalk and six sets with maximized crosstalk. Supplementary Figures 1 and 2 however show that crosstalk turned out to be a much worse indicator of performance than the melting temperatures between BO and DNA part.

bioRxiv preprint doi: https://doi.org/10.1101/510768; this version posted May 29, 2019. The copyright holder for this preprint (which was not certified by peer review) is the author/funder. All rights reserved. No reuse allowed without permission.

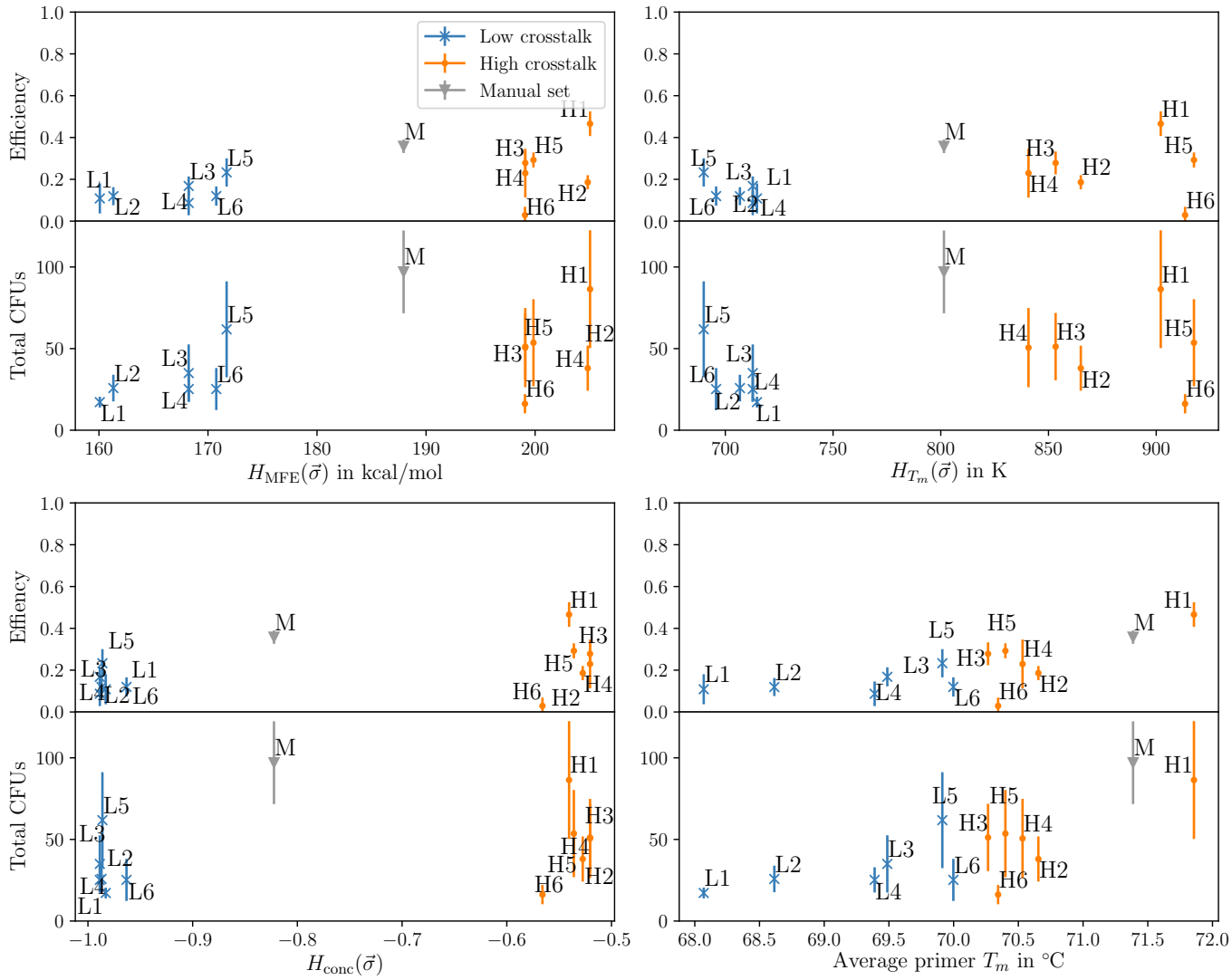

Supplementary Figure 1. Efficiency and total number of CFUs depending on crosstalk and melting temperatures of BO sets with crosstalk optimized towards high (H) or low (L) values plus one manually designed set (M). The data is from the LCRs with 8 %v/v DMSO and 0.45 M betaine of the seven-part toy-plasmid. All LCRs were performed as quintuplets. The optimization criterion for each set can be seen in the crosstalk plots, e.g. sets L1 and L2 appear at the very left of the MFE crosstalk plot because they were optimized for low MFE crosstalk. High-crosstalk sets perform better than low-crosstalk sets because greater crosstalk is usually accompanied by greater melting temperatures; this counteracts the effect of DMSO and betaine, which lower the melting temperature. Ultimately, secondary structure was inhibited so much by DMSO and betaine that crosstalk could not occur and the BOs could barely attach to their complementary DNA parts. Thus the melting temperatures were a better criterion for performance than crosstalk.

bioRxiv preprint doi: https://doi.org/10.1101/510768; this version posted May 29, 2019. The copyright holder for this preprint (which was not certified by peer review) is the author/funder. All rights reserved. No reuse allowed without permission.

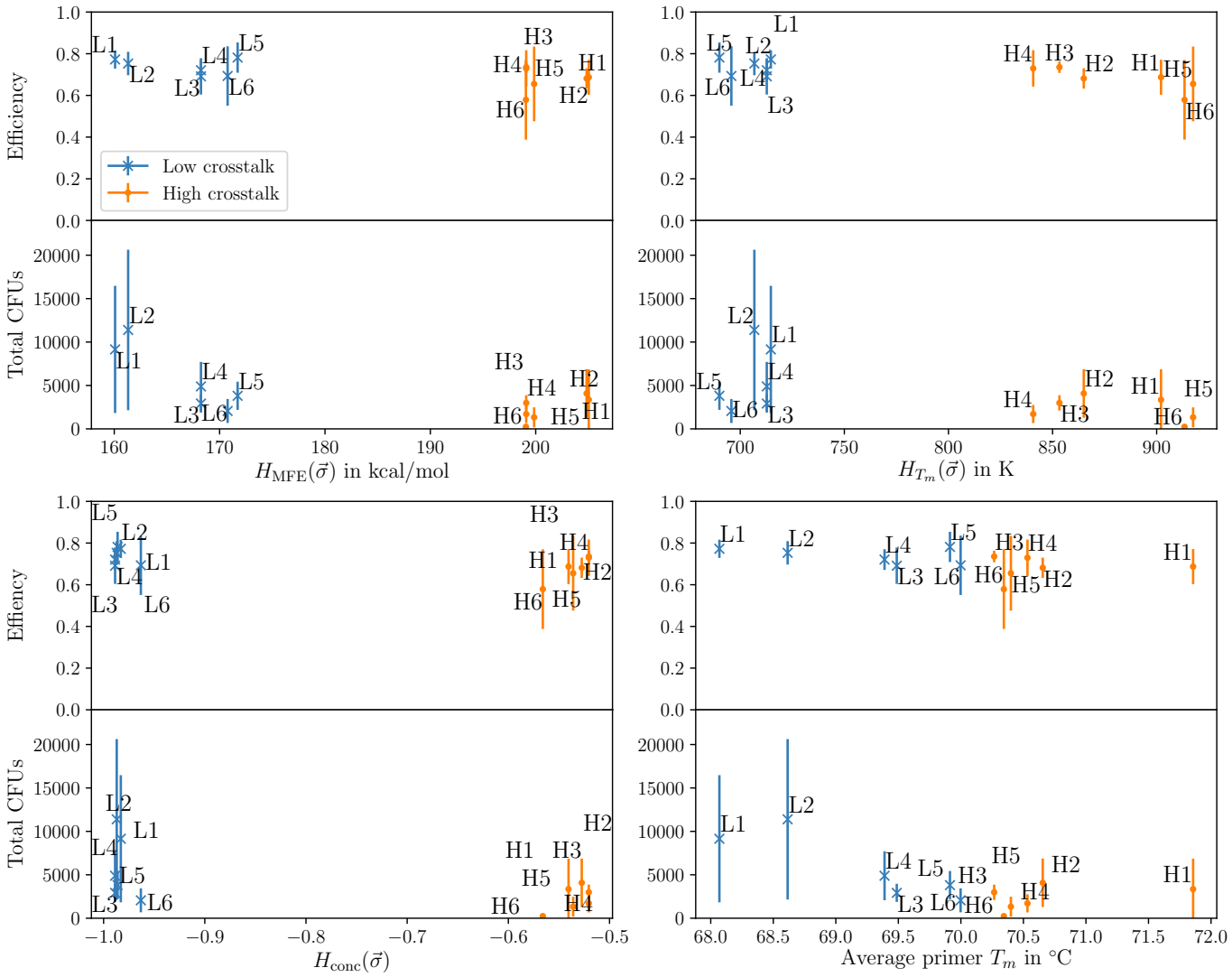

Supplementary Figure 2. Efficiency and total number of CFUs depending on crosstalk and melting temperatures. The data is from the LCRs without DMSO and betaine of the seven-part toy-plasmid. All LCRs were performed as quintuplets. MFE-minimized sets perform better than the remaining sets, but the reason is likely their low melting temperature and not their low crosstalk. Their crosstalk evaluated by H_{T_m} and H_{conc} does not differ from the other low-crosstalk sets, which further suggests that the melting temperature is the main reason for the performance.

bioRxiv preprint doi: https://doi.org/10.1101/510768; this version posted May 29, 2019. The copyright holder for this preprint (which was not certified by peer review) is the author/funder. All rights reserved. No reuse allowed without permission.

Phenotypes of the colonies obtained by the LCRs with the toy-model plasmid

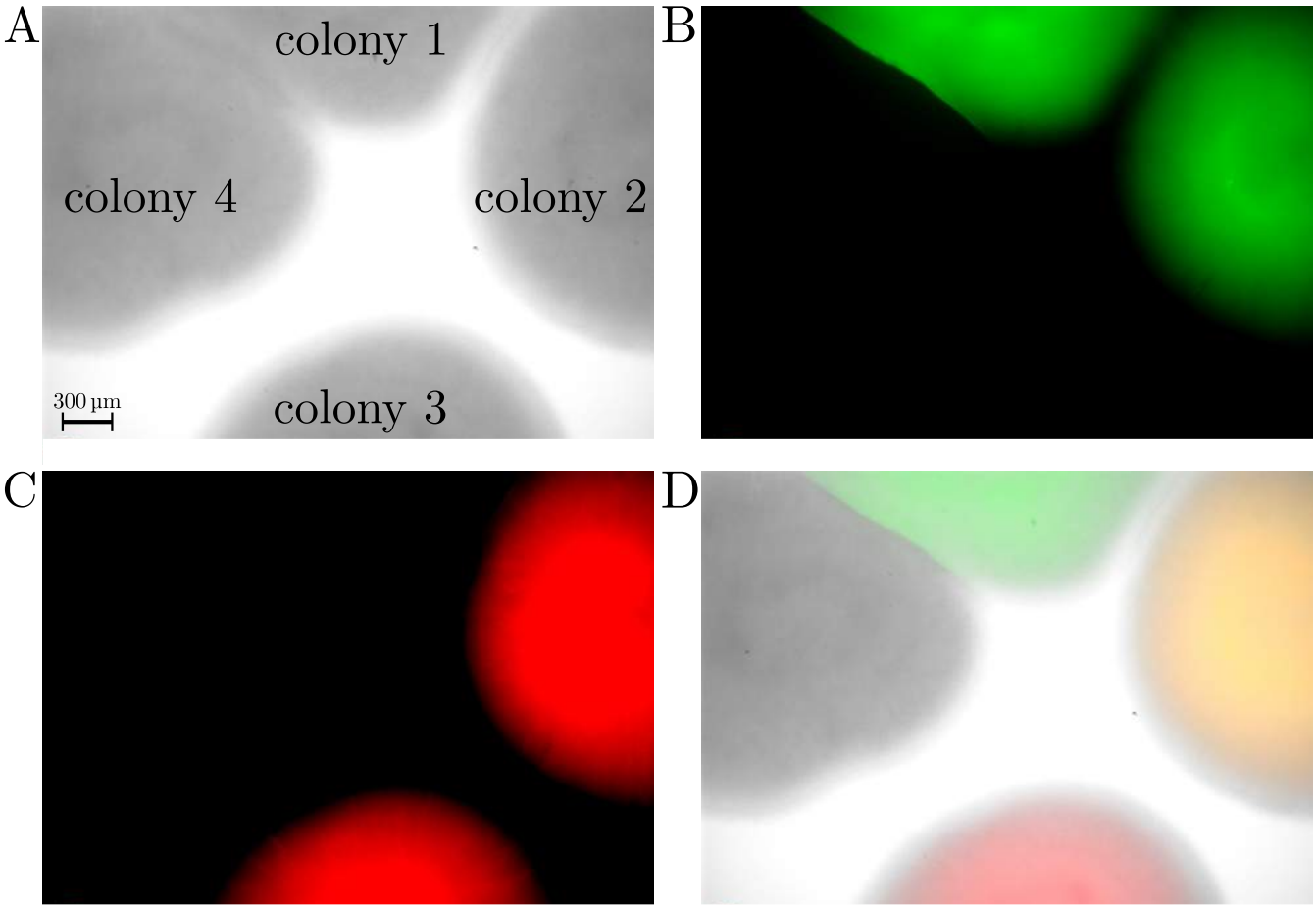

Supplementary Figure 3. The four observed phenotypes of CFUs after the transformation of the LCRs of the toy-model plasmid. The ”colony 2” with the red and green phenotype contained the correct sequence of the toy-model plasmid. The magnification of the images is 40×. **A**. Brightfield image of four colonies. **B**. Image of the colonies shown in A with (colonies 1 and 2) and without sfGFP. **C**. Image of colonies shown in A and B with and without mRFP1 (colonies 2 and 3). **D**. Overlay of the images A-C. CFU: colony forming unit, mRFP1: monomeric red fluorescent protein 1, sfGFP: superfolder green fluorescent protein.

bioRxiv preprint doi: https://doi.org/10.1101/510768; this version posted May 29, 2019. The copyright holder for this preprint (which was not certified by peer review) is the author/funder. All rights reserved. No reuse allowed without permission.

Optimization experiments with the toy-model plasmid

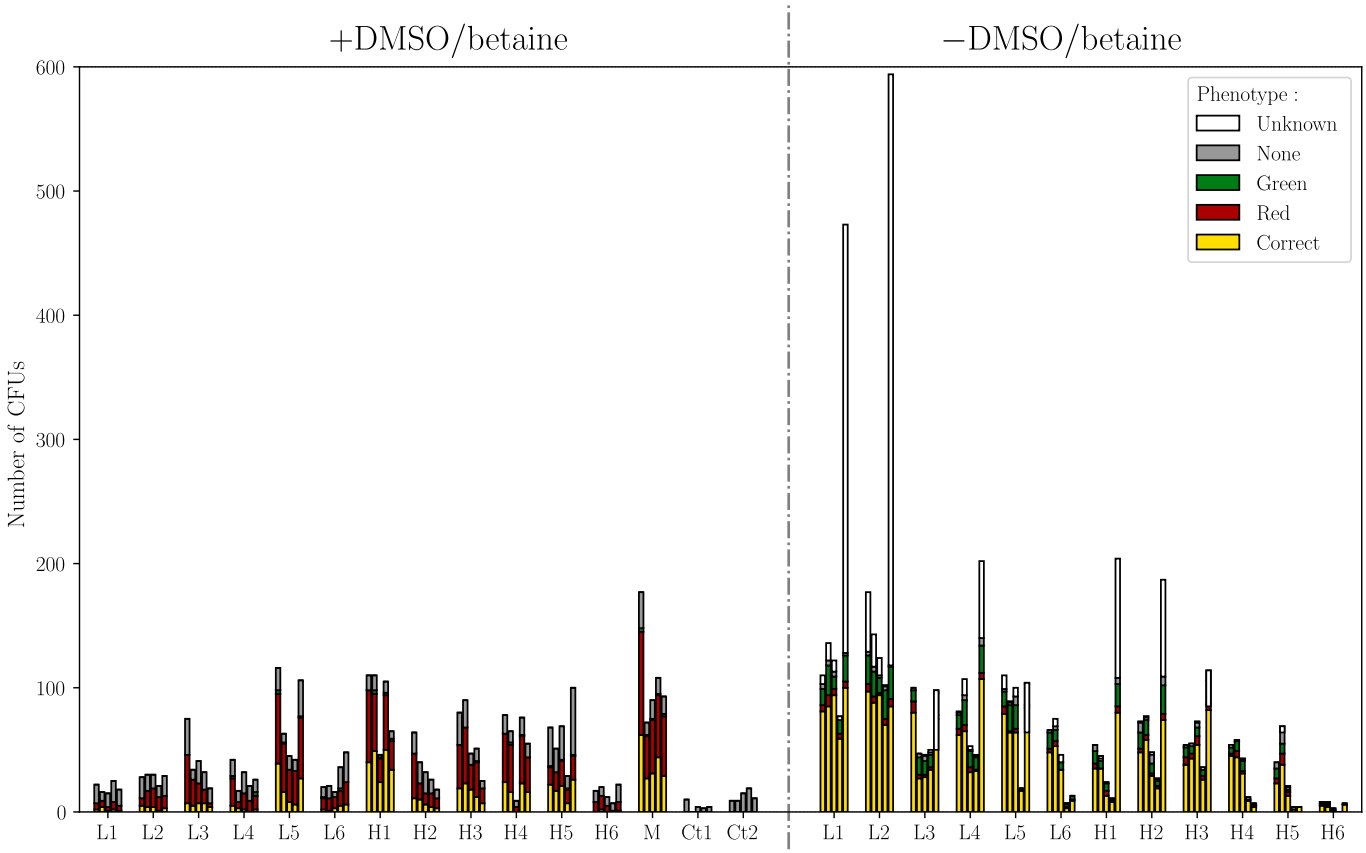

Supplementary Figure 4. Overview of raw data of the experiments to investigate and calculate the influence/omission of DMSO and betaine of the seven-part toy-plasmid (Supplementary Figure 5). All LCRs were performed as quintuplets. Bridging oligo sets with minimized (L1-L6) crosstalk, maximized (H1-H6) crosstalk and the manually designed set (M) are presented. The negative control reactions with BOs without ligase (Ct1) and without BOs and ligase (Ct2) resulted in no fluorescent colonies and were only performed for the LCRs with DMSO/betaine. For the LCRs without DMSO and betaine the amount of CFUs presented here were corrected by multiplying them with the correction factor of 50. All CFUs were counted, but only the phenotypes of about 100 CFUs per LCR were determined. White bars indicate CFUs where the phenotype was not determined. All BO sequences are shown in Supplementary Table 3. BO: bridging oligo, CFU: colony forming unit, DMSO: dimethyl sulfoxide, T_m: melting temperature of a BO-half.

bioRxiv preprint doi: https://doi.org/10.1101/510768; this version posted May 29, 2019. The copyright holder for this preprint (which was not certified by peer review) is the author/funder. All rights reserved. No reuse allowed without permission.

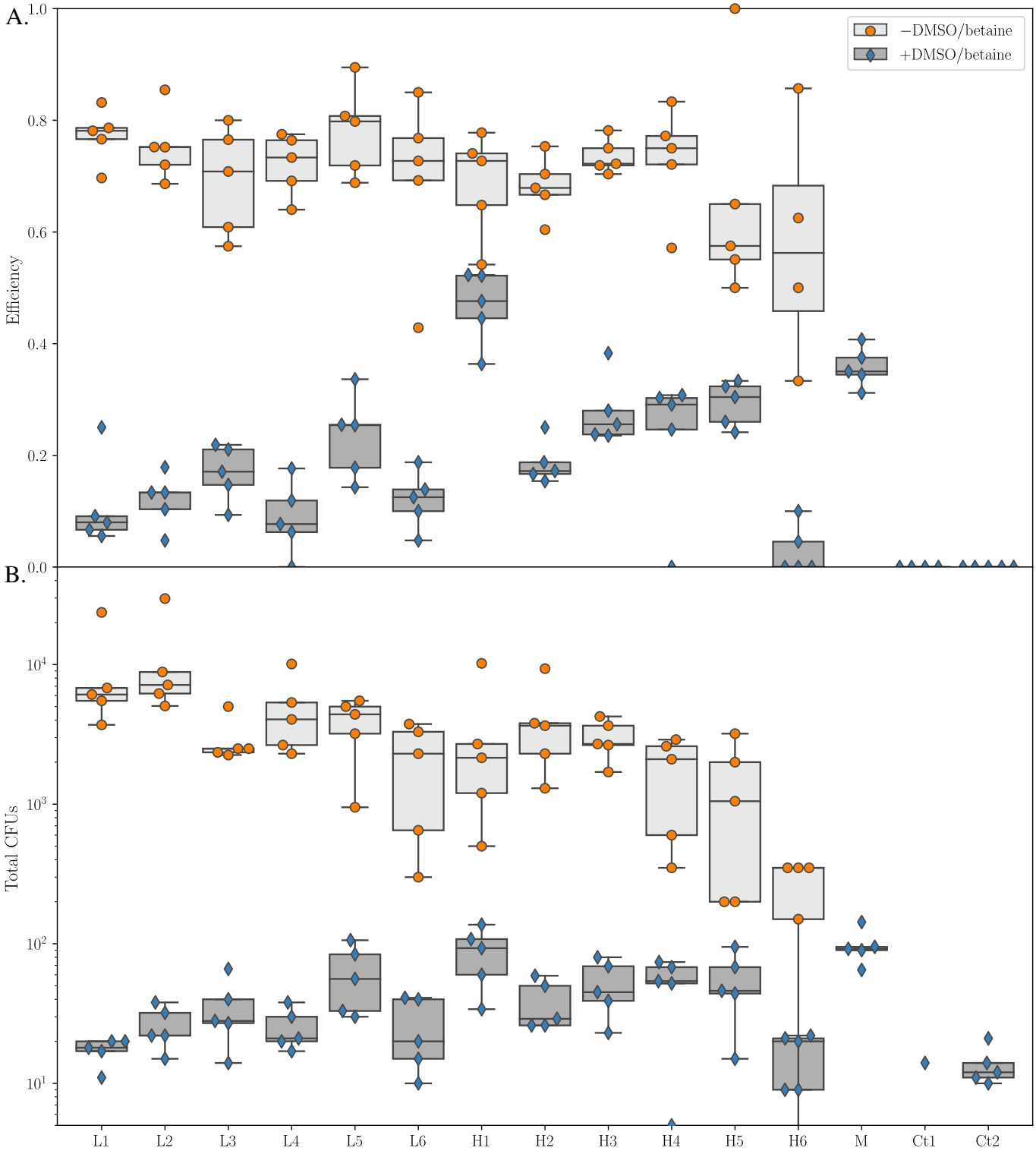

Supplementary Figure 5. LCRs of a seven-part toy-plasmid by utilizing bridging oligo-sets (BO-sets) with high crosstalk (sets H1-H6) and low crosstalk (sets L1-L6). Each LCR was performed as a quintuplet. The standard deviation for each LCR is indicated by error bars. In addition to these twelve sets, a 13th set ("manual" set M) was utilized for the baseline LCR (8 %v/v DMSO and 0.45 M betaine). **A.** All LCRs without DMSO/betaine resulted in higher efficiencies in comparison to the LCRs with both detergents. No correlation between crosstalk and BO performance was found. Additionally, BO-set dependent differences were found for the baseline LCRs, e.g., BO-set H1 resulted in a higher efficiency than BO-set L1. The negative control reactions with BOs without ligase (Ct1) and without BOs and ligase (Ct2) resulted in no fluorescent colonies. **B.** LCRs without DMSO/betaine resulted in more colonies in comparison to the baseline-conditions. The raw data of the LCRs presented here are shown in Supplementary Figure 4. The sequences of all BO-sets are shown in Supplementary Table 3. BO: bridging oligo, CFU: colony forming unit, DMSO: dimethyl sulfoxide.

bioRxiv preprint doi: https://doi.org/10.1101/510768; this version posted May 29, 2019. The copyright holder for this preprint (which was not certified by peer review) is the author/funder. All rights reserved. No reuse allowed without permission.

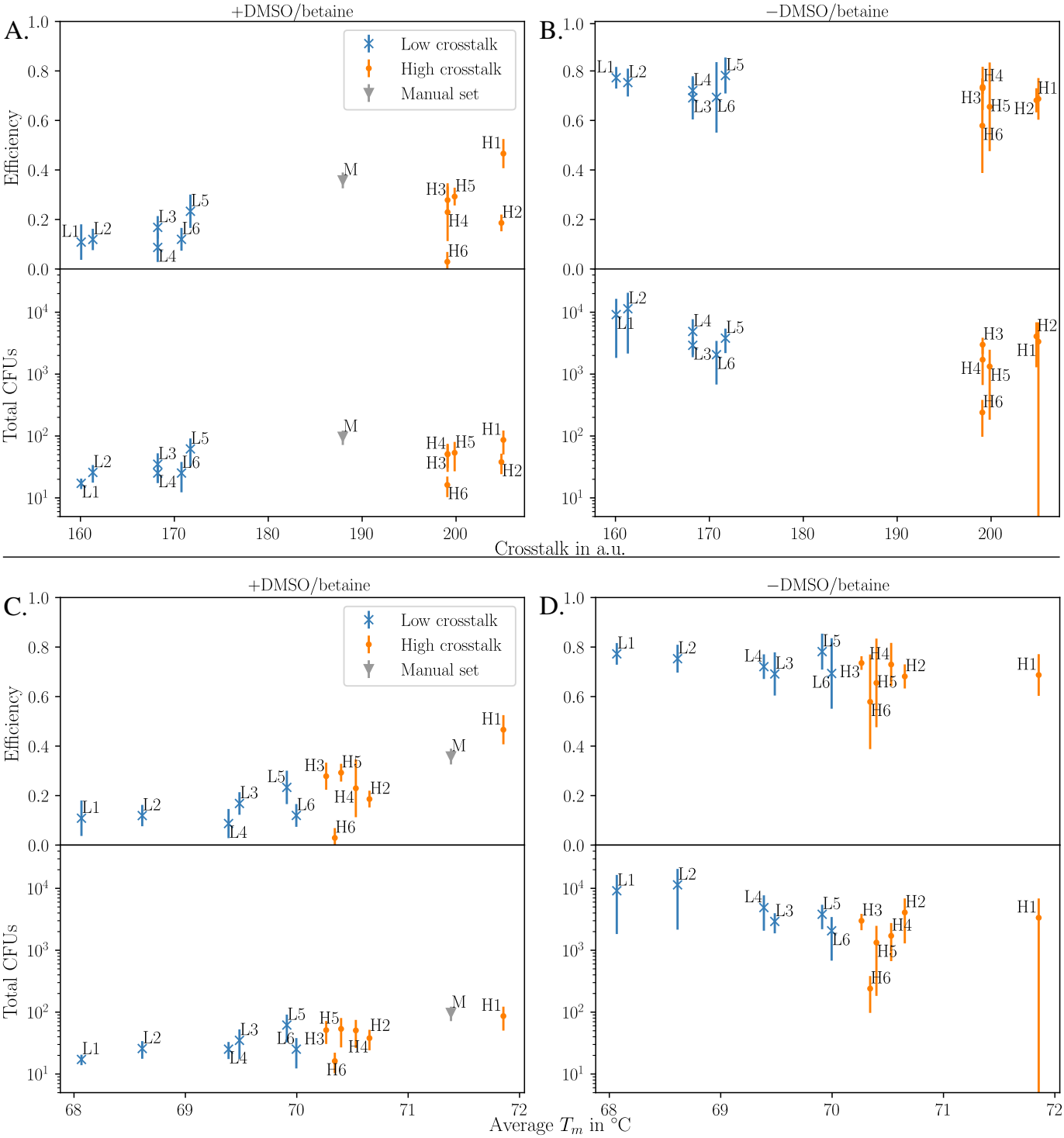

Supplementary Figure 6. Graphical analysis of the bridging oligo sets (BO-sets) utilized for the assembly of a seven-part toy-plasmid, based on the results shown in Supplementary Figure 5. **A+B.** No crosstalk-dependent effects of the BOs were observed for the LCR with (A) and without (B) DMSO/betaine. Both clusters (L1-L6 and H1-H6) were distinguishable by the crosstalk but without affecting the LCR efficiency and total amount of colonies. Slightly higher efficiencies and more colonies were observed for the cluster of the sets H1-H6 when DMSO/betaine was used. **C+D.**: The average melting temperature of the BO-sets influenced the LCRs. Higher T_ms resulted in higher efficiencies and more colonies when DMSO and betaine were used (C). Without DMSO and betaine, all BO-sets resulted in similar efficiencies suggesting no impact of crosstalk of BOs with the DNA parts in the LCR-assembly of the seven-part toy-plasmid. More colonies were observed for sets L1-L6. In contrast to LCRs with DMSO and betaine (C), the total amount of colonies was found to be increasing with decreasing melting temperatures. All T_ms presented here were calculated by using the formula of SantaLucia (20) for the T_m calculation and salt correction. The manual set ("M", used for LCRs with DMSO and betaine) was designed in `Geneious` with the same algorithms and a target temperature of 70 °C. The difference of ∼1.5 °C in comparison to the target T_m of 70 °C is due to the lack of an option to specify the DNA part concentration in the software. The raw data of the LCRs presented here are shown in Supplementary Figure 4. a.u.: arbitrary unit, BO: bridging oligo, CFU: colony forming unit, DMSO: dimethyl sulfoxide, M: manually designed BO-set, T_m: melting temperature of a BO-half.

bioRxiv preprint doi: https://doi.org/10.1101/510768; this version posted May 29, 2019. The copyright holder for this preprint (which was not certified by peer review) is the author/funder. All rights reserved. No reuse allowed without permission.

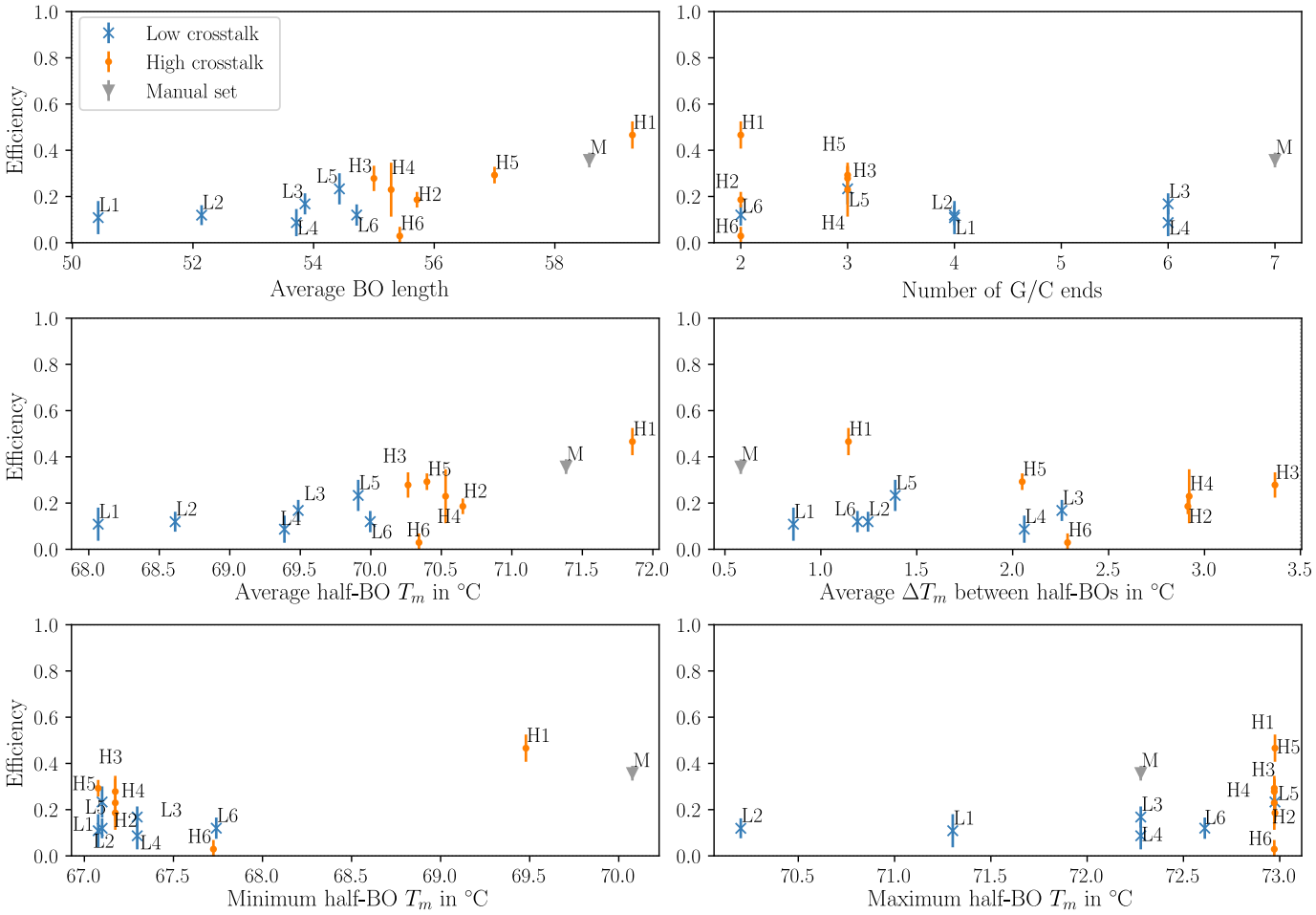

Supplementary Figure 7. Graphical analysis of LCRs with 8 %v/v DMSO and 0.45 M betaine of the seven-part toy-plasmid and the influence of various predictors on the efficiencies by utilizing different bridging oligo sets. All LCRs were performed as quintuplets. The standard deviation for each LCR is indicated by error bars. All BO sequences are shown in Supplementary Table 3. BO: bridging oligo, DMSO: dimethyl sulfoxide, G/C end: 3'-end of one BO ending with the nucleobase guanine or cytosine, T_m: melting temperature.

bioRxiv preprint doi: https://doi.org/10.1101/510768; this version posted May 29, 2019. The copyright holder for this preprint (which was not certified by peer review) is the author/funder. All rights reserved. No reuse allowed without permission.

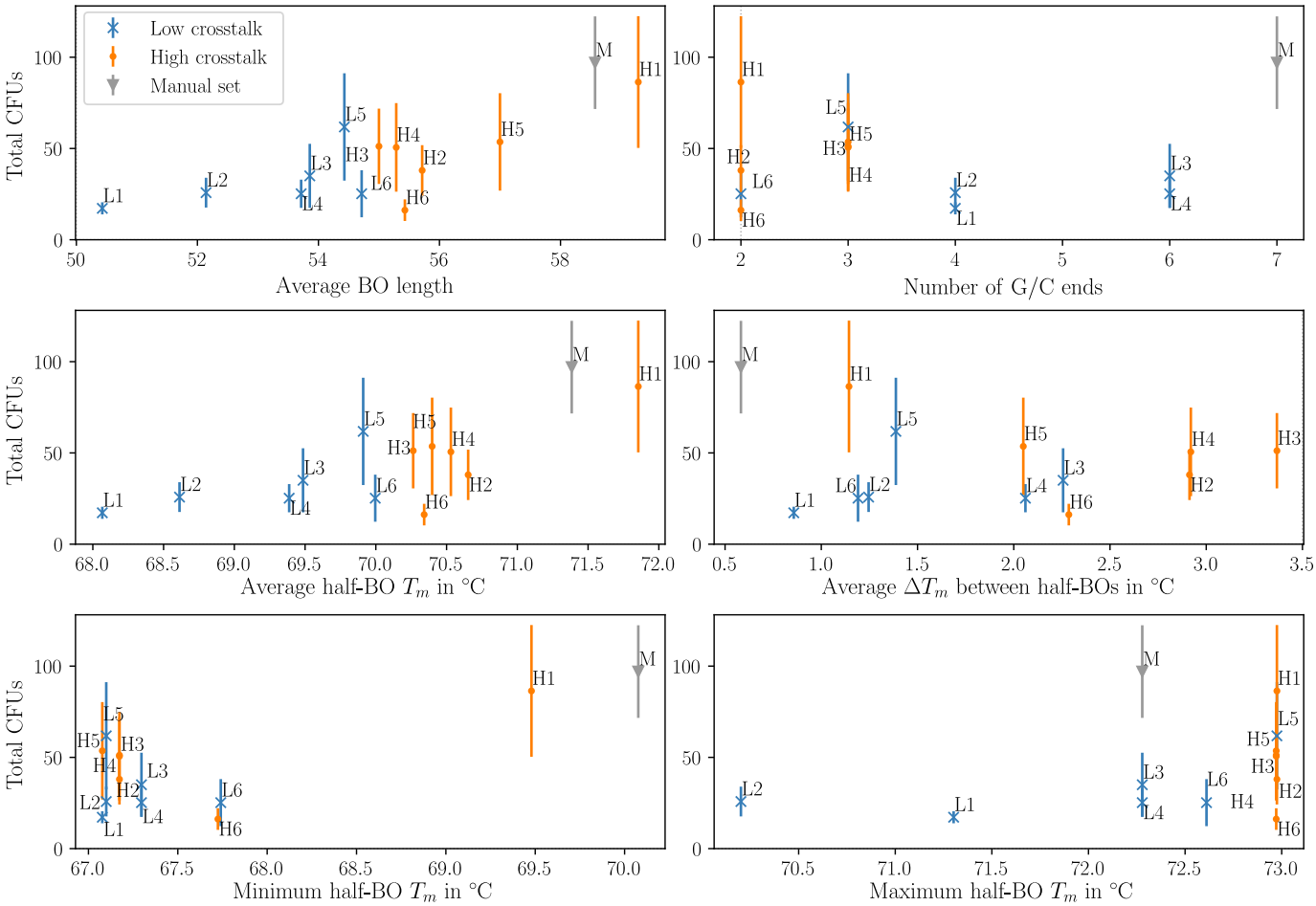

Supplementary Figure 8. Graphical analysis of LCRs with 8 %v/v DMSO and 0.45 M betaine of the seven-part toy-plasmid and the influence of various predictors on the total amount of colonies by utilizing different bridging oligo sets. All LCRs were performed as quintuplets. The standard deviation for each LCR is indicated by error bars. All BO sequences are shown in Supplementary Table 3. BO: bridging oligo, CFU: colony forming unit, DMSO: dimethyl sulfoxide, G/C end: 3'-end of one BO ending with the nucleobase guanine or cytosine, T_m: melting temperature.

bioRxiv preprint doi: https://doi.org/10.1101/510768; this version posted May 29, 2019. The copyright holder for this preprint (which was not certified by peer review) is the author/funder. All rights reserved. No reuse allowed without permission.

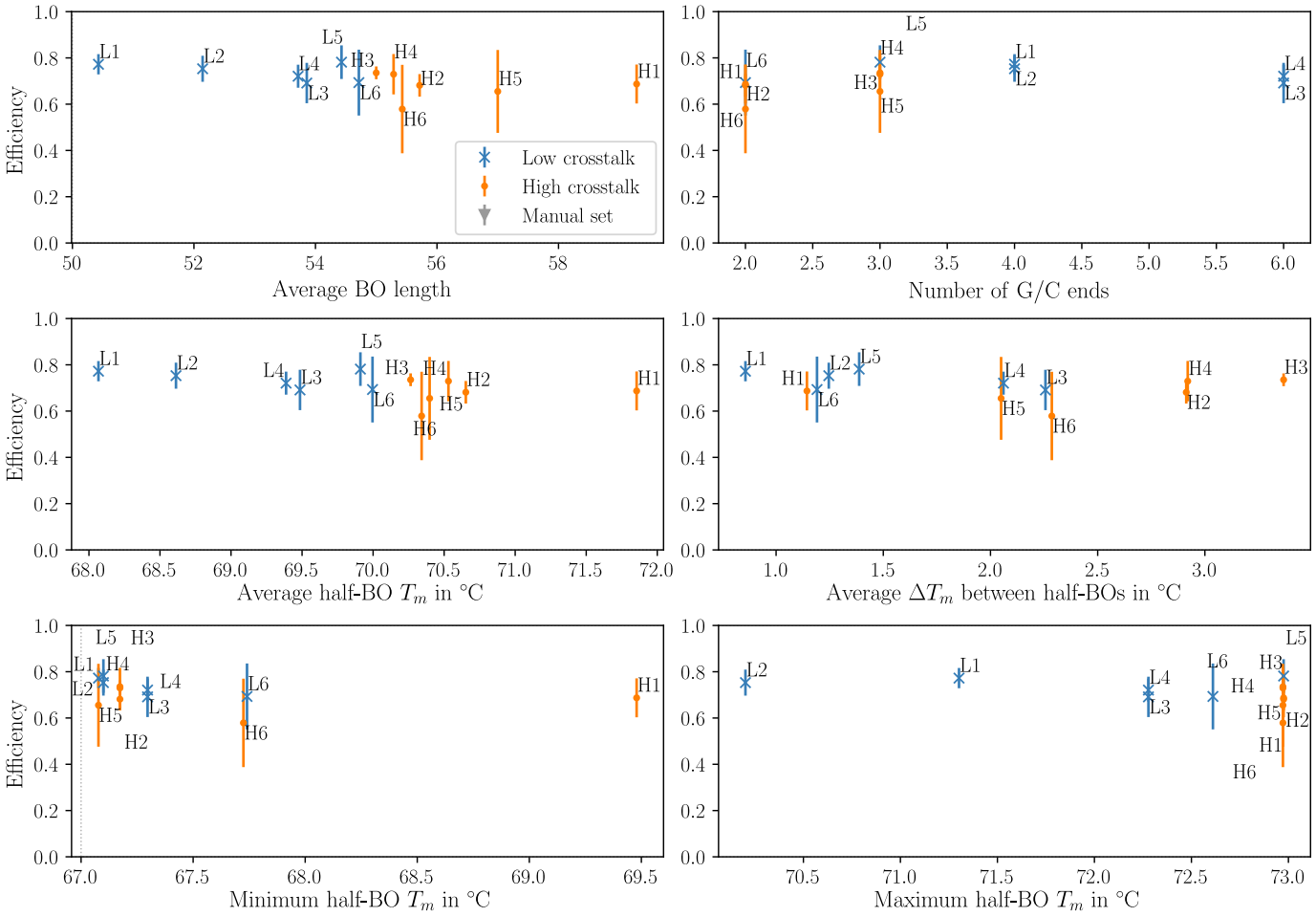

Supplementary Figure 9. Graphical analysis of LCRs without 8 %v/v DMSO and 0.45 M betaine of the seven-part toy-plasmid and the influence of various predictors on the efficiencies by utilizing different bridging oligo sets. All LCRs were performed as quintuplets. The standard deviation for each LCR is indicated by error bars. All BO sequences are shown in Supplementary Table 3. BO: bridging oligo, DMSO: dimethyl sulfoxide, G/C end: 3'-end of one BO ending with the nucleobase guanine or cytosine, T_m: melting temperature.

bioRxiv preprint doi: https://doi.org/10.1101/510768; this version posted May 29, 2019. The copyright holder for this preprint (which was not certified by peer review) is the author/funder. All rights reserved. No reuse allowed without permission.

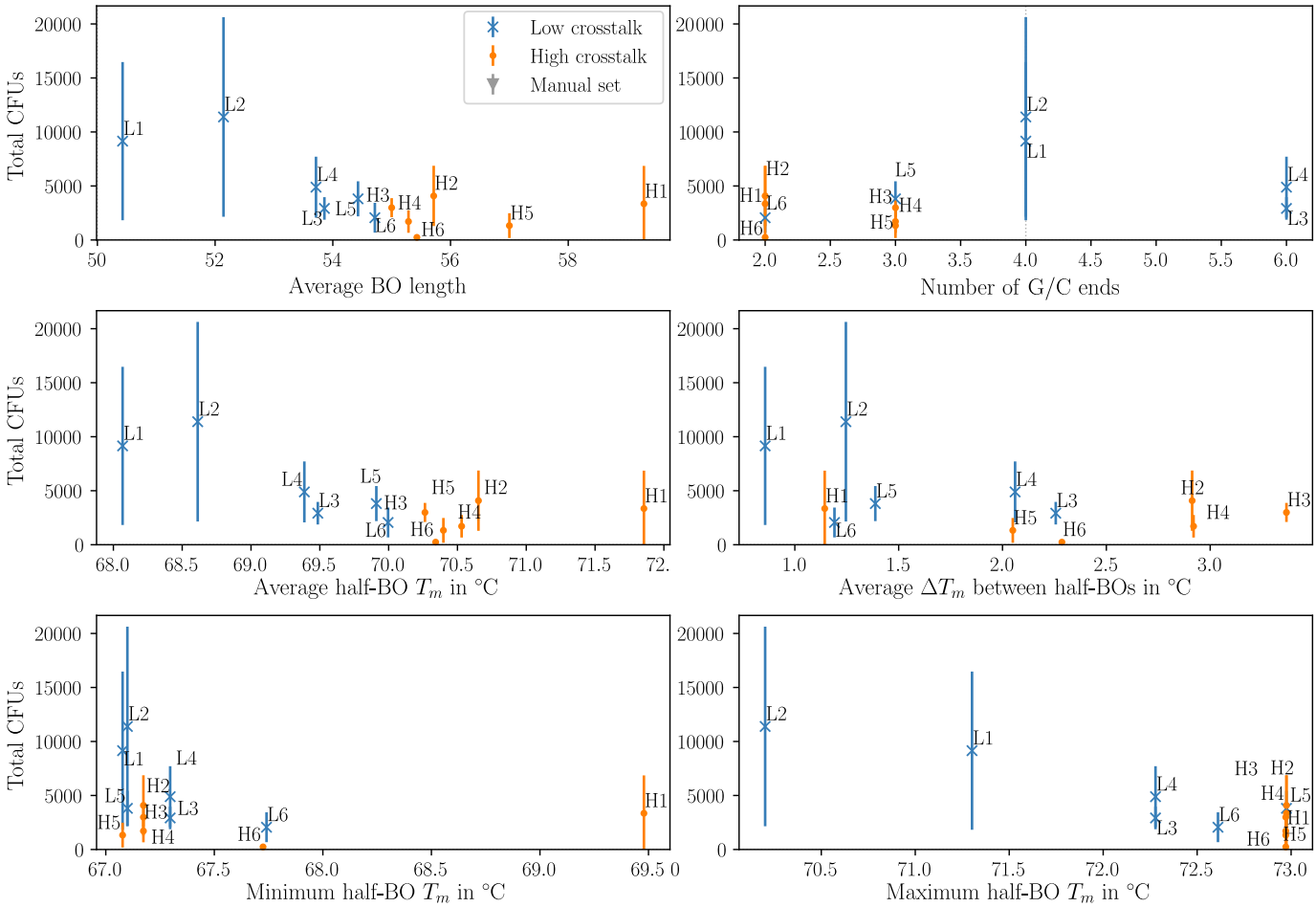

Supplementary Figure 10. Graphical analysis of LCRs without 8 %v/v DMSO and 0.45 M betaine of the seven-part toy-plasmid and the influence of various predictors on the total amount of colonies by utilizing different bridging oligo sets. All LCRs were performed as quintuplets.
The standard deviation for each LCR is indicated by error bars. All BO sequences are shown in Supplementary Table 3. BO: bridging oligo, CFU: colony forming unit, DMSO: dimethyl sulfoxide, G/C end: 3'-end of one BO ending with the nucleobase guanine or cytosine, T_m: melting temperature.

bioRxiv preprint doi: https://doi.org/10.1101/510768; this version posted May 29, 2019. The copyright holder for this preprint (which was not certified by peer review) is the author/funder. All rights reserved. No reuse allowed without permission.

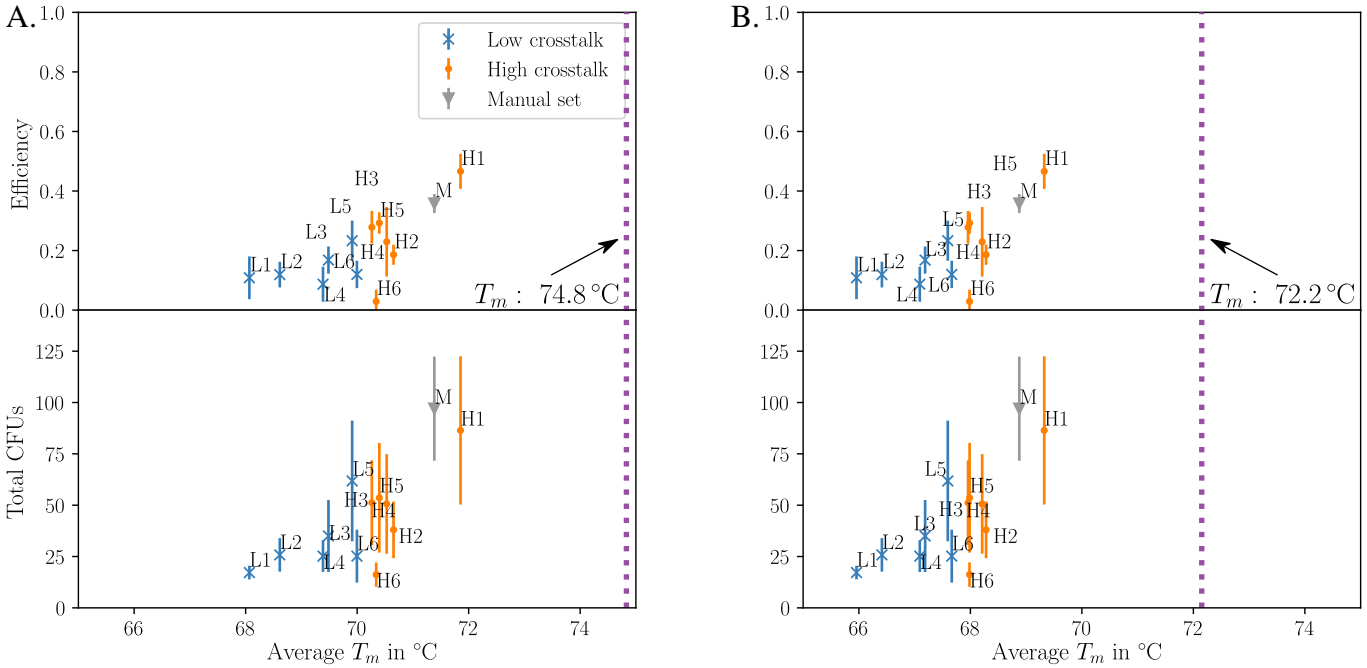

Supplementary Figure 11. Effect of salt corrections on melting temperature. The results for the LCRs with 8 %v/v DMSO and 0.45 M are presented here. The thermodynamic parameters used were SantaLucia (20). The standard deviation for each LCR is indicated by error bars. **A**. SantaLucia (20) salt correction. **B**. Owczarzy (35) salt correction. The optimized melting temperature indicated by the dotted line is obtained from recalculation of the optimized BO-set of the de Kok et al. (8) study. BO: bridging oligo, CFU: colony forming unit, DMSO: dimethyl sulfoxide, T_m: melting temperature of one BO-half.

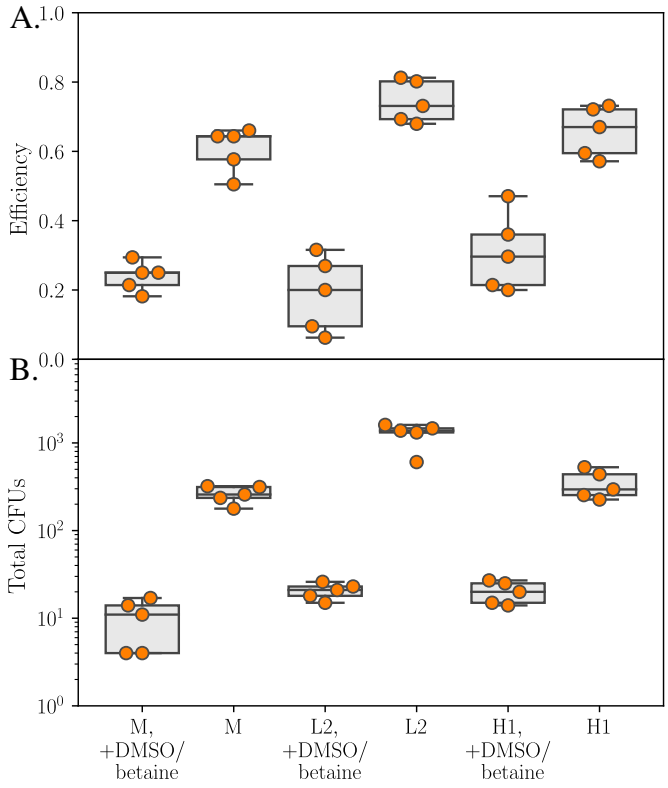

Supplementary Figure 12. Influence of DMSO and betaine in the LCR. All LCRs were performed as quintuplets using the same batches of DNA parts, electrocompetent cells and a master-mix (excluding the BO-sets and the ligase). **A.** For all three BO-sets (H1, L2 and the manually set) the DMSO/betaine-free LCRs were more efficient. As observed in Supplementary Figure 5, the efficiency of the set "H1" was higher than the manual set "M" and set "L2" in the baseline LCR (with DMSO and betaine). **B.** The omission of DMSO/betaine highly increased the total amount of colonies. This is consistent with the results shown in Supplementary Figures 5B and 6H for DMSO/betaine-free conditions: a lower T_m is beneficial and resulted in more colonies. All BO sequences are shown in Supplementary Table 3.

bioRxiv preprint doi: https://doi.org/10.1101/510768; this version posted May 29, 2019. The copyright holder for this preprint (which was not certified by peer review) is the author/funder. All rights reserved. No reuse allowed without permission.

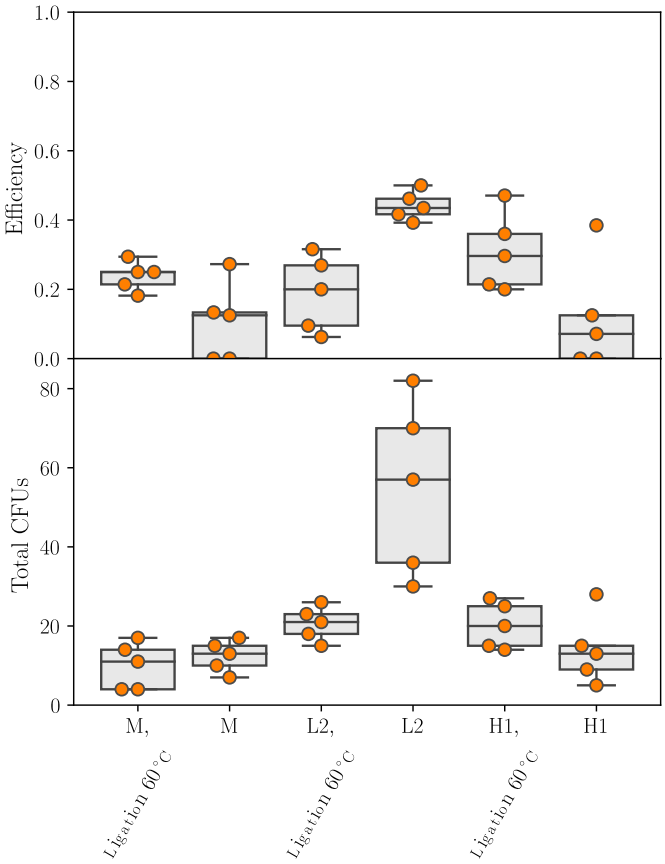

Supplementary Figure 13. Impact of the ligation temperature on LCR performance with DMSO and betaine. All LCRs were performed as quintuplets. A lower ligation temperature is beneficial for the efficiencies and total amount of colonies for the LCR using BO-set L2. This set had a lower T_m of 68.6 °C compared to the manual set with a T_m of 71.4 °C and the set H1 with a T_m of 71.9 °C. Due to the lowered ligation temperature, more BOs of set L2 remained attached to the DNA parts to guide the ligase. All BO sequences are shown in Supplementary Table 3.

bioRxiv preprint doi: https://doi.org/10.1101/510768; this version posted May 29, 2019. The copyright holder for this preprint (which was not certified by peer review) is the author/funder. All rights reserved. No reuse allowed without permission.

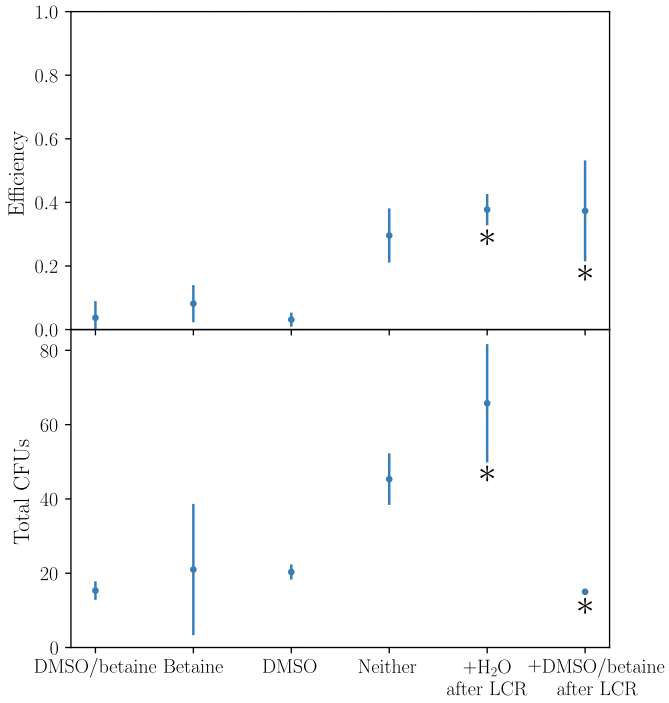

Supplementary Figure 14. DMSO and betaine negatively affect the LCR of the seven-part plasmid. The LCRs to investigate the impact of DMSO and/or betaine were performed as triplicates. To investigate the direct influence of DMSO and betaine on the electroporation process, the LCRs were performed as quadruplets (indicated with a *). The standard deviation for each LCR is indicated by error bars and the manual set "M" was used. The combination of DMSO and betaine negatively affects the efficiency and the total amount of colonies (comparing the results for DMSO/betaine with none of both). Further investigation revealed a direct negative impact of DMSO/betaine in the electroporation. An LCR was performed without DMSO/betaine. Both detergents were added before the electroporation to simulate the transformation conditions (8 %v/v DMSO and 0.45 M betaine, mix of 3 µL LCR and 30 µL competent cells). As a control *dd*H_2O was added. All BO sequences are shown in Supplementary Table 3. BO: bridging oligo, CFU: colony forming unit, DMSO: dimethyl sulfoxide.

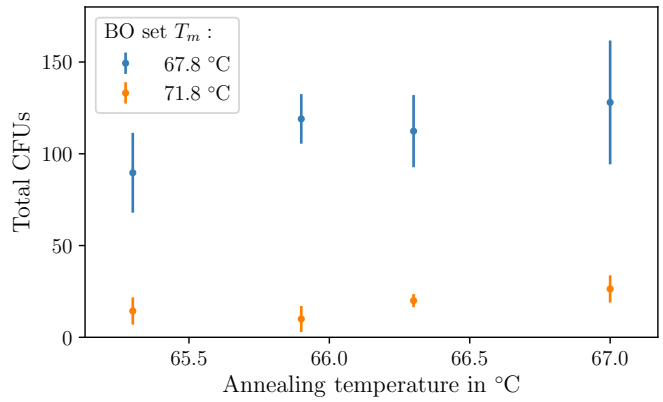

Supplementary Figure 15. Total amount of colonies for the bridging oligo sets "67.8 °C" and "71.8 °C" in the annealing temperature range of 65-67 °C (larger temperature range shown in Figure 3A+B). All LCRs were performed as triplicates. The standard deviation for each LCR is indicated by error bars. All BO sequences are shown in Supplementary Table 4. BO: bridging oligo, CFU: colony forming unit, DMSO: dimethyl sulfoxide, T_m: melting temperature of one BO-half.

bioRxiv preprint doi: https://doi.org/10.1101/510768; this version posted May 29, 2019. The copyright holder for this preprint (which was not certified by peer review) is the author/funder. All rights reserved. No reuse allowed without permission.

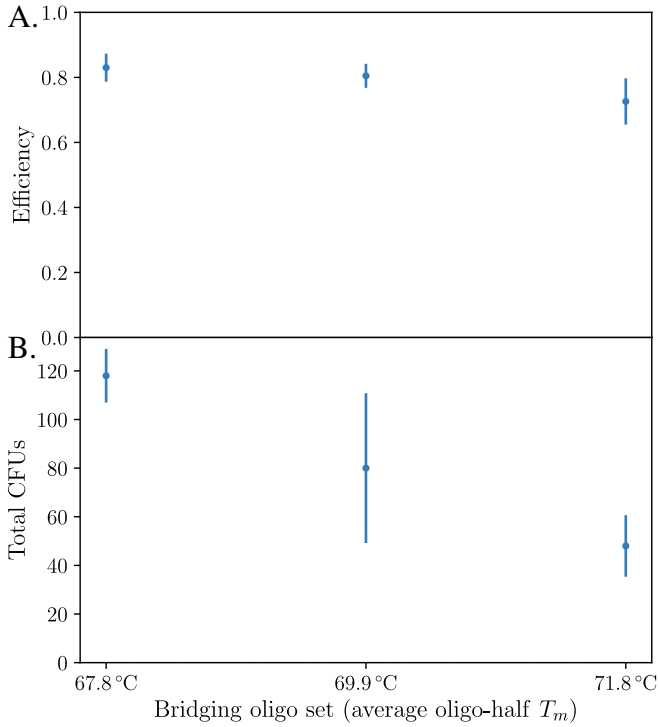

Supplementary Figure 16. LCR without DMSO and betaine at the annealing temperature of 67.9 °C using three bridging oligo sets ($T_m = 67.8$, 69.9 and 71.8 °C). All LCRs were performed as triplicates. The standard deviation for each LCR is indicated by error bars. A larger range of the annealing temperature is shown in Figure 3A+B. **A.** The efficiencies of the LCRs were similar. **B.** The total amount of colonies increased with lower melting temperatures of the BOs. All BO sequences are shown in Supplementary Table 4. BO: bridging oligo, CFU: colony forming unit, DMSO: dimethyl sulfoxide, T_m: melting temperature of one BO-half.

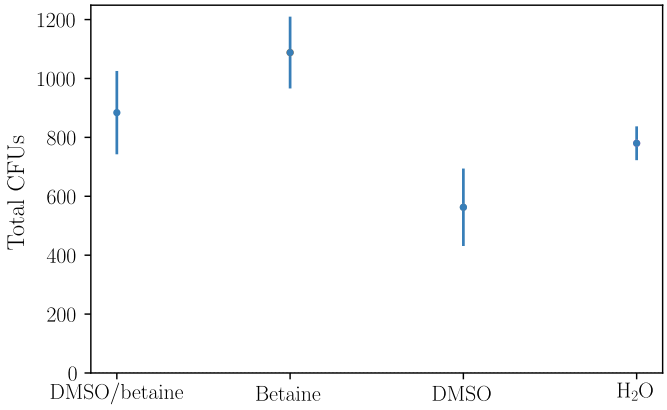

Supplementary Figure 17. DMSO and betaine in chemical transformations. All transformations were performed as triplicates. The standard deviation for each LCR is indicated by error bars. The plasmid pUC19 was mixed with DMSO and/or betaine or *aq. dest.* followed by chemical transformation of *E. coli*. DMSO had a negative impact whereas betaine had a positive impact on the number of colonies. Adding both yielded similar results as adding neither. CFU: colony forming unit, DMSO: dimethyl sulfoxide.

bioRxiv preprint doi: https://doi.org/10.1101/510768; this version posted May 29, 2019. The copyright holder for this preprint (which was not certified by peer review) is the author/funder. All rights reserved. No reuse allowed without permission.

Sequences of the toy-model plasmid and the utilized amplification primers and bridging oligos

Supplementary Table 1: Sequences of the seven-part split of the toy-model (Figure 1B). For the three-part split parts 1-3, 4-6 and 7 were used. The bridging oligos were designed by concatenating subsequences of these parts. It was not necessary to use the reverse complement for the design because the experiments contained both strands of these parts. A GenBank-file of the toy-model plasmid is available in the digital supplement and at www.kabisch-lab.de/data/SynBio_Supp_BO_fasta.zip. *mRFP1*: monomeric red fluorescent protein 1, *sfGFP*: superfolder green fluorescent protein.

Toy-Plasmid Part	Size (bp)	Sequence (5'→3')
mRFP1 (Addgene: pYTK090)		
part 1 (*mRFP1*-part 1)	79	TCCCTATCAGTGATAGAGATTGACATCCCTATCAGTGATAGAGATACTGAGCACGGATCTGAA-AGAGGAGAAAGGATCT
part 2 (*mRFP1*-part 2)	330	ATGGCGAGTAGCGAAGACGTTATCAAAGAGTTCATGCGTTTCAAAGTTCGTATGGAAGGTTCC-GTTAACGGTCACGAGTTCGAAATCGAAGGTGAAGGTGAAGGTCGTCCGTACGAAGGTACTCA-GACCGCTAAACTGAAAGTTACCAAAGGTGGTCCGCTGCCGTTCGCTTGGGACATCCTGTCCCC-GCAGTTCCAGTACGGTTCCAAAGCTTACGTTAAACACCCGGCTGACATCCCGGACTACCTGAA-ACTGTCCTTCCCGGAAGGTTTCAAATGGGAACGTGTTATGAACTTCGAAGACGGTGGTGTTGTT-ACCGTTACCCAGGAC
part 3 (*mRFP1*-part 3)	523	TCCTCCCTGCAAGACGGTGAGTTCATCTACAAAGTTAAACTGCGTGGTACTAACTTCCCGTCCG-ACGGTCCGGTTATGCAGAAAAAAACCATGGGTTGGGAAGCTTCCACCGAACGTATGTACCCGG-AAGACGGTGCTCTGAAAGGTGAAATCAAAATGCGTCTGAAACTGAAAGACGGTGGTCACTAC-GACGCTGAAGTTAAAACCACCTACATGGCTAAAAAACCGGTTCAGCTGCCGGGTGCTTACAAA-ACCGACATCAAACTGGACATCACCTCCCACAACGAAGACTACACCATCGTTGAACAGTACGAA-CGTGCTGAAGGTCGTCACTCCACCGGTGCTTAATAAGGATCTCCAGGCATCAAATAAAACGAA-AGGCTCAGTCGAAAGACTGGGCCTTTCGTTTTATCTGTTGTTTGTCGGTGAACGCTCTCTACTA-GAGTCACACTGGCTCACCTTCGGGTGGGCCTTTCTGCGTTTATAAGTCGGTCTCACCGAGCGGC-CGCGTGTTACAACCAAT
sfGFP (Addgene: pYTK001)		
part 4 (*sfGFP*-part 1)	305	GAAAGTGAAACGTGATTTCATGCGTCATTTTGAACATTTTGTAAATCTTATTTAATAATGTGTG-CGGCAATTCACATTTAATTTATGAATGTTTTCTTAACATCGCGGCAACTCAAGAAACGGCAGGT-TCGGATCTTAGCTACTAGAGAAAGAGGAGAAATACTAGATGCGTAAAGGCGAAGAGCTGTTC-ACTGGTGTCGTCCCTATTCTGGTGGAACTGGATGGTGATGTCAACGGTCATAAGTTTTCCGTGC-GTGGCGAGGGTGAAGGTGACGCAACTAATGGTAAACTGACGCTGAAGTTCA
part 5 (*sfGFP*-part 2)	306	TCTGTACTACTGGTAAACTGCCGGTTCCTTGGCCGACTCTGGTAACGACGCTGACTTATGGTGT-TCAGTGCTTTGCTCGTTATCCGGACCATATGAAGCAGCATGACTTCTTCAAGTCCGCCATGCCG-GAAGGCTATGTGCAGGAACGCACGATTTCCTTTAAGGATGACGGCACGTACAAAACGCGTGCG-GAAGTGAAATTTGAAGGCGATACCCTGGTAAACCGCATTGAGCTGAAAGGCATTGACTTTAAA-GAGGACGGCAATATCCTGGGCCATAAGCTGGAATACAATTTTAACAGCCACA
part 6 (*sfGFP*-part 3)	401	ATGTTTACATCACCGCCGATAAACAAAAAAATGGCATTAAAGCGAATTTTAAAATTCGCCACA-ACGTGGAGGATGGCAGCGTGCAGCTGGCTGATCACTACCAGCAAAACACTCCAATCGGTGATG-GTCCTGTTCTGCTGCCAGACAATCACTATCTGAGCACGCAAAGCGTTCTGTCTAAAGATCCGA-ACGAGAAACGCGATCATATGGTTCTGCTGGAGTTCGTAACCGCAGCGGGCATCACGCATGGTA-TGGATGAACTGTACAAATGACCAGGCATCAAATAAAACGAAAGGCTCAGTCGAAAGACTGGG-CCTTTCGTTTTATCTGTTGTTTGTCGGTGAACGCTCTCTACTAGAGTCACACTGGCTCACCTTCG-GGTGGGCCTTTCTGCGTTTATA
Backbone (Thermo Fisher: pJET1.2/blunt)		

bioRxiv preprint doi: https://doi.org/10.1101/510768; this version posted May 29, 2019. The copyright holder for this preprint (which was not certified by peer review) is the author/funder. All rights reserved. No reuse allowed without permission.

Supplementary Table 1: Sequences of the toy-model parts (continued)

Toy-Plasmid Part	Size (bp)	Sequence (5'→3')
part 7	2974	ATCTTTCTAGAAGATCTCCTACAATATTCTCAGCTGCCATGGAAAATCGATGTTCTTCTTTTATT- CTCTCAAGATTTTCAGGCTGTATATTAAAACTTATATTAAGAACTATGCTAACCACCTCATCAG- GAACCGTTGTAGGTGGCGTGGGTTTTCTTGGCAATCGACTCTCATGAAAACTACGAGCTAAAT- ATTCAATATGTTCCTCTTGACCAACTTTATTCTGCATTTTTTTTGAACGAGGTTTAGAGCAAGCT- TCAGGAAACTGAGACAGGAATTTTATTAAAAATTTAAATTTTGAAGAAAGTTCAGGGTTAATA- GCATCCATTTTTTGCTTTGCAAGTTCCTCAGCATTCTTAACAAAAGACGTCTCTTTTGACATGTT- TAAAGTTTAAACCTCCTGTGTGAAATTATTATCCGCTCATAATTCCACACATTATACGAGCCGG- AAGCATAAAGTGTAAAGCCTGGGGTGCCTAATGAGTGAGCTAACTCACATTAATTGCGTTGCG- CTCACTGCCAATTGCTTTCCAGTCGGGAAACCTGTCGTGCCAGCTGCATTAATGAATCGGCCAA- CGCGCGGGGAGAGGCGGTTTGCGTATTGGGCGCTCTTCCGCTTCCTCGCTCACTGACTCGCTGC- GCTCGGTCGTTCGGCTGCGGCGAGCGGTATCAGCTCACTCAAAGGCGGTAATACGGTTATCCA- CAGAATCAGGGGATAACGCAGGAAAGAACATGTGAGCAAAAGGCCAGCAAAAGGCCAGGAA- CCGTAAAAAGGCCGCGTTGCTGGCGTTTTTCCATAGGCTCCGCCCCCCTGACGAGCATCACAA- AAATCGACGCTCAAGTCAGAGGTGGCGAAACCCGACAGGACTATAAAGATACCAGGCGTTTC- CCCCTGGAAGCTCCCTCGTGCGCTCTCCTGTTCCGACCCTGCCGCTTACCGGATACCTGTCCGC- CTTTCTCCCTTCGGGAAGCGTGGCGCTTTCTCATAGCTCACGCTGTAGGTATCTCAGTTCGGTG- TAGGTCGTTCGCTCCAAGCTGGGCTGTGTGCACGAACCCCCCGTTCAGCCCGACCGCTGCGCCT- TATCCGGTAACTATCGTCTTGAGTCCAACCCGGTAAGACACGACTTATCGCCACTGGCAGCAG- CCACTGGTAACAGGATTAGCAGAGCGAGGTATGTAGGCGGTGCTACAGAGTTCTTGAAGTGGT- GGCCTAACTACGGCTACACTAGAAGGACAGTATTTGGTATCTGCGCTCTGCTGAAGCCAGTTA- CCTTCGGAAAAAGAGTTGGTAGCTCTTGATCCGGCAAACAAACCACCGCTGGTAGCGGTGGTT- TTTTTGTTTGCAAGCAGCAGATTACGCGCAGAAAAAAAGGATCTCAAGAAGATCCTTTGATCT- TTTCTACGGGGTCTGACGCTCAGTGGAACGAAAACTCACGTTAAGGGATTTTGGTCATGAGAT- TATCAAAAAGGATCTTCACCTAGATCCTTTTAAATTAAAAATGAAGTTTTAAATCAATCTAAAG- TATATATGAGTAAACTTGGTCTGACAGTTACCAATGCTTAATCAGTGAGGCACCTATCTCAGCG- ATCTGTCTATTTCGTTCATCCATAGTTGCCTGACTCCCCGTCGTGTAGATAACTACGATACGGG- AGGGCTTACCATCTGGCCCCAGTGCTGCAATGATACCGCGAGACCCACGCTCACCGGCTCCAG- ATTTATCAGCAATAAACCAGCCAGCCGGAAGGGCCGAGCGCAGAAGTGGTCCTGCAACTTTAT- CCGCCTCCATCCAGTCTATTAATTGTTGCCGGGAAGCTAGAGTAAGTAGTTCGCCAGTTAATAG- TTTGCGCAACGTTGTTGCCATTGCTACAGGCATCGTGGTGTCACGCTCGTCGTTTGGTATGGCT- TCATTCAGCTCCGGTTCCCAACGATCAAGGCGAGTTACATGATCCCCCATGTTGTGCAAAAAA- GCGGTTAGCTCCTTCGGTCCTCCGATCGTTGTCAGAAGTAAGTTGGCCGCAGTGTTATCACTCA- TGGTTATGGCAGCACTGCATAATTCTCTTACTGTCATGCCATCCGTAAGATGCTTTTCTGTGAC- TGGTGAGTACTCAACCAAGTCATTCTGAGAATAGTGTATGCGGCGACCGAGTTGCTCTTGCCC- GGCGTCAATACGGGATAATACCGCGCCACATAGCAGAACTTTAAAAGTGCTCATCATTGGAAA- ACGTTCTTCGGGGCGAAAACTCTCAAGGATCTTACCGCTGTTGAGATCCAGTTCGATGTAACCC- ACTCGTGCACCCAACTGATCTTCAGCATCTTTTACTTTCACCAGCGTTTCTGGGTGAGCAAAAA- CAGGAAGGCAAAATGCCGCAAAAAAGGGAATAAGGGCGACACGGAAATGTTGAATACTCATA- CTCTTCCTTTTTCAATATTATTGAAGCATTTATCAGGGTTATTGTCTCATGAGCGGATACATATT- TGAATGTATTTAGAAAAATAAACAAATAGGGGTTCCGCGCACATTTCCCCGAAAAGTGCCACC- TGACGTCTAAGAAACCATTATTATCATGACATTAACCTATAAAAATAGGCGTATCACGAGGCC- GCCCCTGCAGCCGAATTATATTATTTTTGCCAAATAATTTTTAACAAAAGCTCTGAAGTCTTCT- TCATTTAAATTCTTAGATGATACTTCATCTGGAAAATTGTCCCAATTAGTAGCATCACGCTGTG- AGTAAGTTCTAAACCATTTTTTTATTGTTGTATTATCTCTAATCTTACTACTCGATGAGTTTTCG- GTATTATCTCTATTTTTAACTTGGAGCAGGTTCCATTCATTGTTTTTTTCATCATAGTGAATAAA- ATCAACTGCTTTAACACTTGTGCCTGAACACCATATCCATCCGGCGTAATACGACTCACTATAG- GGAGAGCGGCCGCCAGATCTTCCGGATGGCTCGAGTTTTTCAGCAAGAT

bioRxiv preprint doi: https://doi.org/10.1101/510768; this version posted May 29, 2019. The copyright holder for this preprint (which was not certified by peer review) is the author/funder. All rights reserved. No reuse allowed without permission.

Supplementary Table 2: Oligonucleotides for the amplification of all toy-model plasmid parts (shown in Figure 1B). [1] The complete part was ordered as two oligonucleotides, which were phosphorylated and annealed to double stranded DNA before the LCR (described in the methods). [2] For sequencing from the vector into the inserts. fw: forward direction, *mRFP1*: monomeric red fluorescent protein 1, rv: reverse direction, *sfGFP*: superfolder green fluorescent protein.

Toy-Plasmid Part	**OligoID**	**Sequence (5'→3')**
mRFP1 (Addgene: pYTK090)		
part 1 (*mRFP1*-part 1)[1]	10141-fw	TCCCTATCAGTGATAGAGATTGACATCCCTATCAGTGATAGAGATACTGAGCACGGATCTGAA-AGAGGAGAAAGGATCT
	10142-rv	AGATCCTTTCTCCTCTTTCAGATCCGTGCTCAGTATCTCTATCACTGATAGGGATGTCAATCTCT-ATCACTGATAGGGA
part 2 (*mRFP1*-part 2)	10127-fw	ATGGCGAGTAGCGAAGACG
	10128-rv	GTCCTGGGTAACGGTAACAAC
part 3 (*mRFP1*-part 3)	10129-fw	TCCTCCCTGCAAGACGG
	10132-rv	TATAAACGCAGAAAGGCCCAC
sfGFP (Addgene: pYTK001)		
part 4 (*sfGFP*-part 1)	10108-fw	GAAAGTGAAACGTGATTTCATGCG
	10110-rv	TGAACTTCAGCGTCAGTTTAC
part 5 (*sfGFP*-part 2)	10111-fw	TCTGTACTACTGGTAAACTGC
	10112-rv	TGTGGCTGTTAAAATTGTATTCC
part 6 (*sfGFP*-part 3)	10113-fw	ATGTTTACATCACCGCCG
	10109-rv	TATAAACGCAGAAAGGCCCAC
pJET1.2/blunt (Thermo Fisher)		
part 7	23043-fw	ATCTTGCTGAAAAACTCGAGC
	23044-rv	ATCTTTCTAGAAGATCTCC
Sequencing Primers[2]		
forward	14013	CGACTCACTATAGGGAGAGCGGC
reverse	14014	AAGAACATCGATTTTCCATGGCAG

bioRxiv preprint doi: https://doi.org/10.1101/510768; this version posted May 29, 2019. The copyright holder for this preprint (which was not certified by peer review) is the author/funder. All rights reserved. No reuse allowed without permission.
main — 2019/5/22 — 19:03 — page 31 — #31

Supplementary Table 3: Oligonucleotides for crosstalk LCRs (results shown in Supplementary Figures 5 and 6). All melting temperatures (T_ms) presented here are calculated for each BO-half using the formula of SantaLucia (20) for the T_m-calculation and the salt correction. T_m: melting temperature of a BO-half.

Bridging Oligo Set (T_m per BO-half)	OligoID	Sequence (5'→3')
Manually Designed		
M (71.4±0.7°C)	10133	CGGATGGCTCGAGTTTTTCAGCAAGATTCCCTATCAGTGATAGAGATTGACATCCCTATCAG
	10134	GCACGGATCTGAAAGAGGAGAAAGGATCTATGGCGAGTAGCGAAGACGTTATCAAAG
	10135	GTGGTGTTGTTACCGTTACCCAGGACTCCTCCCTGCAAGACGGTGAGTTC
	10137	CGGCCGCGTGTTACAACCAATGAAAGTGAAACGTGATTTCATGCGTCATTTTGAAC
	10116	GCAACTAATGGTAAACTGACGCTGAAGTTCATCTGTACTACTGGTAAACTGCCGGTTCC
	10117	CCATAAGCTGGAATACAATTTTAACAGCCACAATGTTTACATCACCGCCGATAAACAAAAAAATG
	10118	CGGGTGGGCCTTTCTGCGTTTATAATCTTTCTAGAAGATCTCCTACAATATTCTCAGCTGC
Low Crosstalk		
L1 (68.1±1.1°C)	10232	TGGCTCGAGTTTTTCAGCAAGATTCCCTATCAGTGATAGAGATTGACATCC
	10233	CGGATCTGAAAGAGGAGAAAGGATCTATGGCGAGTAGCGAAGACGT
	10234	GTGTTGTTACCGTTACCCAGGACTCCTCCCTGCAAGACGGTG
	10235	GGCCGCGTGTTACAACCAATGAAAGTGAAACGTGATTTCATGCGT
	10236	AATGGTAAACTGACGCTGAAGTTCATCTGTACTACTGGTAAACTGCCGG
	10237	CATAAGCTGGAATACAATTTTAACAGCCACAATGTTTACATCACCGCCGATAAACAAAAAAA
	10238	CGGGTGGGCCTTTCTGCGTTTATAATCTTTCTAGAAGATCTCCTACAATATTCTCAGC
L2 (68.6±0.9°C)	10235	GGCCGCGTGTTACAACCAATGAAAGTGAAACGTGATTTCATGCGT
	10239	GATGGCTCGAGTTTTTCAGCAAGATTCCCTATCAGTGATAGAGATTGACATCCCT
	10240	ACGGATCTGAAAGAGGAGAAAGGATCTATGGCGAGTAGCGAAGACGTTATC
	10241	GGTGTTGTTACCGTTACCCAGGACTCCTCCCTGCAAGACGGTG
	10242	CAACTAATGGTAAACTGACGCTGAAGTTCATCTGTACTACTGGTAAACTGCCGG
	10243	ATAAGCTGGAATACAATTTTAACAGCCACAATGTTTACATCACCGCCGATAAACAAAAAA
	10244	GGGTGGGCCTTTCTGCGTTTATAATCTTTCTAGAAGATCTCCTACAATATTCTCAGC
L3 (69.5±1.7°C)	10244	GGGTGGGCCTTTCTGCGTTTATAATCTTTCTAGAAGATCTCCTACAATATTCTCAGC
	10268	GGCCGCGTGTTACAACCAATGAAAGTGAAACGTGATTTCATGCGTC
	10283	GGATGGCTCGAGTTTTTCAGCAAGATTCCCTATCAGTGATAGAGATTGACATCCC
	10284	GCACGGATCTGAAAGAGGAGAAAGGATCTATGGCGAGTAGCGAAGACGTTATC
	10285	GTGTTGTTACCGTTACCCAGGACTCCTCCCTGCAAGACGGTGAGTTC
	10286	GCAACTAATGGTAAACTGACGCTGAAGTTCATCTGTACTACTGGTAAACTGCCGGT
	10287	TAAGCTGGAATACAATTTTAACAGCCACAATGTTTACATCACCGCCGATAAACAAAAAAATGG
L4 (69.4±1.6°C)	10244	GGGTGGGCCTTTCTGCGTTTATAATCTTTCTAGAAGATCTCCTACAATATTCTCAGC
	10268	GGCCGCGTGTTACAACCAATGAAAGTGAAACGTGATTTCATGCGTC
	10283	GGATGGCTCGAGTTTTTCAGCAAGATTCCCTATCAGTGATAGAGATTGACATCCC
	10284	GCACGGATCTGAAAGAGGAGAAAGGATCTATGGCGAGTAGCGAAGACGTTATC
	10285	GTGTTGTTACCGTTACCCAGGACTCCTCCCTGCAAGACGGTGAGTTC
	10286	GCAACTAATGGTAAACTGACGCTGAAGTTCATCTGTACTACTGGTAAACTGCCGGT
	10288	TAAGCTGGAATACAATTTTAACAGCCACAATGTTTACATCACCGCCGATAAACAAAAAAATG

bioRxiv preprint doi: https://doi.org/10.1101/510768; this version posted May 29, 2019. The copyright holder for this preprint (which was not certified by peer review) is the author/funder. All rights reserved. No reuse allowed without permission.

Supplementary Table 3: Oligonucleotides for crosstalk LCRs (continued).

Bridging Oligo Set (T_m per BO-half)	OligoID	Sequence (5'→3')
L5 (69.9±2.1°C)	10235	GGCCGCGTGTTACAACCAATGAAAGTGAAACGTGATTTCATGCGT
	10260	CGGATGGCTCGAGTTTTTCAGCAAGATTCCCTATCAGTGATAGAGATTGACATCCCTAT
	10261	CGGATCTGAAAGAGGAGAAAGGATCTATGGCGAGTAGCGAAGACGTTATC
	10262	TGGTGTTGTTACCGTTACCCAGGACTCCTCCCTGCAAGACGGTGAGTTC
	10263	GCAACTAATGGTAAACTGACGCTGAAGTTCATCTGTACTACTGGTAAACTGCCGGTTCCTT
	10264	TAAGCTGGAATACAATTTTAACAGCCACAATGTTTACATCACCGCCGATAAACAAA
	10265	GGGTGGGCCTTTCTGCGTTTATAATCTTTCTAGAAGATCTCCTACAATATTCTCAGCTGCC
L6 (70.0±1.7°C)	10259	GTGGTGTTGTTACCGTTACCCAGGACTCCTCCCTGCAAGACGGTGAGTT
	10266	CGGATGGCTCGAGTTTTTCAGCAAGATTCCCTATCAGTGATAGAGATTGACATCCCTA
	10267	CGGATCTGAAAGAGGAGAAAGGATCTATGGCGAGTAGCGAAGACGTT
	10268	GGCCGCGTGTTACAACCAATGAAAGTGAAACGTGATTTCATGCGTC
	10269	CAACTAATGGTAAACTGACGCTGAAGTTCATCTGTACTACTGGTAAACTGCCGGTT
	10270	GCCATAAGCTGGAATACAATTTTAACAGCCACAATGTTTACATCACCGCCGATAAACAAAAAAATG
	10271	TTCGGGTGGGCCTTTCTGCGTTTATAATCTTTCTAGAAGATCTCCTACAATATTCTCAGCT
High Crosstalk		
H1 (71.9±1.1°C)	10245	CGGATGGCTCGAGTTTTTCAGCAAGATTCCCTATCAGTGATAGAGATTGACATCCCTATCAGT
	10246	GCACGGATCTGAAAGAGGAGAAAGGATCTATGGCGAGTAGCGAAGACGTTATCAAAG
	10247	GTGGTGTTGTTACCGTTACCCAGGACTCCTCCCTGCAAGACGGTGAGT
	10248	GCGGCCGCGTGTTACAACCAATGAAAGTGAAACGTGATTTCATGCGTCATTTTGAACA
	10249	CAACTAATGGTAAACTGACGCTGAAGTTCATCTGTACTACTGGTAAACTGCCGGTTCCTT
	10250	GCCATAAGCTGGAATACAATTTTAACAGCCACAATGTTTACATCACCGCCGATAAACAAAAAAAT
	10251	TTCGGGTGGGCCTTTCTGCGTTTATAATCTTTCTAGAAGATCTCCTACAATATTCTCAGCTGCC
H2 (70.7±2.4°C)	10248	GCGGCCGCGTGTTACAACCAATGAAAGTGAAACGTGATTTCATGCGTCATTTTGAACA
	10252	ATGGCTCGAGTTTTTCAGCAAGATTCCCTATCAGTGATAGAGATTGACATCCCTATCAGT
	10253	AGCACGGATCTGAAAGAGGAGAAAGGATCTATGGCGAGTAGCGAAGACGTT
	10254	GTGGTGTTGTTACCGTTACCCAGGACTCCTCCCTGCAAGACGGTGAGTTC
	10255	AATGGTAAACTGACGCTGAAGTTCATCTGTACTACTGGTAAACTGCCGGTTCCTT
	10256	AAGCTGGAATACAATTTTAACAGCCACAATGTTTACATCACCGCCGATAAACAA
	10257	TTCGGGTGGGCCTTTCTGCGTTTATAATCTTTCTAGAAGATCTCCTACAATATTCTCAGCTG
H3 (70.3±2.3°C)	10248	GCGGCCGCGTGTTACAACCAATGAAAGTGAAACGTGATTTCATGCGTCATTTTGAACA
	10265	GGGTGGGCCTTTCTGCGTTTATAATCTTTCTAGAAGATCTCCTACAATATTCTCAGCTGCC
	10289	GATGGCTCGAGTTTTTCAGCAAGATTCCCTATCAGTGATAGAGATTGACATCCCTATCA
	10290	AGCACGGATCTGAAAGAGGAGAAAGGATCTATGGCGAGTAGCGAAGACGTTA
	10291	GTGGTGTTGTTACCGTTACCCAGGACTCCTCCCTGCAAGACGGTG
	10292	AATGGTAAACTGACGCTGAAGTTCATCTGTACTACTGGTAAACTGCCGGTTC
	10293	GCCATAAGCTGGAATACAATTTTAACAGCCACAATGTTTACATCACCGCCGATAAACA
H4 (70.5±2.2°C)	10248	GCGGCCGCGTGTTACAACCAATGAAAGTGAAACGTGATTTCATGCGTCATTTTGAACA
	10265	GGGTGGGCCTTTCTGCGTTTATAATCTTTCTAGAAGATCTCCTACAATATTCTCAGCTGCC
	10290	AGCACGGATCTGAAAGAGGAGAAAGGATCTATGGCGAGTAGCGAAGACGTTA

bioRxiv preprint doi: https://doi.org/10.1101/510768; this version posted May 29, 2019. The copyright holder for this preprint (which was not certified by peer review) is the author/funder. All rights reserved. No reuse allowed without permission.

Supplementary Table 3: Oligonucleotides for crosstalk LCRs (continued).

Bridging Oligo Set (T_m per BO-half)	**OligoID**	**Sequence (5'→3')**
	10291	GTGGTGTTGTTACCGTTACCCAGGACTCCTCCCTGCAAGACGGTG
	10292	AATGGTAAACTGACGCTGAAGTTCATCTGTACTACTGGTAAACTGCCGGTTC
	10293	GCCATAAGCTGGAATACAATTTTAACAGCCACAATGTTTACATCACCGCCGATAAACA
	10294	CGGATGGCTCGAGTTTTTCAGCAAGATTCCCTATCAGTGATAGAGATTGACATCCCTATCA
H5 (70.4±1.9°C)	10248	GCGGCCGCGTGTTACAACCAATGAAAGTGAAACGTGATTTCATGCGTCATTTTGAACA
	10272	TGGCTCGAGTTTTTCAGCAAGATTCCCTATCAGTGATAGAGATTGACATCCCTATCAGT
	10273	CACGGATCTGAAAGAGGAGAAAGGATCTATGGCGAGTAGCGAAGACGTTATCAAAGA
	10274	GTGTTGTTACCGTTACCCAGGACTCCTCCCTGCAAGACGGTGA
	10275	CAACTAATGGTAAACTGACGCTGAAGTTCATCTGTACTACTGGTAAACTGCCGGTTC
	10276	CATAAGCTGGAATACAATTTTAACAGCCACAATGTTTACATCACCGCCGATAAACAAAAAAATGG
	10277	CGGGTGGGCCTTTCTGCGTTTATAATCTTTCTAGAAGATCTCCTACAATATTCTCAGCTG
H6 (70.3±2.2°C)	10242	CAACTAATGGTAAACTGACGCTGAAGTTCATCTGTACTACTGGTAAACTGCCGG
	10248	GCGGCCGCGTGTTACAACCAATGAAAGTGAAACGTGATTTCATGCGTCATTTTGAACA
	10278	GATGGCTCGAGTTTTTCAGCAAGATTCCCTATCAGTGATAGAGATTGACATCCCTATCAGT
	10279	AGCACGGATCTGAAAGAGGAGAAAGGATCTATGGCGAGTAGCGAAGACGTTATCAA
	10280	GTGGTGTTGTTACCGTTACCCAGGACTCCTCCCTGCAAGACGGTGA
	10281	AGCTGGAATACAATTTTAACAGCCACAATGTTTACATCACCGCCGATAAACAA
	10282	TTCGGGTGGGCCTTTCTGCGTTTATAATCTTTCTAGAAGATCTCCTACAATATTCTCAGC

bioRxiv preprint doi: https://doi.org/10.1101/510768; this version posted May 29, 2019. The copyright holder for this preprint (which was not certified by peer review) is the author/funder. All rights reserved. No reuse allowed without permission.
main — 2019/5/22 — 19:03 — page 34 — #34

Supplementary Table 4: Bridging oligo sets for the gradient-LCR (composed of bridging oligos for crosstalk experiments; Supplementary Table 3). The results of the gradient-LCRs are shown in Figure 3A+B. All melting temperatures (T_ms) presented here are calculated for each BO-half using the formula of SantaLucia (20) for the T_m-calculation and the salt correction. T_m: melting temperature of a BO-half.

Bridging Oligo Set (T_m per BO-half)	**OligoID**	**Sequence (5'→3')**
67.8±0.5°C	10232	TGGCTCGAGTTTTTCAGCAAGATTCCCTATCAGTGATAGAGATTGACATCC
	10233	CGGATCTGAAAGAGGAGAAAGGATCTATGGCGAGTAGCGAAGACGT
	10234	GTGTTGTTACCGTTACCCAGGACTCCTCCCTGCAAGACGGTG
	10236	AATGGTAAACTGACGCTGAAGTTCATCTGTACTACTGGTAAACTGCCGG
	10244	GGGTGGGCCTTTCTGCGTTTATAATCTTTCTAGAAGATCTCCTACAATATTCTCAGC
	10268	GGCCGCGTGTTACAACCAATGAAAGTGAAACGTGATTTCATGCGTC
	10281	AGCTGGAATACAATTTTAACAGCCACAATGTTTACATCACCGCCGATAAACAA
69.9±1.3°C	10117	CCATAAGCTGGAATACAATTTTAACAGCCACAATGTTTACATCACCGCCGATAAACAAAAAAATG
	10118	CGGGTGGGCCTTTCTGCGTTTATAATCTTTCTAGAAGATCTCCTACAATATTCTCAGCTGC
	10240	ACGGATCTGAAAGAGGAGAAAGGATCTATGGCGAGTAGCGAAGACGTTATC
	10247	GTGGTGTTGTTACCGTTACCCAGGACTCCTCCCTGCAAGACGGTGAGT
	10268	GGCCGCGTGTTACAACCAATGAAAGTGAAACGTGATTTCATGCGTC
	10269	CAACTAATGGTAAACTGACGCTGAAGTTCATCTGTACTACTGGTAAACTGCCGGTT
	10283	GGATGGCTCGAGTTTTTCAGCAAGATTCCCTATCAGTGATAGAGATTGACATCCC
71.8±0.8°C	10116	GCAACTAATGGTAAACTGACGCTGAAGTTCATCTGTACTACTGGTAAACTGCCGGTTCC
	10117	CCATAAGCTGGAATACAATTTTAACAGCCACAATGTTTACATCACCGCCGATAAACAAAAAAATG
	10133	CGGATGGCTCGAGTTTTTCAGCAAGATTCCCTATCAGTGATAGAGATTGACATCCCTATCAG
	10134	GCACGGATCTGAAAGAGGAGAAAGGATCTATGGCGAGTAGCGAAGACGTTATCAAAG
	10248	GCGGCCGCGTGTTACAACCAATGAAAGTGAAACGTGATTTCATGCGTCATTTTGAACA
	10251	TTCGGGTGGGCCTTTCTGCGTTTATAATCTTTCTAGAAGATCTCCTACAATATTCTCAGCTGCC
	10259	GTGGTGTTGTTACCGTTACCCAGGACTCCTCCCTGCAAGACGGTGAGTT

bioRxiv preprint doi: https://doi.org/10.1101/510768; this version posted May 29, 2019. The copyright holder for this preprint (which was not certified by peer review) is the author/funder. All rights reserved. No reuse allowed without permission.

Supplementary Table 5: Bridging oligo sets with temperatures in the range of 62.0 °C to 67 °C. The results of the LCRs are shown in Figure 3C+D. All melting temperatures (T_ms) presented here are calculated for each BO-half using the formula of SantaLucia (20) for the T_m-calculation and the salt correction. T_m: melting temperature of a BO-half.

Bridging Oligo Set (T_m per BO-half)	**OligoID**	**Sequence (5'→3')**
62.0±0.9°C	10331	GGAATACAATTTTAACAGCCACAATGTTTACATCACCGCCG
	10333	GCTCGAGTTTTTCAGCAAGATTCCCTATCAGTGATAGAGATTGAC
	10334	ATCTGAAAGAGGAGAAAGGATCTATGGCGAGTAGCGAAGAC
	10335	TGTTACCGTTACCCAGGACTCCTCCCTGCAAGACG
	10336	CCGCGTGTTACAACCAATGAAAGTGAAACGTGATTTCATGC
	10337	AAACTGACGCTGAAGTTCATCTGTACTACTGGTAAACTGC
	10338	GGGCCTTTCTGCGTTTATAATCTTTCTAGAAGATCTCCTACAATAT
63.3±0.7°C	10333	GCTCGAGTTTTTCAGCAAGATTCCCTATCAGTGATAGAGATTGAC
	10336	CCGCGTGTTACAACCAATGAAAGTGAAACGTGATTTCATGC
	10339	GATCTGAAAGAGGAGAAAGGATCTATGGCGAGTAGCGAAGAC
	10340	GTTGTTACCGTTACCCAGGACTCCTCCCTGCAAGACGG
	10341	GTAAACTGACGCTGAAGTTCATCTGTACTACTGGTAAACTGCC
	10342	TGGAATACAATTTTAACAGCCACAATGTTTACATCACCGCCGATA
	10343	TGGGCCTTTCTGCGTTTATAATCTTTCTAGAAGATCTCCTACAATATTCT
65.1±0.6°C	10340	GTTGTTACCGTTACCCAGGACTCCTCCCTGCAAGACGG
	10344	GGCTCGAGTTTTTCAGCAAGATTCCCTATCAGTGATAGAGATTGACATC
	10345	GGATCTGAAAGAGGAGAAAGGATCTATGGCGAGTAGCGAAGACG
	10346	GCCGCGTGTTACAACCAATGAAAGTGAAACGTGATTTCATGCG
	10347	GGTAAACTGACGCTGAAGTTCATCTGTACTACTGGTAAACTGCCG
	10348	CTGGAATACAATTTTAACAGCCACAATGTTTACATCACCGCCGATAAA
	10349	GTGGGCCTTTCTGCGTTTATAATCTTTCTAGAAGATCTCCTACAATATTCTC
66.0±0.5°C	10344	GGCTCGAGTTTTTCAGCAAGATTCCCTATCAGTGATAGAGATTGACATC
	10345	GGATCTGAAAGAGGAGAAAGGATCTATGGCGAGTAGCGAAGACG
	10346	GCCGCGTGTTACAACCAATGAAAGTGAAACGTGATTTCATGCG
	10350	TGTTGTTACCGTTACCCAGGACTCCTCCCTGCAAGACGGT
	10351	TGGTAAACTGACGCTGAAGTTCATCTGTACTACTGGTAAACTGCCG
	10352	GCTGGAATACAATTTTAACAGCCACAATGTTTACATCACCGCCGATAAAC
	10353	GGTGGGCCTTTCTGCGTTTATAATCTTTCTAGAAGATCTCCTACAATATTCTCAG
67.3±0.6°C	10350	TGTTGTTACCGTTACCCAGGACTCCTCCCTGCAAGACGGT
	10353	GGTGGGCCTTTCTGCGTTTATAATCTTTCTAGAAGATCTCCTACAATATTCTCAG
	10354	ATGGCTCGAGTTTTTCAGCAAGATTCCCTATCAGTGATAGAGATTGACATCC
	10355	CGGATCTGAAAGAGGAGAAAGGATCTATGGCGAGTAGCGAAGACGT
	10356	GGCCGCGTGTTACAACCAATGAAAGTGAAACGTGATTTCATGCGTC
	10357	CTAATGGTAAACTGACGCTGAAGTTCATCTGTACTACTGGTAAACTGCCGG
	10358	GCTGGAATACAATTTTAACAGCCACAATGTTTACATCACCGCCGATAAACA

bioRxiv preprint doi: https://doi.org/10.1101/510768; this version posted May 29, 2019. The copyright holder for this preprint (which was not certified by peer review) is the author/funder. All rights reserved. No reuse allowed without permission.

Validation experiments

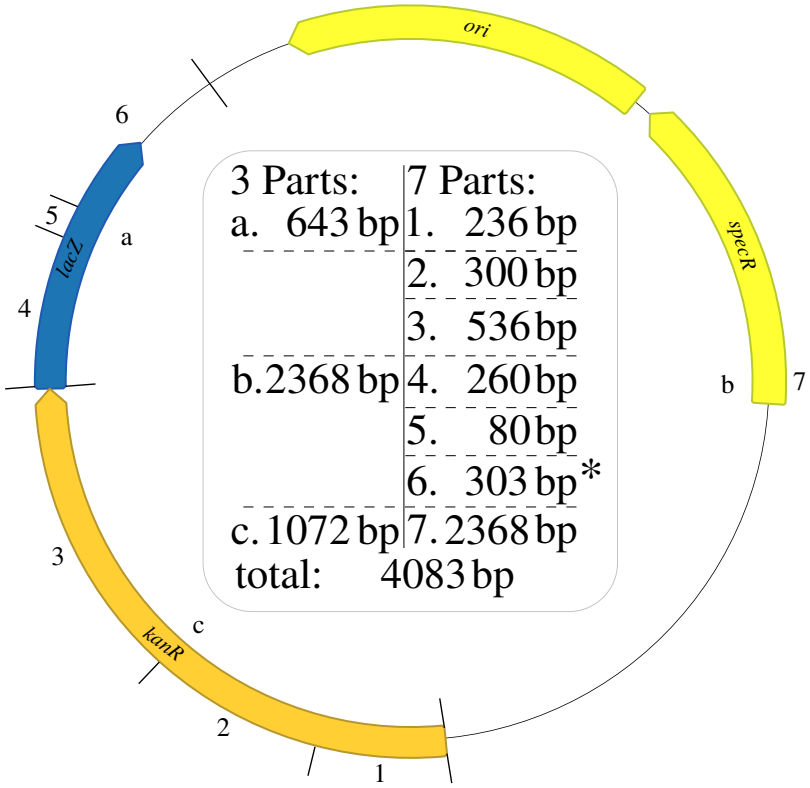

Supplementary Figure 18. Plasmid 1 ("VP1") for the validation experiments of the improved LCR conditions (Figure 4, Table 1). The plasmid was split in three and seven parts. Only if all parts were assembled the cells were able to replicate, were resistant to spectinomycin and turned blue by using the blue-white screening. Part 7 was PCR-amplified from the already existing plasmid build for scar-free deletions in *Bacillus subtilis* (41). The *lacZ* gene was inserted to enable a blue-white screening and was derived from the TALEN Kit 2.0 from Addgene (42). In comparison to the original flanking regions of the *lacZ* some mutations were present due to subcloning. *: Part 6 was amplified from the existing validation plasmid 2 ("VP2") shown in Supplementary Figure 19. The *kanR* gene was derived from (43). Before PCR-amplification, all templates were digested by restriction enzymes. Afterwards, all PCR-products were additionally digested by a DpnI-digestion. *lacZ*: β-galactosidase, *ori*: origin of replication, *specR*: spectinomycin resistance gene.

bioRxiv preprint doi: https://doi.org/10.1101/510768; this version posted May 29, 2019. The copyright holder for this preprint (which was not certified by peer review) is the author/funder. All rights reserved. No reuse allowed without permission.

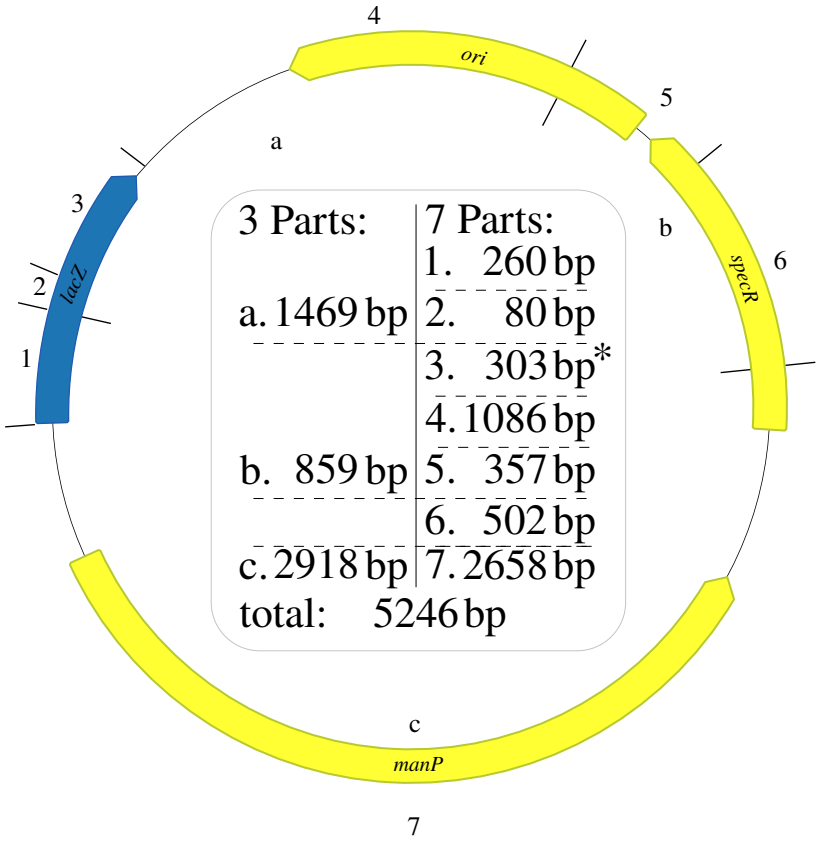

Supplementary Figure 19. Plasmid 2 ("VP2") for the validation experiments of the improved LCR conditions (Figure 4, Table 1). The plasmid was split in three and seven parts. Only if all parts were assembled the cells were able to replicate, were resistant to spectinomycin and kanamycin and turned blue by using blue-white screening. Parts 1-3 were derived by PCR-amplification of a plasmid from Wenzel et al. (41) and . Part 3 (*) begins in the *lacZ* of the plasmid derived from TALEN Kit 2.0 from Addgene (42) and ends in the plasmid derived from Wenzel et al. (41). Parts 4-7 were PCR-amplified from the already existing plasmid build for scar-free deletions in *Bacillus subtilis* (41). Before PCR-amplification, all templates were digested by restriction enzymes. Afterwards, all PCR-products were digested by DpnI. *lacZ*: β-galactosidase, *manP*: D-mannose permease (for *Bacillus* spp.), *ori*: origin of replication), *specR*: spectinomycin resistance gene.

bioRxiv preprint doi: https://doi.org/10.1101/510768; this version posted May 29, 2019. The copyright holder for this preprint (which was not certified by peer review) is the author/funder. All rights reserved. No reuse allowed without permission.

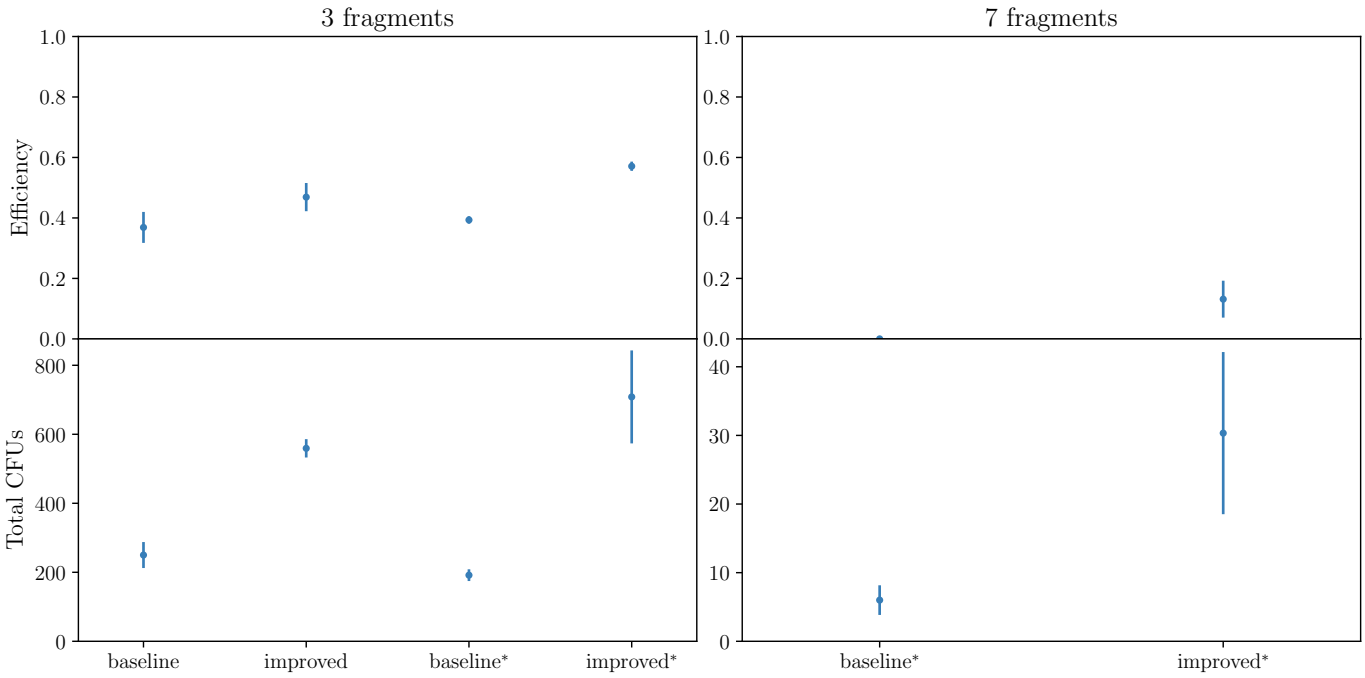

Supplementary Figure 20. Results of the baseline and improved LCR-protocol for the toy-model plasmid ("TP"). For the three-part split, the same LCRs were transformed in chemical and in * electrocompetent cells to prove that the results are independent of the transformation method. For the seven-part LCR only electroporation resulted in CFUs. For all LCRs, 3 µL were transformed in 30 µL cells. All LCRs were performed as triplicates. BO: bridging oligo, CFU: colony forming unit, DMSO: dimethyl sulfoxide, T_m: melting temperature of one BO-half.

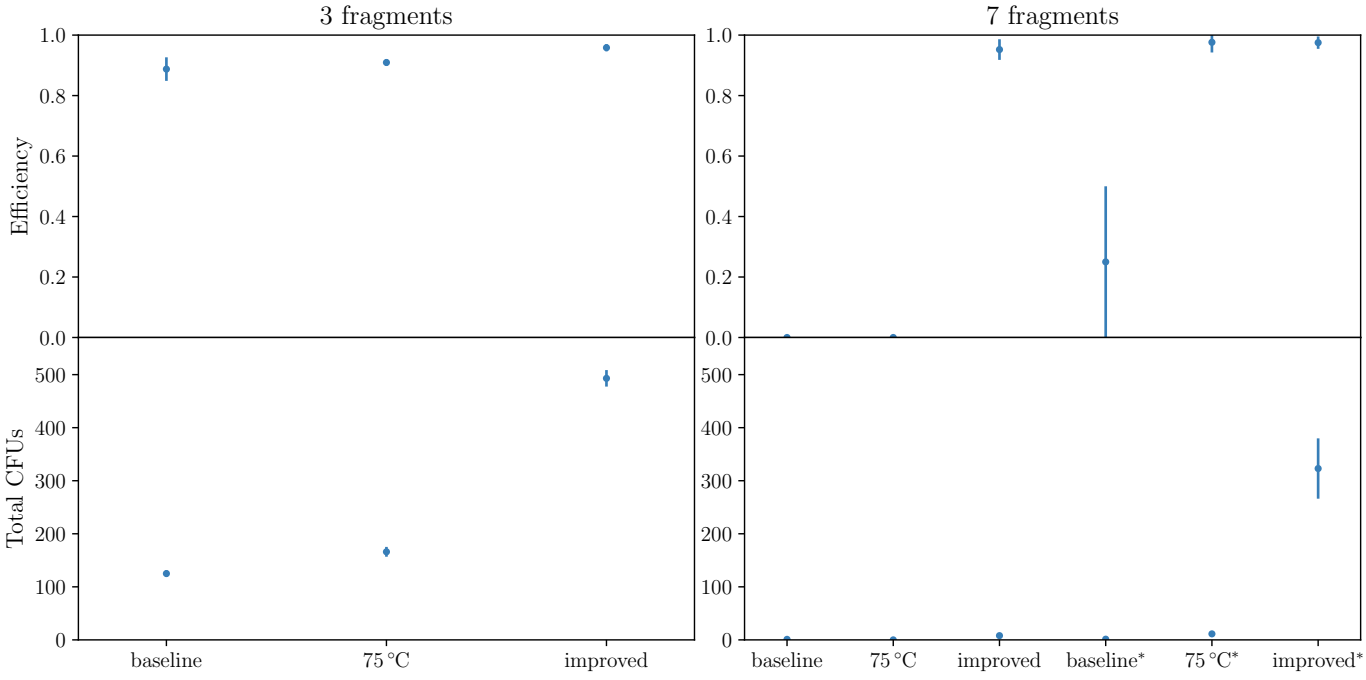

Supplementary Figure 21. Results of the baseline, 75 °C and improved LCR-protocol for the validation plasmid 1 ("VP1"). For the seven-part split the same LCRs were transformed in chemical cells and electrocompetent cells (indicated by an *) due to no CFUs for the baseline and 75 °C protocol when chemical transformation was used. For all LCRs, 3 µL were transformed in 30 µL cells. As a negative control, the LCR-mix without BOs and without Ampligase® was used and resulted in no colonies (not shown). All LCRs were performed as triplicates. CFU: colony forming unit.

bioRxiv preprint doi: https://doi.org/10.1101/510768; this version posted May 29, 2019. The copyright holder for this preprint (which was not certified by peer review) is the author/funder. All rights reserved. No reuse allowed without permission.

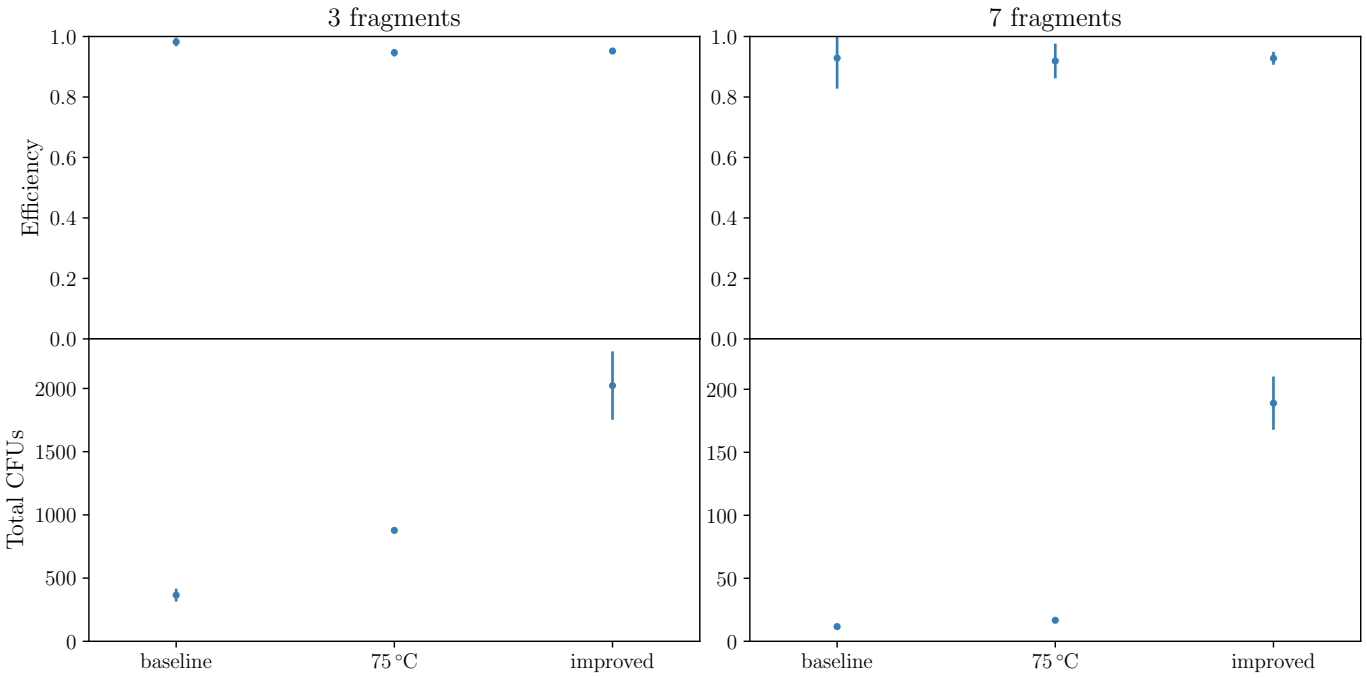

Supplementary Figure 22. Results of the baseline, 75 °C and improved LCR-protocol for the validation plasmid 2 ("VP2"). All LCRs were transformed in chemical competent cells. For this, 3 µL were transformed in 30 µL cells. As a negative control, the LCR mix without BOs and without Ampligase® were used and resulted in no colonies (not shown). All LCRs were performed as triplicates. BO: bridging oligo, CFU: colony forming unit.

bioRxiv preprint doi: https://doi.org/10.1101/510768; this version posted May 29, 2019. The copyright holder for this preprint (which was not certified by peer review) is the author/funder. All rights reserved. No reuse allowed without permission.

Step-by-step protocol for the ligase cycling reaction

Niels Schlichting, Felix Reinhardt, Sven Jager, Michael Schmidt, Johannes Kabisch

Correspondence: johannes@kabisch-lab.de

Abstract

The ligase cycling reaction (LCR) is a scarless and efficient method to assemble plasmids from fragments of DNA. This assembly method is based on the hybridization of DNA fragments with complementary oligonucleotides, so-called bridging oligos (BOs), and an experimental procedure of thermal denaturation, annealing and ligation. In this study, we explore the effect of molecular crosstalk of BOs and various experimental parameters on the LCR by utilizing a fluorescence-based screening system. The results indicate an impact of the melting temperatures of BOs on the overall success of the LCR assembly. Secondary structure inhibitors, such as DMSO and betaine, are shown to negatively impact the number of correctly assembled plasmids. Adjustments of the annealing, ligation and BO-melting temperature further improved the LCR. The optimized LCR was confirmed by validation experiments. Based on these findings, a step-by-step protocol is offered within this study to ensure a routine for high efficient LCR assemblies.

Reagents

- amplification of DNA fragments:
  - proof-reading polymerase, no T/A overhangs
  - phosphorylated primers for the amplification of DNA fragments (use T4-polynucleotide kinase (T4-PNK; New England Biolabs, Ipswich, USA) and T4-PNK buffer (10×) or order as synthetically modified oligos
- LCR:
  - Ampligase® thermostable DNA (Lucigen, Wisconsin, USA) ligase (Epicentre) and 10×-buffer
  - *aq. dest.*
  - competent cells

bioRxiv preprint doi: https://doi.org/10.1101/510768; this version posted May 29, 2019. The copyright holder for this preprint (which was not certified by peer review) is the author/funder. All rights reserved. No reuse allowed without permission.

Amplification of DNA fragments

- use phosphorylated amplification primers for the amplification of DNA fragments (inserts and backbone)
- phosphorylation of the amplification primers by T4-PNK (on ice):

  2 µL of 100 µM primer
  + 5 µL 10× T4-PNK buffer (1x)
  + 1 µL 10 000 U ml^{-1} T4-PNK (10 U)
  + 2 µL 100 mM ATP (4 mM)
  + 41.0 µL *aq. dest*/MilliQ

  $\sum$ 50 µL of 4 µM primer
- incubate for 1 h at 37 °C and 20 min at 65 °C
- use 6.25 µL of each phosphorylated amplification primer in a 50 µL PCR (primer concentration in PCR: 500 nM)[1,2]
- Recommended: DpnI digestion of all parts before the purification
- store parts at −20 °C; prepare aliquots for multiple usage of the same part (loss of function due to repeated freeze-thaw cycles [1, 2])

Bridging Oligo Design

For the LCRs the addition of DMSO/betaine is NOT recommended. The target-T_m of the BO design depends on the algorithms you are applying (1):

- SantaLucia 1998 (T_m calculation and salt correction [3])
  - target $T_m \approx 67.8$ °C

or

- SantaLucia 1998 (T_m calculation [3]) and Owczarzy 2008 (salt correction [4])
  - target $T_m \approx 65.2$ °C

or

- `Geneious` (www.geneious.com, [5]) utilizing `Primer3` [6]:
  - a Geneious-plugin for the design of bridging oligos is available at www.gitlab.com/kabischlab.de/lcr-publication-synthetic-biology

  to use Geneious without the plugin:

bioRxiv preprint doi: https://doi.org/10.1101/510768; this version posted May 29, 2019. The copyright holder for this preprint (which was not certified by peer review) is the author/funder. All rights reserved. No reuse allowed without permission.

- restrictions in adjusting parameters for DNA-part concentration (only "Oligo" can be adjusted)
- to get correct melting temperatures use 114 nM for the input of "Oligo"
- then use SantaLucia 1998 [3] for the T_m calculation and salt correction (Owczarzy 2008 [4] is not available for the calculations in `Geneious` versions$\leq$ 11.0.5)
- target $T_m \approx 67.8\,^{\circ}\mathrm{C}$

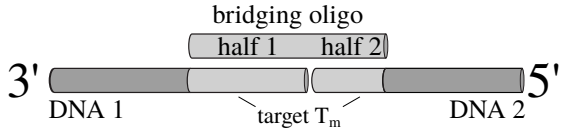

Figure 1: Scheme of the bridging oligo design. Half 1: 100% complementary to the 5-end of the first DNA part. Half 2: 100% complementary to the 3-end of the second DNA part.

Ligation

- use inserts:vector ratio of 10:1 (use 0.3 nM of the backbone) to reduce the background (religation of the backbone occurs due to the phosphorylation of all parts)
- for 25 µl (in brackets: final concentration):

  DNA inserts (3 nM of each fragment)
  + vector (0.3 nM)
  + 0.5 µL of each 1.5 µM bridging oligo (30 nM of each oligo)
  + 2.5 µL 10× Ampligase® buffer (includes 0.5 mM NAD^+)
  (+ 1.25 µL of 10 mM NAD^+ (0.5 mM))[3]
  + 1.5 µL of 5 U μL^{-1} Ampligase® (7.5 U)

  fill up with *aq. dest* to 25 µL
- use low-profile tubes or low-profile PCR plates (96-well) in a cycler for volumes of less than 10 µL
- for more than 25 cycles of small volumes ($\leq$ 10 µL): use 384-well plates
- start cycling (figure 2)

Initial denaturation :	94° C 2 min	
Denaturation :	94° C 10 s	25-50x
Annealing :	66° C 30 s	
Ligation :	66° C 1 min	
Hold :	10° C ∞	

Figure 2: Cycling parameters for the LCR.

bioRxiv preprint doi: https://doi.org/10.1101/510768; this version posted May 29, 2019. The copyright holder for this preprint (which was not certified by peer review) is the author/funder. All rights reserved. No reuse allowed without permission.

– store at -20 °C or directly use for transformation of chemically- or electrocompetent cells or use LCR-mix as template in a PCR (1 µl of 1:100 dilution works in general)

Notes

1. This is the recommended primer concentration for the Q5® High-Fidelity Polymerase (New England Biolabs, Ipswich, USA). Probably, the concentration has to be adjusted for your polymerase. For this please ask your supplier.
2. For some PCRs the sum of the forward and reverse primers 12.5 µL in a total PCR-volume of 50 µL can result in no product. In those cases, a dialysis of the phosphorylated primers for 20 min with *aq. dest.* and a floating membrane (Merck-Millipore™Membrane Filter, 0.025 µm; order-#: VSWP02500) is helpful.
3. Self-made 10×-buffer without NAD^+ is recommended. NAD^+ is sensitive to freeze-thaw cycles, long-term storage and light exposure. Prepare a stock solution of NAD^+ and store in aliquots at −80 °C up to 6 months. 10× Ampligase® buffer: 200 mM TRIS-HCl (pH 8.3), 250 mM KCl, 100 mM $MgCl_2$, 0.1% Triton X-100.

References

[1] Robinson, C. J., Dunstan, M. S., Swainston, N., Titchmarsh, J., Takano, E., Scrutton, N. S., and Jervis, A. J. (January, 2018) Chapter Thirteen - Multifragment DNA Assembly of Biochemical Pathways via Automated Ligase Cycling Reaction. In Scrutton, N., (ed.), *Methods in Enzymology*, Vol. 608 of Enzymes in synthetic biology, pp. 369–392 Academic Press.

[2] Davis, D. L., O'Brie, E. P., and Bentzley, C. M. (October, 2000) Analysis of the degradation of oligonucleotide strands during the freezing/thawing processes using MALDI-MS. *Analytical Chemistry,* **72**(20), 5092–5096.

[3] SantaLucia, J. (February, 1998) A unified view of polymer, dumbbell, and oligonucleotide DNA nearest-neighbor thermodynamics. *Proceedings of the National Academy of Sciences,* **95**(4), 1460–1465.

[4] Owczarzy, R., Moreira, B. G., You, Y., Behlke, M. A., and Walder, J. A. (May, 2008) Predicting stability of DNA duplexes in solutions containing magnesium and monovalent cations. *Biochemistry,* **47**(19), 5336–5353.

[5] Kearse, M., Moir, R., Wilson, A., Stones-Havas, S., Cheung, M., Sturrock, S., Buxton, S., Cooper, A., Markowitz, S., Duran, C., Thierer, T., Ashton, B., Meintjes, P., and Drummond, A. (June, 2012) Geneious basic: an integrated and extendable desktop software platform for the organization and analysis of sequence data. *Bioinformatics,* **28**(12), 1647–1649.

[6] Untergasser, A., Cutcutache, I., Koressaar, T., Ye, J., Faircloth, B. C., Remm, M., and Rozen, S. G. (August, 2012) Primer3-new capabilities and interfaces. *Nucleic Acids Research,* **40**(15), e115.

bioRxiv preprint doi: https://doi.org/10.1101/510768; this version posted May 29, 2019. The copyright holder for this preprint (which was not certified by peer review) is the author/funder. All rights reserved. No reuse allowed without permission.

Supplementary Table 6: Sequences of the seven-part split of the validation plasmid 1 (Supplementary Figure 18). For the three-part split parts 1-3, 4-6 and 7 were used. The bridging oligos were designed by concatenating subsequences of these parts. It was not necessary to use the reverse complement for the design because the experiments contained both strands of these parts. [1] Part 6 begins in the *lacZ* of a plasmid derived from the TALEN Kit 2.0 from Addgene (42) and ends in the plasmid derived from Wenzel et al. (41). *kanR*: kanamycin resistance gene, *lacZ*: β-galactosidase.

Validation Plasmid 1 Part	Size (bp)	Sequence (5'→3')
kanR (pMSE3, 43)		
part 1 (*kanR*-part 1)	236	GTCGATACTATGTTATACGCCAACTTTGAAAACAACTTTGAAAAAGCTGTTTTCTGGTATTTAA-GGTTTTAGAATGCAAGGAACAGTGAATTGGAGTTCGTCTTGTTATAATTAGCTTCTTGGGGTAT-CTTTAAATACTGTAGAAAAGAGGAAGGAAATAATAAATGGCTAAAATGAGAATATCACCGGA-ATTGAAAAAACTGATCGAAAAATACCGCTGCGTAAAAGATACGGAA
part 2 (*kanR*-part 2)	300	GGAATGTCTCCTGCTAAGGTATATAAGCTGGTGGGAGAAAATGAAAACCTATATTTAAAAATG-ACGGACAGCCGGTATAAAGGGACCACCTATGATGTGGAACGGGAAAAGGACATGATGCTATG-GCTGGAAGGAAAGCTGCCTGTTCCAAAGGTCCTGCACTTTGAACGGCATGATGGCTGGAGCAA-TCTGCTCATGAGTGAGGCCGATGGCGTCCTTTGCTCGGAAGAGTATGAAGATGAACAAAGCCC-TGAAAAGATTATCGAGCTGTATGCGGAGTGCATCAGGCTCTTTCACTCC
part 3 (*kanR*-part 3)	536	ATCGACATATCGGATTGTCCCTATACGAATAGCTTAGACAGCCGCTTAGCCGAATTGGATTACT-TACTGAATAACGATCTGGCCGATGTGGATTGCGAAAACTGGGAAGAAGACACTCCATTTAAAG-ATCCGCGCGAGCTGTATGATTTTTTAAAGACGGAAAAGCCCGAAGAGGAACTTGTCTTTTCCC-ACGGCGACCTGGGAGACAGCAACATCTTTGTGAAAGATGGCAAAGTAAGTGGCTTTATTGATC-TTGGGAGAAGCGGCAGGGCGGACAAGTGGTATGACATTGCCTTCTGCGTCCGGTCGATCAGGG-AGGATATCGGGGAAGAACAGTATGTCGAGCTATTTTTTGACTTACTGGGGATCAAGCCTGATT-GGGAGAAAATAAAATATTATATTTTACTGGATGAATTGTTTTAGTACCTAGATTTAGATGTCTA-AAAAGCCTGCAGTCGCGAGGCCTCGACGGATCCCCAAAGCACTTGCATAGGCTAATGCCTGGC-TTGGTTTTTCAGCTAAAATAACCGTACTCA
lacZ (pTAL3_His, Addgene: TALEN Kit 2.0)		
part 4 (*lacZ*-part 1)	260	CGCTGCACCGTTTCGAAGAGACCGCCGGTGGAGAGCGGGCAGTGAGCGCAACGCAATTAATG-TGAGTTAGCTCACTCATTAGGCACCCCAGGCTTTACACTTTATGCCTCCGGCTCGTATGTTGTG-TGGAATTGTGAGCGGATAACAATTTCACACAGGAAACAGCTATGACCATGATTACGCCAAGCG-CGCAATTAACCCTCACTAAAGGGAACAAAAGCTGGAGGACCTCGAGGGGGGGCCCGGTACCC-AATTCGCCC
part 5 (*lacZ*-part 2)	80	TATAGTGAGTCGTATTACGCGCGCTCACTGGCCGTCGTTTTACAACGTCGTGACTGGGAAAAC-CCTGGCGTTACCCAACT
part 6 (*lacZ*-part 3)[1]	303	TAATCGCCTTGCAGCACATCCCCCTTTCGCCAGCTGGCGTAATAGCGAAGAGGCCCGCACCGA-TCGCCCTTCCCAACAGTTGCGCAGCCTGAATGGCGAATGGGACGCGCCCTGTAGCGGCGCCGG-TCTCGATAGCCACCACTGATATCTTTCTAGAAGATCTCCTACAATATTCTCAGCTAGTGATTTTT-CTCTGGTCCCGCCGCATCCATACCGCCAGTTGTTTACCCTCACAACGTTCCAGTAACCGGGCAT-GTTCATCATCAGTAACCCGTATCGTGAGCATCCTCTCTCGTTTCATCG
Backbone (pJOE8739.1, 41)		

bioRxiv preprint doi: https://doi.org/10.1101/510768; this version posted May 29, 2019. The copyright holder for this preprint (which was not certified by peer review) is the author/funder. All rights reserved. No reuse allowed without permission.

Supplementary Table 6: Sequences of the validation plasmid 1 (continued)

Validation Plasmid 1 Part	Size (bp)	Sequence (5'→3')
part 7	2368	GTATCATTACCCCCATGAACAGAAATCCCCCTTACACGGAGGCATCAGTGACCAAACAGGAAA-AAACCGCCCTTAACATGGCCCGCTTTATCAGAAGCCAGACATTAACGCTTCTGGAGAAACTCA-ACGAGCTGGACGCGGATGAACAGGCAGACATCTGTGAATCGCTTCACGACCACGCTGATGAG-CTTTACCGCAGCTGCCTCGCGCGTTTCGGTGATGACGGTGAAAACCTCTGACACATGCAGCTCC-CGGAGACGGTCACAGCTTGTCTGTAAGCGGATGCCGGGAGCAGACAAGCCCGTCAGGGCGCG-TCAGCGGGTGTTGGCGGGTGTCGGGGCGCAGCCATGACCCAGTCACGTAGCGATAGCGGAGT-GTATACTGGCTTAACTATGCGGCATCAGAGCAGATTGTACTGAGAGTGCACCATATATGCGGT-GTGAAATACCGCACAGATGCGTAAGGAGAAAATACCGCATCAGGCGCTCTTCCGCTTCCTCGC-TCACTGACTCGCTGCGCTCGGTCGTTCGGCTGCGGCGAGCGGTATCAGCTCACTCAAAGGCGG-TAATACGGTTATCCACAGAATCAGGGGATAACGCAGGAAAGAACATGTGAGCAAAAGGCCAG-CAAAAGGCCAGGAACCGTAAAAAGGCCGCGTTGCTGGCGTTTTTCCATAGGCTCCGCCCCCCT-GACGAGCATCACAAAAATCGACGCTCAAGTCAGAGGTGGCGAAACCCGACAGGACTATAAAG-ATACCAGGCGTTTCCCCCTGGAAGCTCCCTCGTGCGCTCTCCTGTTCCGACCCTGCCGCTTACC-GGATACCTGTCCGCCTTTCTCCCTTCGGGAAGCGTGGCGCTTTCTCATAGCTCACGCTGTAGGT-ATCTCAGTTCGGTGTAGGTCGTTCGCTCCAAGCTGGGCTGTGTGCACGAACCCCCCGTTCAGCC-CGACCGCTGCGCCTTATCCGGTAACTATCGTCTTGAGTCCAACCCGGTAAGACACGACTTATCG-CCACTGGCAGCAGCCACTGGTAACAGGATTAGCAGAGCGAGGTATGTAGGCGGTGCTACAGA-GTTCTTGAAGTGGTGGCCTAACTACGGCTACACTAGAAGGACAGTATTTGGTATCTGCGCTCTG-CTGAAGCCAGTTACCTTCGGAAAAAGAGTTGGTAGCTCTTGATCCGGCAAACAAACCACCGCT-GGTAGCGGTGGTTTTTTTGTTTGCAAGCAGCAGATTACGCGCAGAAAAAAAGGATCTCAAGAA-GATCCTTTGATCTTTTCTACGGGGTTTAAACGTGTTTCCACCATTTTTTCAATTTTTTTATAATTT-TTTTAATCTGTTATTTAAATAGTTTATAGTTAAATTTACATTTTCATTAGTCCATTCAATATTCT-CTCCAAGATAACTACGAACTGCTAACAAAATTCTCTCCCTATGTTCTAATGGAGAAGATTCAG-CCACTGCATTTCCCGCAATATCTTTTGGTATGATTTTACCCGTGTCCATAGTTAAAATCATACG-GCATAAAGTTAATATAGAGTTGGTTTCATCATCCTGATAATTATCTATTAATTCCTCTGACGAA-TCCATAATGGCTCTTCTCACATCAGAAAATGGAATATCAGGTAGTAATTCCTCTAAGTCATAAT-TTCCGTATATTCTTTTATTTTTTCGTTTTGCTTGGTAAAGCATTATGGTTAAATCTGAATTTAATT-CCTTCTGAGGAATGTATCCTTGTTCATAAAGCTCTTGTAACCATTCTCCATAAATAAATTCTTGT-TTGGGAGGATGATTCCACGGTACCATTTCTTGCTGAATAATAATTGTTAATTCAATATATCGTA-AGTTGCTTTTATCTCCTATTTTTTTTGAAATAGGTCTAATTTTTTGTATAAGTATTTCTTTACTTT-GATCTGTCAATGGTTCAGATACGACGACTAAAAAGTCAAGATCACTATTTGGTTTTAGTCCACT-CTCAACTCCTGATCCAAACATGTAAGTACCAATAAGGTTATTTTTTAAATGTTTCCGAAGTATT-TTTTTCACTTTATTAATTTGTTCGTATGTATTCAAATATATCCTCCTCACTATTTTGATTAGTACC-TATTTTATATCCATAGTTGTTAATTAAATAAACTTAATTTAGTTTATTTATAGATTTCATTGGCT-TCTAAATTTTTTATCTAGATAATAATTATTTTAGTTAATTTTATTCTAGATTATATATGATATGA-TCTTTCATTTCCATAAAACTAAAGTAAGTGTAAACCTATTCATTGTTTTAAAAATATCTCTTGCC-AGTCACGTTACGTTATTAGTTATAGTTATTATAACATGTATTCACGAACGAAAATCGCCATTCG-CCAGGGGT

bioRxiv preprint doi: https://doi.org/10.1101/510768; this version posted May 29, 2019. The copyright holder for this preprint (which was not certified by peer review) is the author/funder. All rights reserved. No reuse allowed without permission.

Supplementary Table 7: Oligonucleotides for the amplification of all validation plasmid 1 parts (shown in Supplementary Figure 18 and Supplementary Table 6). For the amplification of the parts of the three-part split the oligonucleotides of parts 1 (fw)+3 (rv), 4 (fw)+6 (rv) and 7 (fw and rv) were used. [1] The complete part was ordered as two oligonucleotides, which were phosphorylated and annealed to double stranded DNA before the LCR (described in the methods). [2] Part 6 begins in the *lacZ* of the plasmid derived from the TALEN Kit 2.0 from Addgene (42) and ends in the plasmid derived from Wenzel et al. (41). [3] For sequencing from the vector into the inserts. fw: forward direction, *kanR*: kanamycin resistance gene, *lacZ*: β-galactosidase, rv: reverse direction.

Part	**OligoID**	**Sequence (5'→3')**
kanR (pMSE3, 43)		
part 1 (*kanR*-part 1)	10404-fw	GTCGATACTATGTTATACGCCAAC
	10407-rv	TTCCGTATCTTTTACGCAGC
part 2 (*kanR*-part 2)	10408-fw	GGAATGTCTCCTGCTAAGG
	10409-rv	GGAGTGAAAGAGCCTGATG
part 3 (*kanR*-part 3)	10410-fw	ATCGACATATCGGATTGTCC
	10433-rv	TGAGTACGGTTATTTTAGCTGAAAAACCAAGCCAGGCATTAGC
lacZ (pTAL3_His, Addgene: TALEN Kit 2.0)		
part 4 (*lacZ*-part 1)	10185-fw	CGCTGCACCGTTTCGAAG
	10382-rv	GGGCGAATTGGGTACCG
part 5 (*lacZ*-part 2)[1]	10387-fw	TATAGTGAGTCGTATTACGCGCGCTCACTGGCCGTCGTTTTACAACGTCGTGACTGGGAAAAC-CCTGGCGTTACCCAACT
	10388-rv	AGTTGGGTAACGCCAGGGTTTTCCCAGTCACGACGTTGTAAAACGACGGCCAGTGAGCGCGCG-TAATACGACTCACTATA
part 6 (*lacZ*-part 3)[2]	10187-fw	TAATCGCCTTGCAGCACATC
	10383-rv	CGATGAAACGAGAGAGGATG
Backbone (pJOE8739.1, 41)		
part 7	10384-fw	GTATCATTACCCCCATGAACAG
	10406-rv	ACCCCTGGCGAATGGC
Sequencing primers[3]		
forward	10419-fw	CTTGCCAGTCACGTTACG
reverse	10420-rv	CCTGTTTGGTCACTGATGCC

bioRxiv preprint doi: https://doi.org/10.1101/510768; this version posted May 29, 2019. The copyright holder for this preprint (which was not certified by peer review) is the author/funder. All rights reserved. No reuse allowed without permission.
main — 2019/5/22 — 19:03 — page 47 — #47

Supplementary Table 8: Sequences of the seven-part split of the validation plasmid 2 (Supplementary Figure 19). For the three-part split parts 2-4, 5+6 and 7+1 were used. The bridging oligos were designed by concatenating subsequences of these parts. It was not necessary to use the reverse complement for the design because the experiments contained both strands of these parts. [1] Part 3 begins in the *lacZ* of the plasmid derived from the TALEN Kit 2.0 from Addgene (42) and ends in the plasmid derived from Wenzel et al. (41). *kanR*: kanamycin resistance gene, *lacZ*: β-galactosidase.

Validation Plasmid 2 Part	Size (bp)	Sequence (5'→3')
lacZ (pTAL3_His, Addgene: TALEN Kit 2.0)		
part 1 (*lacZ*-part 1)	260	CGCTGCACCGTTTCGAAGAGACCGCCGGTGGAGAGCGGGCAGTGAGCGCAACGCAATTAATG-TGAGTTAGCTCACTCATTAGGCACCCCAGGCTTTACACTTTATGCCTCCGGCTCGTATGTTGTG-TGGAATTGTGAGCGGATAACAATTTCACACAGGAAACAGCTATGACCATGATTACGCCAAGCG-CGCAATTAACCCTCACTAAAGGGAACAAAAGCTGGAGGACCTCGAGGGGGGGCCCGGTACCC-AATTCGCCC
part 2 (*lacZ*-part 2)	80	TATAGTGAGTCGTATTACGCGCGCTCACTGGCCGTCGTTTTACAACGTCGTGACTGGGAAAAC-CCTGGCGTTACCCAACT
part 3 (*lacZ*-part 3)[1]	303	TAATCGCCTTGCAGCACATCCCCCTTTCGCCAGCTGGCGTAATAGCGAAGAGGCCCGCACCGA-TCGCCCTTCCCAACAGTTGCGCAGCCTGAATGGCGAATGGGACGCGCCCTGTAGCGGCGCCGG-TCTCGATAGCCACCACTGATATCTTTCTAGAAGATCTCCTACAATATTCTCAGCTAGTGATTTTT-CTCTGGTCCCGCCGCATCCATACCGCCAGTTGTTTACCCTCACAACGTTCCAGTAACCGGGCAT-GTTCATCATCAGTAACCCGTATCGTGAGCATCCTCTCTCGTTTCATCG
Backbone (pJOE8739.1, 41)		
part 4 (*ori*-part 1)	1086	GTATCATTACCCCCATGAACAGAAATCCCCCTTACACGGAGGCATCAGTGACCAAACAGGAAA-AAACCGCCCTTAACATGGCCCGCTTTATCAGAAGCCAGACATTAACGCTTCTGGAGAAACTCA-ACGAGCTGGACGCGGATGAACAGGCAGACATCTGTGAATCGCTTCACGACCACGCTGATGAG-CTTTACCGCAGCTGCCTCGCGCGTTTCGGTGATGACGGTGAAAACCTCTGACACATGCAGCTCC-CGGAGACGGTCACAGCTTGTCTGTAAGCGGATGCCGGGAGCAGACAAGCCCGTCAGGGCGCG-TCAGCGGGTGTTGGCGGGTGTCGGGGCGCAGCCATGACCCAGTCACGTAGCGATAGCGGAGT-GTATACTGGCTTAACTATGCGGCATCAGAGCAGATTGTACTGAGAGTGCACCATATATGCGGT-GTGAAATACCGCACAGATGCGTAAGGAGAAAATACCGCATCAGGCGCTCTTCCGCTTCCTCGC-TCACTGACTCGCTGCGCTCGGTCGTTCGGCTGCGGCGAGCGGTATCAGCTCACTCAAAGGCGG-TAATACGGTTATCCACAGAATCAGGGGATAACGCAGGAAAGAACATGTGAGCAAAAGGCCAG-CAAAAGGCCAGGAACCGTAAAAAGGCCGCGTTGCTGGCGTTTTTCCATAGGCTCCGCCCCCCT-GACGAGCATCACAAAAATCGACGCTCAAGTCAGAGGTGGCGAAACCCGACAGGACTATAAAG-ATACCAGGCGTTTCCCCCTGGAAGCTCCCTCGTGCGCTCTCCTGTTCCGACCCTGCCGCTTACC-GGATACCTGTCCGCCTTTCTCCCTTCGGGAAGCGTGGCGCTTTCTCATAGCTCACGCTGTAGGT-ATCTCAGTTCGGTGTAGGTCGTTCGCTCCAAGCTGGGCTGTGTGCACGAACCCCCCGTTCAGCC-CGACCGCTGCGCCTTATCCGGTAACTATCGTCTTGAGTCCAACCCGGTAAGACACGACTTATCG-CCACTGGCAGCAGCCACTGGTAACAGGATTAGCAGAGCGAGGTATGTAGGCGGTGCTACAGA-GTTCTTGAAGTGGTGG
part 5 (*ori*-part 2+*specR*-part 1)	357	CCTAACTACGGCTACACTAGAAGGACAGTATTTGGTATCTGCGCTCTGCTGAAGCCAGTTACCT-TCGGAAAAAGAGTTGGTAGCTCTTGATCCGGCAAACAAACCACCGCTGGTAGCGGTGGTTTTT-TTGTTTGCAAGCAGCAGATTACGCGCAGAAAAAAAGGATCTCAAGAAGATCCTTTGATCTTTT-CTACGGGGTTTAAACGTGTTTCCACCATTTTTTCAATTTTTTTTATAATTTTTTTAATCTGTTATTT-AAATAGTTTATAGTTAAATTTACATTTTCATTAGTCCATTCAATATTCTCTCCAAGATAACTAC-GAACTGCTAACAAAATTCTCTCCCTATGTTCTAATGG
part 6 (*specR*-part 2)	502	AGAAGATTCAGCCACTGCATTTCCCGCAATATCTTTTGGTATGATTTTACCCGTGTCCATAGTT-AAAATCATACGGCATAAAGTTAATATAGAGTTGGTTTCATCATCCTGATAATTATCTATTAATT-CCTCTGACGAATCCATAATGGCTCTTCTCACATCAGAAAATGGAATATCAGGTAGTAATTCCTC-TAAGTCATAATTTCCGTATATTCTTTTATTTTTTCGTTTTGCTTGGTAAAGCATTATGGTTAAAT-CTGAATTTAATTCCTTCTGAGGAATGTATCCTTGTTCATAAAGCTCTTGTAACCATTCTCCATAA-ATAAATTCTTGTTTGGGAGGATGATTCCACGGTACCATTTCTTGCTGAATAATAATTGTTAATT-CAATATATCGTAAGTTGCTTTTATCTCCTATTTTTTTTGAAATAGGTCTAATTTTTTGTATAAGT-ATTTCTTTACTTTGATCTGTCAATGGTTCAGATACGACGACTAAAAAGTCA

bioRxiv preprint doi: https://doi.org/10.1101/510768; this version posted May 29, 2019. The copyright holder for this preprint (which was not certified by peer review) is the author/funder. All rights reserved. No reuse allowed without permission.

Supplementary Table 8: Sequences of the validation plasmid 2 (continued)

Validation Plasmid 2 Part	Size (bp)	Sequence (5'→3')
part 7 (*specR*-part 3+*manP*)	2658	AGATCACTATTTGGTTTTAGTCCACTCTCAACTCCTGATCCAAACATGTAAGTACCAATAAGGT- TATTTTTTAAATGTTTCCGAAGTATTTTTTTCACTTTATTAATTTGTTCGTATGTATTCAAATATA- TCCTCCTCACTATTTTGATTAGTACCTATTTTATATCCATAGTTGTTAATTAAATAAACTTAATT- TAGTTTATTTATAGATTTCATTGGCTTCTAAATTTTTTATCTAGATAATAATTATTTTAGTTAAT- TTTATTCTAGATTATATATGATATGATCTTTCATTTCCATAAAACTAAAGTAAGTGTAAACCTA- TTCATTGTTTTAAAAATATCTCTTGCCAGTCACGTTACGTTATTAGTTATAGTTATTATAACATG- TATTCACGAACGAAAATCGCCATTCGCCAGGGGTTTAATTGCGTCGAGACCCCTGTGGGTCTC- GTTTTTTGGATCACCGGTATGGCGCCATATGCTTTATTCGATTTCTTCTAGCAGCTTGTATGCTT- CTTCTGTTGTTTGCACGGAGAGCAGCCGCTCCCTATAATTGTCATCCATTAGCTTTCGAGATAG- CATCTGCAGTATTTTGAGATGCTGGTTTCCCCCGCTCTCTTTCGGTACAGCAATCATAAAGATT- AATTTAGCTTCTGATCCATCCAGGCTATTCCAATCAACGCCTGATCGTTTGATCCCAAAGGCAA- CACTCGGCTCCCTGACCGCCTCAGACTTTCCGTGCGGAATCGCGATATTCATGCCAATCGCCGT- TGTTCCCTGTTGTTCACGATTCAAAATGGCTTGTTTAAACCCGCTCTCTGAAAGCAGCGCACCT- CTTCGTGACAATTTCTGAATCAATTCATCTATGATGTCATCACTCGTTTCCCCCGATAAATTTGG- TTCAATTAATTCCGGGCTGATAATGTCTGTCAGTTTTTTAAATTCCGACATCTCAGCTTTTTGGC- TTTGAATTGGCTGCTTTATTTCATTTGCTGCCGCAGCTTCACTTGGCGCGGAGGTCGGTGCAGT- TTCACTGAGCACAGGAGACGCCGTAATATCCTTTTTTAGTACATTGACGAACAGAGCAGTGAC- AAGAGATCCTGCAATCACAGCAATAAAAAACATCAAGACATGATCAACTGCGCCAAGCACTG- CAACGATAGGTCCGCCGTGCGCCACTCTGTCTCCCACATTGCCAATCATGGCTATCACAGAAC- CTGTCATTGAGCCTGCCATAATACTTGGAATAACGCGCAGAGGGTCCTGCGCCGCAAATGGAA- TCGCTCCTTCAGTAATGCCGAAGAGCCCCATCGTAAATGCCGCTTTCCCCATTTCTCTTTGAGA- TGCCTCGAATTTTCTTTTTCCTAAAAACGTCGCAATGCCAAGGCCAATCGGGGGGATACAAAT- GGCGACAGCAATTGGTCCCATAATTTCATAATTTCCTTCTCCAATCATTGCCGATCCAAACAGA- AACGCCACCTTATTTACGGGACCGCCCATATCAAATGAGATCATCGCCCCTAAAATCAATGCC- AGAAGGATCGAGCTCGACCCTTTCATCCCCGCCAGCCAAACTGTTAAAGAGGCGAAAATTTGA- GCTACAGGCGCGCCGATCAAAAACACAAACGCTAAACCTACAATCAGTGATGCAAACACCGG- AATAATAATAATCGGCATAATCGGCTGGATGGCTTTTGGAACTTTTAATTTTTTGATCCAAAGT- GCCGCGTATCCGGCCAAAAACCCGGCAATAATCCCCCCGAGGAATCCGGCGCCGCTTGCGCTG- TCATAAAAACTTCCAGTCGCCGCAATATAACCGCCGATCATACCTGGCACAAGCCCCGGTTTA- TCAGCGATGCTATAGGCGATATAGCCGGCTAAAATCGGAATCATAAATGAAAATGAAGCACT- GCCGATCTGTTCAATCGTTTTCCAGAAGGAATCATCCGGAATAACTAAGCCTTTAGGTGTTTTC- TCCCCTCCAAGCGTTAATGCAACCGCTATCAATAATCCGCCGACAACAATGAAAGGAACCATA- AATGAAACGCCGTTCATTAAATGACGGTAAATTGGATTTTGTTTCTTCTCCTGATGATTACCGG- ATTCCGATTTTGTAGCGGAACGATAGACCGGTATATCCCCGTTAAGAGCTTTTTGAATCAATTC- TTCCGGTTTGCGGATACCGTCCTGTACCCCCACAGACAGCAGTTTTTTGCCTATAAACCGGTCT- TTGTTTACCGAACGGTCTGCAGCAATAATGATTGCGTCCGCTTCGCGAATTTCCTCTTCGGTTA- GCTTATTTTCAACACCAATCCCTCCCTGGGTCTCAACTTTGATGCTAACGCCCAGTCTGTCAGC- AGCTTTTTGCAGATTTTCTGCTGCCATATACGTATGGGCGATTCCATTCGGACAAGATGTAATC- GCTAACAGTTTCATAGGAAACCTCCTTTAAAGTGTGAATAATAAGATCTTGTCTCAACTGTATA- CCGAAATCAGCTCATTAAAATCGCTTTTTTTACCATAGGTTCCGGTAATAAAGGCATTTTTCCC- ATATGGCGATTAAGTTGGGTAACGCCAGGGTTTTCCCAGTCACGACGTTGTAAAACGACGGCC- AGTGCAGATCTTCCGGATGGCTCGAGTTTTTCAGCAAGATATC

bioRxiv preprint doi: https://doi.org/10.1101/510768; this version posted May 29, 2019. The copyright holder for this preprint (which was not certified by peer review) is the author/funder. All rights reserved. No reuse allowed without permission.
main — 2019/5/22 — 19:03 — page 49 — #49

Supplementary Table 9: Oligonucleotides for the amplification of all validation plasmid 2 parts (shown in Supplementary Figure 19 and Supplementary Table 9). For the amplification of the parts of the three-part split the oligonucleotides of parts 2 (fw)+4 (rv), 5 (fw)+6 (rv) and 7 (fw)+1 (rv) were used. [1] The complete part was ordered as two oligonucleotides, which were phosphorylated and annealed to double stranded DNA before the LCR (described in the methods). [2] Part 3 begins in the *lacZ* of the plasmid derived from the TALEN Kit 2.0 from Addgene (42) and ends in the plasmid derived from Wenzel et al. (41). [3] For sequencing from the vector into the inserts. fw: forward direction, *ori*: origin of replication, *lacZ*: β-galactosidase, rv: reverse direction, *specR*: spectinomycin resistance gene.

Part	**OligoID**	**Sequence (5'→3')**
lacZ (pTAL3_His, Addgene: TALEN Kit 2.0)		
part 1 (*lacZ*-part 1)	10185-fw	CGCTGCACCGTTTCGAAG
	10382-rv	GGGCGAATTGGGTACCG
part 2 (*lacZ*-part 2)[1]	10387-fw	TATAGTGAGTCGTATTACGCGCGCTCACTGGCCGTCGTTTTACAACGTCGTGACTGGGAAAAC-CCTGGCGTTACCCAACT
	10388-rv	AGTTGGGTAACGCCAGGGTTTTCCCAGTCACGACGTTGTAAAACGACGGCCAGTGAGCGCGCG-TAATACGACTCACTATA
part 3 (*lacZ*-part 3)[2]	10187-fw	TAATCGCCTTGCAGCACATC
	10383-rv	CGATGAAACGAGAGAGGATG
Backbone (pJOE8739.1, 41)		
part 4 (ori-part 1)	10384-fw	GTATCATTACCCCCATGAACAG
	11313-rv	CCACCACTTCAAGAACTCTGTAG
part 5 (*ori*-part 2+*specR*-part 1)	11315-fw	CCTAACTACGGCTACACTAGAAGG
	11308-rv	CCATTAGAACATAGGGAGAGAATTTTG
part 6 (*specR*-part 2)	10385-fw	AGAAGATTCAGCCACTGCATTTC
	10389-rv	TGACTTTTTAGTCGTCGTATCTG
part 7 (*specR*-part 3+*manP*)	10381-fw	AGATCACTATTTGGTTTTAGTCCAC
	10386-rv	GATATCTTGCTGAAAAACTCGAGC
Sequencing primers[3]		
forward	11253	GCAGAGCGAGGTATGTAGG
reverse	10420	CCTGTTTGGTCACTGATGCC

bioRxiv preprint doi: https://doi.org/10.1101/510768; this version posted May 29, 2019. The copyright holder for this preprint (which was not certified by peer review) is the author/funder. All rights reserved. No reuse allowed without permission.

Supplementary Table 10: Bridging oligonucleotides for the assembly of the three-part and seven-part toy-plasmid consisting of *mRFP1*, *sfGFP* and pJET1.2/blunt by using the baseline and improved protocol (results and protocols shown in Figure 4). The BO-set for the baseline LCR consists of BOs of the manual set shown in Supplementary Table 3. The BO-set for the improved LCR consists of BOs of the "67.8 °C"-set of the gradient-LCR (Supplementary Table 4). All melting temperatures (T_ms) presented here are calculated for each BO-half using the formula of SantaLucia (20) for the T_m-calculation and the salt correction. [1] Bridging oligos with a target T$_m$ of 70.0 °C for each half, with 8 %v/v DMSO and 0.45 M betaine and the experimental annealing temperature of 55 °C. [2] Bridging oligos with a target T$_m$ of 67.8 °C for each half, without DMSO and betaine and the experimental annealing temperature of 66 °C. T_m: melting temperature of a BO-half.

Bridging Oligo Set (T_m per BO-half)	**OligoID**	**Sequence (5'→3')**
Three-part split		
Baseline (71.4±0.6°C)[1]	10133	CGGATGGCTCGAGTTTTTCAGCAAGATTCCCTATCAGTGATAGAGATTGACATCCCTATCAG
	10137	CGGCCGCGTGTTACAACCAATGAAAGTGAAACGTGATTTCATGCGTCATTTTGAAC
	10118	CGGGTGGGCCTTTCTGCGTTTATAATCTTTCTAGAAGATCTCCTACAATATTCTCAGCTGC
Improved (67.9±0.7°C)[2]	10232	TGGCTCGAGTTTTTCAGCAAGATTCCCTATCAGTGATAGAGATTGACATCC
	10244	GGGTGGGCCTTTCTGCGTTTATAATCTTTCTAGAAGATCTCCTACAATATTCTCAGC
	10268	GGCCGCGTGTTACAACCAATGAAAGTGAAACGTGATTTCATGCGTC
Seven-part split		
Baseline (71.4±0.7°C)[1]	10133	CGGATGGCTCGAGTTTTTCAGCAAGATTCCCTATCAGTGATAGAGATTGACATCCCTATCAG
	10134	GCACGGATCTGAAAGAGGAGAAAGGATCTATGGCGAGTAGCGAAGACGTTATCAAAG
	10135	GTGGTGTTGTTACCGTTACCCAGGACTCCTCCCTGCAAGACGGTGAGTTC
	10137	CGGCCGCGTGTTACAACCAATGAAAGTGAAACGTGATTTCATGCGTCATTTTGAAC
	10116	GCAACTAATGGTAAACTGACGCTGAAGTTCATCTGTACTACTGGTAAACTGCCGGTTCC
	10117	CCATAAGCTGGAATACAATTTTAACAGCCACAATGTTTACATCACCGCCGATAAACAAAAAAATG
	10118	CGGGTGGGCCTTTCTGCGTTTATAATCTTTCTAGAAGATCTCCTACAATATTCTCAGCTGC
Improved (67.8±0.5°C)[2]	10232	TGGCTCGAGTTTTTCAGCAAGATTCCCTATCAGTGATAGAGATTGACATCC
	10233	CGGATCTGAAAGAGGAGAAAGGATCTATGGCGAGTAGCGAAGACGT
	10234	GTGTTGTTACCGTTACCCAGGACTCCTCCCTGCAAGACGGTG
	10236	AATGGTAAACTGACGCTGAAGTTCATCTGTACTACTGGTAAACTGCCGG
	10244	GGGTGGGCCTTTCTGCGTTTATAATCTTTCTAGAAGATCTCCTACAATATTCTCAGC
	10268	GGCCGCGTGTTACAACCAATGAAAGTGAAACGTGATTTCATGCGTC
	10281	AGCTGGAATACAATTTTAACAGCCACAATGTTTACATCACCGCCGATAAACAA

bioRxiv preprint doi: https://doi.org/10.1101/510768; this version posted May 29, 2019. The copyright holder for this preprint (which was not certified by peer review) is the author/funder. All rights reserved. No reuse allowed without permission.

Supplementary Table 11: Bridging oligos for the assembly of the validation plasmid 1 (Supplementary Figure 18; results shown in Figure 4). All melting temperatures (T_ms) presented here are calculated for each BO-half using the formula of SantaLucia (20) for the T_m-calculation and the salt correction. [1] Bridging oligos with a target T$_m$ of 70.0 °C for each half, with 8 %v/v DMSO and 0.45 M betaine and the experimental annealing temperature of 55 °C. [2] Bridging oligos with a target T$_m$ of 74.8 °C for each half, with 8 %v/v DMSO and 0.45 M betaine and the experimental annealing temperature of 55 °C. [3] Bridging oligos with a target T$_m$ of 67.8 °C for each half, without DMSO and betaine and the experimental annealing temperature of 66 °C. DMSO: dimethyl sulfoxide, T_m: melting temperature of a BO-half, w/o: without.

Bridging Oligo Set (T_m per BO-half)	**OligoID**	**Sequence (5'→3')**
Three-part split		
Baseline (70.8±0.4°C)[1]	10425	CGTGAGCATCCTCTCTCGTTTCATCGGTATCATTACCCCCATGAACAGAAATCCCC
	10429	AAATCGCCATTCGCCAGGGGTGTCGATACTATGTTATACGCCAACTTTGAAAACAAC
	10432	GCTTGGTTTTTCAGCTAAAATAACCGTACTCACGCTGCACCGTTTCGAAGAGAC
75 °C (74.5±0.9°C)[2]	10396	CCGTATCGTGAGCATCCTCTCTCGTTTCATCGGTATCATTACCCCCATGAACAGAAATCCCCCTTACA
	10411	CGAAAATCGCCATTCGCCAGGGGTGTCGATACTATGTTATACGCCAACTTTGAAAACAACTTTGAAA
	10417	GCCTGGCTTGGTTTTTCAGCTAAAATAACCGTACTCACGCTGCACCGTTTCGAAGAGACCG
Improved (68.1±0.4°C)[3]	10400	TGAGCATCCTCTCTCGTTTCATCGGTATCATTACCCCCATGAACAGAAATCC
	10412	CGCCATTCGCCAGGGGTGTCGATACTATGTTATACGCCAACTTTGAAA
	10418	TGGTTTTTCAGCTAAAATAACCGTACTCACGCTGCACCGTTTCGAAGAG
Seven-part split		
Baseline (70.9±0.6°C)[1]	10429	AAATCGCCATTCGCCAGGGGTGTCGATACTATGTTATACGCCAACTTTGAAAACAAC
	10430	GAAAAATACCGCTGCGTAAAAGATACGGAAGGAATGTCTCCTGCTAAGGTATATAAGCTGG
	10431	GGAGTGCATCAGGCTCTTTCACTCCATCGACATATCGGATTGTCCCTATACGAATAG
	10432	GCTTGGTTTTTCAGCTAAAATAACCGTACTCACGCTGCACCGTTTCGAAGAGAC
	10423	GCCCGGTACCCAATTCGCCCTATAGTGAGTCGTATTACGCGCGCTC
	10424	GGAAAACCCTGGCGTTACCCAACTTAATCGCCTTGCAGCACATCCCC
	10425	CGTGAGCATCCTCTCTCGTTTCATCGGTATCATTACCCCCATGAACAGAAATCCCC
75 °C (74.6±0.7°C)[2]	10411	CGAAAATCGCCATTCGCCAGGGGTGTCGATACTATGTTATACGCCAACTTTGAAAACAACTTTGAAA
	10413	ACTGATCGAAAAATACCGCTGCGTAAAAGATACGGAAGGAATGTCTCCTGCTAAGGTATATAAGCTGGTGGG
	10415	GCGGAGTGCATCAGGCTCTTTCACTCCATCGACATATCGGATTGTCCCTATACGAATAGCTTAGAC
	10417	GCCTGGCTTGGTTTTTCAGCTAAAATAACCGTACTCACGCTGCACCGTTTCGAAGAGACCG
	10399	GGCCCGGTACCCAATTCGCCCTATAGTGAGTCGTATTACGCGCGCTCACTGG
	10390	CTGGGAAAACCCTGGCGTTACCCAACTTAATCGCCTTGCAGCACATCCCCCTTT
	10396	CCGTATCGTGAGCATCCTCTCTCGTTTCATCGGTATCATTACCCCCATGAACAGAAATCCCCCTTACA
Improved (68.2±0.5°C)[3]	10412	CGCCATTCGCCAGGGGTGTCGATACTATGTTATACGCCAACTTTGAAA
	10414	ACCGCTGCGTAAAAGATACGGAAGGAATGTCTCCTGCTAAGGTATATAAGCT
	10416	GTGCATCAGGCTCTTTCACTCCATCGACATATCGGATTGTCCCTATACG
	10418	TGGTTTTTCAGCTAAAATAACCGTACTCACGCTGCACCGTTTCGAAGAG
	10403	CCCGGTACCCAATTCGCCCTATAGTGAGTCGTATTACGCGCGC
	10393	AACCCTGGCGTTACCCAACTTAATCGCCTTGCAGCACATCC
	10400	TGAGCATCCTCTCTCGTTTCATCGGTATCATTACCCCCATGAACAGAAATCC

bioRxiv preprint doi: https://doi.org/10.1101/510768; this version posted May 29, 2019. The copyright holder for this preprint (which was not certified by peer review) is the author/funder. All rights reserved. No reuse allowed without permission.

Supplementary Table 12: Bridging oligos for the assembly of the validation plasmid 2 (Supplementary Figure 19; results shown in Figure 4). All melting temperatures (T_ms) presented here are calculated for each BO-half using the formula of SantaLucia (20) for the T_m-calculation and the salt correction. [1] Bridging oligos with a target T$_m$ of 70.0 °C for each half, with 8 %v/v DMSO and 0.45 M betaine and the experimental annealing temperature of 55 °C. [2] Bridging oligos with a target T$_m$ of 74.8 °C for each half, with 8 %v/v DMSO and 0.45 M betaine and the experimental annealing temperature of 55 °C. [3] Bridging oligos with a target T$_m$ of 67.8 °C for each half, without DMSO and betaine and the experimental annealing temperature of 66 °C. DMSO: dimethyl sulfoxide, T_m: melting temperature of a BO-half.

Bridging Oligo Set (T_m per BO-half)	**OligoID**	**Sequence (5'→3')**
Three-part split		
Baseline (70.8±0.8°C)[1]	10423	GCCCGGTACCCAATTCGCCCTATAGTGAGTCGTATTACGCGCGCTC
	10426	GGTGCTACAGAGTTCTTGAAGTGGTGGCCTAACTACGGCTACACTAGAAGGACAG
	10428	GTCAATGGTTCAGATACGACGACTAAAAAGTCAAGATCACTATTTGGTTTTAGTCCACTCTCAACTC
75 °C (74.2±0.5°C)[2]	10399	GGCCCGGTACCCAATTCGCCCTATAGTGAGTCGTATTACGCGCGCTCACTGG
	10391	GCGGTGCTACAGAGTTCTTGAAGTGGTGGCCTAACTACGGCTACACTAGAAGGACAGTATTTGGTAT
	10392	TTGATCTGTCAATGGTTCAGATACGACGACTAAAAAGTCAAGATCACTATTTGGTTTTAGTCCACTCTCAACTCCTGAT
Improved (68.7±0.4°C)[3]	10403	CCCGGTACCCAATTCGCCCTATAGTGAGTCGTATTACGCGCGC
	10394	TGCTACAGAGTTCTTGAAGTGGTGGCCTAACTACGGCTACACTAGAAGGACA
	10395	TGGTTCAGATACGACGACTAAAAAGTCAAGATCACTATTTGGTTTTAGTCCACTCTCA
Seven-part split		
Baseline (70.8±0.7°C)[1]	10422	GGATGGCTCGAGTTTTTCAGCAAGATATCCGCTGCACCGTTTCGAAGAGAC
	10423	GCCCGGTACCCAATTCGCCCTATAGTGAGTCGTATTACGCGCGCTC
	10424	GGAAAACCCTGGCGTTACCCAACTTAATCGCCTTGCAGCACATCCCC
	10425	CGTGAGCATCCTCTCTCGTTTCATCGGTATCATTACCCCCATGAACAGAAATCCCC
	10426	GGTGCTACAGAGTTCTTGAAGTGGTGGCCTAACTACGGCTACACTAGAAGGACAG
	10427	ACTGCTAACAAAATTCTCTCCCTATGTTCTAATGGAGAAGATTCAGCCACTGCATTTCCC
	10428	GTCAATGGTTCAGATACGACGACTAAAAAGTCAAGATCACTATTTGGTTTTAGTCCACTCTCAACTC
75 °C (74.5±0.5°C)[2]	10398	TCTTCCGGATGGCTCGAGTTTTTCAGCAAGATATCCGCTGCACCGTTTCGAAGAGACCG
	10399	GGCCCGGTACCCAATTCGCCCTATAGTGAGTCGTATTACGCGCGCTCACTGG
	10390	CTGGGAAAACCCTGGCGTTACCCAACTTAATCGCCTTGCAGCACATCCCCCTTT
	10396	CCGTATCGTGAGCATCCTCTCTCGTTTCATCGGTATCATTACCCCCATGAACAGAAATCCCCCTTACA
	10391	GCGGTGCTACAGAGTTCTTGAAGTGGTGGCCTAACTACGGCTACACTAGAAGGACAGTATTTGGTAT
	10397	ACTACGAACTGCTAACAAAATTCTCTCCCTATGTTCTAATGGAGAAGATTCAGCCACTGCATTTCCCGCAATATC
	10392	TTGATCTGTCAATGGTTCAGATACGACGACTAAAAAGTCAAGATCACTATTTGGTTTTAGTCCACTCTCAACTCCTGAT
Improved (68.3±0.5°C)[3]	10402	ATGGCTCGAGTTTTTCAGCAAGATATCCGCTGCACCGTTTCGAAGAG
	10403	CCCGGTACCCAATTCGCCCTATAGTGAGTCGTATTACGCGCGC
	10393	AACCCTGGCGTTACCCAACTTAATCGCCTTGCAGCACATCC
	10400	TGAGCATCCTCTCTCGTTTCATCGGTATCATTACCCCCATGAACAGAAATCC
	10394	TGCTACAGAGTTCTTGAAGTGGTGGCCTAACTACGGCTACACTAGAAGGACA
	10401	GCTAACAAAATTCTCTCCCTATGTTCTAATGGAGAAGATTCAGCCACTGCATTTCC
	10395	TGGTTCAGATACGACGACTAAAAAGTCAAGATCACTATTTGGTTTTAGTCCACTCTCA

bioRxiv preprint doi: https://doi.org/10.1101/510768; this version posted May 29, 2019. The copyright holder for this preprint (which was not certified by peer review) is the author/funder. All rights reserved. No reuse allowed without permission.

GENBANK FILES

Toy-model plasmid

```
LOCUS       ToyModelPlasmid          4918 bp    DNA     circular UNA 20-MAY-2019
DEFINITION  toy-model plasmid; mRPF1 (from pYTK090), sfGFP (from pYTK001),
pJET1.2/blunt (Thermo Fisher); manually designed bridging oligos
are indicated by "BO" in the primer annotation.
KEYWORDS    .
SOURCE
ORGANISM    .
FEATURES             Location/Qualifiers
misc_feature    1..4918
/note="Geneious type: Editing History Replacement"
/standard_name="GCCATGGAAAATCGATGTTCTTCTTTTATTCTCTCAAGATTT
TCAGGCTGTATATTAAAACTTATATTAAGAACTATGCTAACCACCTCATCAGGAACCG
TTGTAGGTGGCGTGGGTTTTCTTGGCAATCGACTCTCATGAAAACTACGAGCTAAATA
TTCAATATGTTCCTCTTGACCAACTTTATTCTGCATTTTTTTTGAACGAGGTTTAGAG
CAAGCTTCAGGAAACTGAGACAGGAATTTTATTAAAAATTTAAATTTTGAAGAAAGTT
CAGGGTTAATAGCATCCATTTTTTGCTTTGCAAGTTCCTCAGCATTCTTAACAAAAGA
CGTCTCTTTTGACATGTTTAAAGTTTAAACCTCCTGTGTGAAATTATTATCCGCTCAT
AATTCCACACATTATACGAGCCGGAAGCATAAAGTGTAAAGCCTGGGGTGCCTAATGA
GTGAGCTAACTCACATTAATTGCGTTGCGCTCACTGCCAATTGCTTTCCAGTCGGGAA
ACCTGTCGTGCCAGCTGCATTAATGAATCGGCCAACGCGCGGGGAGAGGCGGTTTGCG
TATTGGGCGCTCTTCCGCTTCCTCGCTCACTGACTCGCTGCGCTCGGTCGTTCGGCTG
CGGCGAGCGGTATCAGCTCACTCAAAGGCGGTAATACGGTTATCCACAGAATCAGGGG
ATAACGCAGGAAAGAACATGTGAGCAAAAGGCCAGCAAAAGGCCAGGAACCGTAAAAA
GGCCGCGTTGCTGGCGTTTTTCCATAGGCTCCGCCCCCCTGACGAGCATCACAAAAAT
CGACGCTCAAGTCAGAGGTGGCGAAACCCGACAGGACTATAAAGATACCAGGCGTTTC
CCCCTGGAAGCTCCCTCGTGCGCTCTCCTGTTCCGACCCTGCCGCTTACCGGATACCT
GTCCGCCTTTCTCCCTTCGGGAAGCGTGGCGCTTTCTCATAGCTCACGCTGTAGGTAT
CTCAGTTCGGTGTAGGTCGTTCGCTCCAAGCTGGGCTGTGTGCACGAACCCCCCGTTC
AGCCCGACCGCTGCGCCTTATCCGGTAACTATCGTCTTGAGTCCAACCCGGTAAGACA
CGACTTATCGCCACTGGCAGCAGCCACTGGTAACAGGATTAGCAGAGCGAGGTATGTA
GGCGGTGCTACAGAGTTCTTGAAGTGGTGGCCTAACTACGGCTACACTAGAAGGACAG
TATTTGGTATCTGCGCTCTGCTGAAGCCAGTTACCTTCGGAAAAAGAGTTGGTAGCTC
TTGATCCGGCAAACAAACCACCGCTGGTAGCGGTGGTTTTTTTGTTTGCAAGCAGCAG
ATTACGCGCAGAAAAAAAGGATCTCAAGAAGATCCTTTGATCTTTTCTACGGGGTCTG
ACGCTCAGTGGAACGAAAACTCACGTTAAGGGATTTTGGTCATGAGATTATCAAAAAG
GATCTTCACCTAGATCCTTTTAAATTAAAAATGAAGTTTTAAATCAATCTAAAGTATA
TATGAGTAAACTTGGTCTGACAGTTACCAATGCTTAATCAGTGAGGCACCTATCTCAG
CGATCTGTCTATTTCGTTCATCCATAGTTGCCTGACTCCCCGTCGTGTAGATAACTAC
GATACGGGAGGGCTTACCATCTGGCCCCAGTGCTGCAATGATACCGCGAGACCCACGC
TCACCGGCTCCAGATTTATCAGCAATAAACCAGCCAGCCGGAAGGGCCGAGCGCAGAA
GTGGTCCTGCAACTTTATCCGCCTCCATCCAGTCTATTAATTGTTGCCGGGAAGCTAG
AGTAAGTAGTTCGCCAGTTAATAGTTTGCGCAACGTTGTTGCCATTGCTACAGGCATC
GTGGTGTCACGCTCGTCGTTTGGTATGGCTTCATTCAGCTCCGGTTCCCAACGATCAA
GGCGAGTTACATGATCCCCCATGTTGTGCAAAAAAGCGGTTAGCTCCTTCGGTCCTCC
GATCGTTGTCAGAAGTAAGTTGGCCGCAGTGTTATCACTCATGGTTATGGCAGCACTG
CATAATTCTCTTACTGTCATGCCATCCGTAAGATGCTTTTCTGTGACTGGTGAGTACT
CAACCAAGTCATTCTGAGAATAGTGTATGCGGCGACCGAGTTGCTCTTGCCCGGCGTC
AATACGGGATAATACCGCGCCACATAGCAGAACTTTAAAAGTGCTCATCATTGGAAAA
CGTTCTTCGGGGCGAAAACTCTCAAGGATCTTACCGCTGTTGAGATCCAGTTCGATGT
AACCCACTCGTGCACCCAACTGATCTTCAGCATCTTTTACTTTCACCAGCGTTTCTGG
GTGAGCAAAAACAGGAAGGCAAAATGCCGCAAAAAAGGGAATAAGGGCGACACGGAAA
TGTTGAATACTCATACTCTTCCTTTTTCAATATTATTGAAGCATTTATCAGGGTTATT
GTCTCATGAGCGGATACATATTTGAATGTATTTAGAAAAATAAACAAATAGGGGTTCC
GCGCACATTTCCCCGAAAAGTGCCACCTGACGTCTAAGAAACCATTATTATCATGACA
TTAACCTATAAAAATAGGCGTATCACGAGGCCGCCCCTGCAGCCGAATTATATTATTT
TTGCCAAATAATTTTTAACAAAAGCTCTGAAGTCTTCTTCATTTAAATTCTTAGATGA
TACTTCATCTGGAAAATTGTCCCAATTAGTAGCATCACGCTGTGAGTAAGTTCTAAAC
```

bioRxiv preprint doi: https://doi.org/10.1101/510768; this version posted May 29, 2019. The copyright holder for this preprint (which was not certified by peer review) is the author/funder. All rights reserved. No reuse allowed without permission.


```
CATTTTTTTATTGTTGTATTATCTCTAATCTTACTACTCGATGAGTTTTCGGTATTAT
CTCTATTTTTAACTTGGAGCAGGTTCCATTCATTGTTTTTTTCATCATAGTGAATAAA
ATCAACTGCTTTAACACTTGTGCCTGAACACCATATCCATCCGGCGTAATACGACTCA
CTATAGGGAGAGCGGCCGCCAGATCTTCCGGATGGCTCGAGTTTTTCAGCAAGATATC
CGCTGCACCGTTTCGAGCGCTTGCTTGCCGCCAGAGACCACCGGTGGAAAGCGGGCAG
TGAGCGCAACGCAATTAATGTGAGTTAGCTCACTCATTAGGCACCCCAGGCTTTACAC
TTTATGCTTCCGGCTCGTATGTTGTGTGGAATTGTGAGCGGATAACAATTTCACACAG
GAAACAGCTATGACCATGATTACGCCAAGCGCGCAATTAACCCTCACTAAAGGGAACA
AAAGCTGGAGGACCTCGAGGGGGGGCCCGGTACCCAATTCGCCCTATAGTGAGTCGTA
TTACGCGCGCTCACTGGCCGTCGTTTTACAACGTCGTGACTGGGAAAACCCTGGCGTT
ACCCAACTTAATCGCCTTGCAGCACATCCCCCTTTCGCCAGCTGGCGTAATAGCGAAG
AGGCCCGCACCGATCGCCCTTCCCAACAGTTGCGCAGCCTGAATGGCGAATGGGACGC
GCCCTGTAGCGGCGCCGGTCTCGATAGCCACCACTGATATCTTTCTAGAAGATCTCCT
ACAATATTCTCAGCT"
misc_feature    1..2974
/note="Geneious type: Vector"
/standard_name="pJET1.2/blunt"
CDS             join(complement(<1..382),complement(2622..>2974))
/standard_name="eco47IR"
primer_bind     1..19
/standard_name="23044_pJET_fw"
misc_feature    complement(34..57)
/note="Geneious type: primer_bind_reverse"
/standard_name="14014_pJET1.2-Seq-rev"
rep_origin      1045..1296
CDS             complement(1554..2411)
/standard_name="bla"
primer_bind     2913..2935
/standard_name="14013_pJET1.2-Seq-fwd"
primer_bind     2948..3009
/standard_name="10133_BO_pJET_mRFP1-P1_fw"
misc_feature    complement(2954..2974)
/note="Geneious type: primer_bind_reverse"
/standard_name="23043_pJET_rv"
misc_feature    2975..3869
/note="Geneious type: Inserted sequence"
/standard_name="mRFP1 insertion"
promoter        2975..3028
/note="Geneious type: promoter prokaryotic"
/standard_name="Bba_R0040 TetR Promoter"
misc_feature    complement(2975..3053)
/note="Geneious type: primer_bind_reverse"
/standard_name="10142_mRFP1_P1_rv"
primer_bind     2975..3053
/standard_name="10141_mRFP1_P1_fw"
primer_bind     3025..3081
/standard_name="10134_BO_mRFP1-P1P2_fw"
RBS             3029..3053
/standard_name="mRFP1 Ribsosome Binding Site"
CDS             3054..3731
/standard_name="mRFP1"
primer_bind     3054..3072
/standard_name="10127_mRFP1_P2_fw"
primer_bind     3358..3407
/standard_name="10135_BO_mRFP1-P2P3_fw"
misc_feature    complement(3363..3383)
/note="Geneious type: primer_bind_reverse"
/standard_name="10128_mRFP1_P2_rv"
primer_bind     3384..3400
/standard_name="10129_mRFP1_P3_fw"
```

bioRxiv preprint doi: https://doi.org/10.1101/510768; this version posted May 29, 2019. The copyright holder for this preprint (which was not certified by peer review) is the author/funder. All rights reserved. No reuse allowed without permission.
main — 2019/5/22 — 19:03 — page 55 — #55


```
primer_bind       3489..3542
/standard_name="10136_BO_mRFP1-P3P4_fw"
misc_feature      complement(3493..3512)
/note="Geneious type: primer_bind_reverse"
/standard_name="10130_mRFP1_P3_rv"
primer_bind       3513..3531
/standard_name="10131_mRFP1_P4_fw"
terminator        3741..3869
/standard_name="BBa_B0015 Terminator"
misc_feature      3870..3906
/note="Geneious type: Spacer"
/standard_name="Spacer (from pYTK009)"
protein_bind      join(3874..3879,3881..3884)
/standard_name="BsaI"
primer_bind       3886..3941
/standard_name="10137_BO_mRFP1-P4_sfGFP_fw"
misc_feature      complement(3888..3906)
/note="Geneious type: primer_bind_reverse"
/standard_name="10132_mRFP1_P4_rv"
misc_feature      3907..4918
/note="Geneious type: Inserted sequence"
/standard_name="sfGFP insertion"
promoter          3907..4036
/note="Geneious type: promoter prokaryotic"
/standard_name="BBa_J72163 GlpT Promoter"
primer_bind       3907..3930
/standard_name="10108_sfGFP_fw"
RBS               4037..4072
/standard_name="sfGFP Ribosome Binding Site"
CDS               4073..4789
/standard_name="sfGFP"
primer_bind       4181..4239
/standard_name="10116_BO_sfGFP_P1_sfGFP_P2_fw"
misc_feature      complement(4191..4211)
/note="Geneious type: primer_bind_reverse"
/standard_name="10110_sfGFP_P1_rv"
primer_bind       4212..4232
/standard_name="10111_sfGFP_P2_fw"
primer_bind       4486..4550
/standard_name="10117_BO_sfGFP_P2_sfGFP_P3_fw"
misc_feature      complement(4495..4517)
/note="Geneious type: primer_bind_reverse"
/standard_name="10112_sfGFP_P2_rv"
primer_bind       4518..4535
/standard_name="10113_sfGFP_P3_fw"
terminator        4790..4918
/standard_name="BBa_B0015 Terminator"
primer_bind       4895..37
/standard_name="10118_BO_sfGFP_P3_pJET_fw"
misc_feature      complement(4898..4918)
/note="Geneious type: primer_bind_reverse"
/standard_name="10109_sfGFP_rv"
ORIGIN
1 atctttctag aagatctcct acaatattct cagctgccat ggaaaatcga tgttcttctt
61 ttattctctc aagattttca ggctgtatat taaaacttat attaagaact atgctaacca
121 cctcatcagg aaccgttgta ggtggcgtgg gttttcttgg caatcgactc tcatgaaaac
181 tacgagctaa atattcaata tgttcctctt gaccaacttt attctgcatt ttttttgaac
241 gaggtttaga gcaagcttca ggaaactgag acaggaattt tattaaaaat ttaaattttg
301 aagaaagttc agggttaata gcatccattt tttgctttgc aagttcctca gcattcttaa
361 caaaagacgt ctcttttgac atgtttaaag tttaaacctc ctgtgtgaaa ttattatccg
```

bioRxiv preprint doi: https://doi.org/10.1101/510768; this version posted May 29, 2019. The copyright holder for this preprint (which was not certified by peer review) is the author/funder. All rights reserved. No reuse allowed without permission.


```
421  ctcataattc cacacattat acgagccgga agcataaagt gtaaagcctg gggtgcctaa
481  tgagtgagct aactcacatt aattgcgttg cgctcactgc caattgcttt ccagtcggga
541  aacctgtcgt gccagctgca ttaatgaatc ggccaacgcg cggggagagg cggtttgcgt
601  attgggcgct cttccgcttc ctcgctcact gactcgctgc gctcggtcgt tcggctgcgg
661  cgagcggtat cagctcactc aaaggcggta atacggttat ccacagaatc aggggataac
721  gcaggaaaga acatgtgagc aaaaggccag caaaaggcca ggaaccgtaa aaaggccgcg
781  ttgctggcgt ttttccatag gctccgcccc cctgacgagc atcacaaaaa tcgacgctca
841  agtcagaggt ggcgaaaccc gacaggacta taaagatacc aggcgtttcc ccctggaagc
901  tccctcgtgc gctctcctgt tccgaccctg ccgcttaccg gatacctgtc cgcctttctc
961  ccttcgggaa gcgtggcgct ttctcatagc tcacgctgta ggtatctcag ttcggtgtag
1021 gtcgttcgct ccaagctggg ctgtgtgcac gaaccccccg ttcagcccga ccgctgcgcc
1081 ttatccggta actatcgtct tgagtccaac ccggtaagac acgacttatc gccactggca
1141 gcagccactg gtaacaggat tagcagagcg aggtatgtag gcggtgctac agagttcttg
1201 aagtggtggc ctaactacgg ctacactaga aggacagtat ttggtatctg cgctctgctg
1261 aagccagtta ccttcggaaa aagagttggt agctcttgat ccggcaaaca aaccaccgct
1321 ggtagcggtg gttttttttgt ttgcaagcag cagattacgc gcagaaaaaa aggatctcaa
1381 gaagatcctt tgatcttttc tacggggtct gacgctcagt ggaacgaaaa ctcacgttaa
1441 gggattttgg tcatgagatt atcaaaaagg atcttcacct agatcctttt aaattaaaaa
1501 tgaagtttta aatcaatcta aagtatatat gagtaaactt ggtctgacag ttaccaatgc
1561 ttaatcagtg aggcacctat ctcagcgatc tgtctatttc gttcatccat agttgcctga
1621 ctccccgtcg tgtagataac tacgatacgg gagggcttac catctggccc cagtgctgca
1681 atgataccgc gagacccacg ctcaccggct ccagatttat cagcaataaa ccagccagcc
1741 ggaagggccg agcgcagaag tggtcctgca actttatccg cctccatcca gtctattaat
1801 tgttgccggg aagctagagt aagtagttcg ccagttaata gtttgcgcaa cgttgttgcc
1861 attgctacag gcatcgtggt gtcacgctcg tcgtttggta tggcttcatt cagctccggt
1921 tcccaacgat caaggcgagt tacatgatcc cccatgttgt gcaaaaaagc ggttagctcc
1981 ttcggtcctc cgatcgttgt cagaagtaag ttggccgcag tgttatcact catggttatg
2041 gcagcactgc ataattctct tactgtcatg ccatccgtaa gatgcttttc tgtgactggt
2101 gagtactcaa ccaagtcatt ctgagaatag tgtatgcggc gaccgagttg ctcttgcccg
2161 gcgtcaatac gggataatac cgcgccacat agcagaactt taaaagtgct catcattgga
2221 aaacgttctt cggggcgaaa actctcaagg atcttaccgc tgttgagatc cagttcgatg
2281 taacccactc gtgcacccaa ctgatcttca gcatctttta ctttcaccag cgtttctggg
2341 tgagcaaaaa caggaaggca aaatgccgca aaaaagggaa taagggcgac acggaaatgt
2401 tgaatactca tactcttcct ttttcaatat tattgaagca tttatcaggg ttattgtctc
2461 atgagcggat acatatttga atgtatttag aaaaataaac aaataggggt tccgcgcaca
2521 tttccccgaa aagtgccacc tgacgtctaa gaaaccatta ttatcatgac attaacctat
2581 aaaaataggc gtatcacgag gccgcccctg cagccgaatt atattatttt tgccaaataa
2641 tttttaacaa aagctctgaa gtcttcttca tttaaattct tagatgatac ttcatctgga
2701 aaattgtccc aattagtagc atcacgctgt gagtaagttc taaaccattt ttttattgtt
2761 gtattatctc taatcttact actcgatgag ttttcggtat tatctctatt tttaacttgg
2821 agcaggttcc attcattgtt tttttcatca tagtgaataa aatcaactgc tttaacactt
2881 gtgcctgaac accatatcca tccggcgtaa tacgactcac tatagggaga gcggccgcca
2941 gatcttccgg atggctcgag tttttcagca agattcccta tcagtgatag agattgacat
3001 ccctatcagt gatagagata ctgagcacgg atctgaaaga ggagaaagga tctatggcga
3061 gtagcgaaga cgttatcaaa gagttcatgc gtttcaaagt tcgtatggaa ggttccgtta
3121 acggtcacga gttcgaaatc gaaggtgaag gtgaaggtcg tccgtacgaa ggtactcaga
3181 ccgctaaact gaaagttacc aaaggtggtc cgctgccgtt cgcttgggac atcctgtccc
3241 cgcagttcca gtacggttcc aaagcttacg ttaaacaccc ggctgacatc ccggactacc
3301 tgaaactgtc cttcccggaa ggtttcaaat gggaacgtgt tatgaacttc gaagacggtg
3361 gtgttgttac cgttacccag gactcctccc tgcaagacgg tgagttcatc tacaaagtta
3421 aactgcgtgg tactaacttc ccgtccgacg gtccggttat gcagaaaaaa accatgggtt
3481 gggaagcttc caccgaacgt atgtacccgg aagacggtgc tctgaaaggt gaaatcaaaa
3541 tgcgtctgaa actgaaagac ggtggtcact acgacgctga agttaaaacc acctacatgg
3601 ctaaaaaacc ggttcagctg ccgggtgctt acaaaaccga catcaaactg gacatcacct
3661 cccacaacga agactacacc atcgttgaac agtacgaacg tgctgaaggt cgtcactcca
3721 ccggtgctta ataaggatct ccaggcatca aataaaacga aaggctcagt cgaaagactg
3781 ggcctttcgt tttatctgtt gtttgtcggt gaacgctctc tactagagtc acactggctc
3841 accttcgggt gggcctttct gcgtttataa gtcggtctca ccgagcggcc gcgtgttaca
3901 accaatgaaa gtgaaacgtg atttcatgcg tcattttgaa cattttgtaa atcttattta
3961 ataatgtgtg cggcaattca catttaattt atgaatgttt tcttaacatc gcggcaactc
```

bioRxiv preprint doi: https://doi.org/10.1101/510768; this version posted May 29, 2019. The copyright holder for this preprint (which was not certified by peer review) is the author/funder. All rights reserved. No reuse allowed without permission.


```
4021 aagaaacggc aggttcggat cttagctact agagaaagag gagaaatact agatgcgtaa
4081 aggcgaagag ctgttcactg gtgtcgtccc tattctggtg gaactggatg gtgatgtcaa
4141 cggtcataag ttttccgtgc gtggcgaggg tgaaggtgac gcaactaatg gtaaactgac
4201 gctgaagttc atctgtacta ctggtaaact gccggttcct tggccgactc tggtaacgac
4261 gctgacttat ggtgttcagt gctttgctcg ttatccggac catatgaagc agcatgactt
4321 cttcaagtcc gccatgccgg aaggctatgt gcaggaacgc acgatttcct ttaaggatga
4381 cggcacgtac aaaacgcgtg cggaagtgaa atttgaaggc gataccctgg taaaccgcat
4441 tgagctgaaa ggcattgact ttaaagagga cggcaatatc ctgggccata agctggaata
4501 caattttaac agccacaatg tttacatcac cgccgataaa caaaaaaatg gcattaaagc
4561 gaattttaaa attcgccaca acgtggagga tggcagcgtg cagctggctg atcactacca
4621 gcaaaacact ccaatcggtg atggtcctgt tctgctgcca gacaatcact atctgagcac
4681 gcaaagcgtt ctgtctaaag atccgaacga gaaacgcgat catatggttc tgctggagtt
4741 cgtaaccgca gcgggcatca cgcatggtat ggatgaactg tacaaatgac caggcatcaa
4801 ataaaacgaa aggctcagtc gaaagactgg gcctttcgtt ttatctgttg tttgtcggtg
4861 aacgctctct actagagtca cactggctca ccttcgggtg ggcctttctg cgtttata
//
```

bioRxiv preprint doi: https://doi.org/10.1101/510768; this version posted May 29, 2019. The copyright holder for this preprint (which was not certified by peer review) is the author/funder. All rights reserved. No reuse allowed without permission.

Validation plasmid 1

```
LOCUS       ValidationPlasmid1          4083 bp    DNA     circular UNA 10-MAY-2019
DEFINITION  kanR, lacZ, pJOE8739.1 Backbone (without manP).
KEYWORDS    .
SOURCE
ORGANISM    .
FEATURES             Location/Qualifiers
     misc_feature    1..2490
     /note="Geneious type: Vector"
     /standard_name="pJEO8739.1"
     primer_bind     97..152
     /standard_name="10425_LCR"
     misc_feature    complement(103..122)
     /note="Geneious type: primer_bind_reverse"
     /standard_name="10383_lacZ_Part3_rv"
     primer_bind     123..144
     /standard_name="10384_Rest+ori_Part1_fw"
     misc_feature    complement(163..182)
     /note="Geneious type: primer_bind_reverse"
     /standard_name="10420_Seq_rv"
     gene            170..361
     /standard_name="ROP"
     CDS             170..361
     /gene="rop"
     /standard_name="rop CDS"
     rep_origin      complement(541..1394)
     CDS             complement(1440..2192)
     /gene="SpcR"
     /standard_name="specR"
     primer_bind     2413..2430
     /standard_name="10419_Seq_fw"
     primer_bind     2470..2526
     /standard_name="10429_LCR"
     misc_feature    complement(2475..2490)
     /note="Geneious type: primer_bind_reverse"
     /standard_name="10406_BB_rv"
     misc_feature    2491..3562
     /note="Geneious type: Editing History Replacement"
     /standard_name="TTAATTGCGTCGAGACCCCTGTGGGTCTCGTTTTTTGGATCA
CCGGTATGGCGCCATATGCTTTATTCGATTTCTTCTAGCAGCTTGTATGCTTCTTCTG
TTGTTTGCACGGAGAGCAGCCGCTCCCTATAATTGTCATCCATTAGCTTTCGAGATAG
CATCTGCAGTATTTTGAGATGCTGGTTTCCCCCGCTCTCTTTCGGTACAGCAATCATA
AAGATTAATTTAGCTTCTGATCCATCCAGGCTATTCCAATCAACGCCTGATCGTTTGA
TCCCAAAGGCAACACTCGGCTCCCTGACCGCCTCAGACTTTCCGTGCGGAATCGCGAT
ATTCATGCCAATCGCCGTTGTTCCCTGTTGTTCACGATTCAAAATGGCTTGTTTAAAC
CCGCTCTCTGAAAGCAGCGCACCTCTTCGTGACAATTTCTGAATCAATTCATCTATGA
TGTCATCACTCGTTTCCCCCGATAAATTTGGTTCAATTAATTCCGGGCTGATAATGTC
TGTCAGTTTTTTAAATTCCGACATCTCAGCTTTTTGGCTTTGAATTGGCTGCTTTATT
TCATTTGCTGCCGCAGCTTCACTTGGCGCGGAGGTCGGTGCAGTTTCACTGAGCACAG
GAGACGCCGTAATATCCTTTTTTAGTACATTGACGAACAGAGCAGTGACAAGAGATCC
TGCAATCACAGCAATAAAAAACATCAAGACATGATCAACTGCGCCAAGCACTGCAACG
ATAGGTCCGCCGTGCGCCACTCTGTCTCCCACATTGCCAATCATGGCTATCACAGAAC
CTGTCATTGAGCCTGCCATAATACTTGGAATAACGCGCAGAGGGTCCTGCGCCGCAAA
TGGAATCGCTCCTTCAGTAATGCCGAAGAGCCCCATCGTAAATGCCGCTTTCCCCATT
TCTCTTTGAGATGCCTCGAATTTTCTTTTTCCTAAAAACGTCGCAATGCCAAGGCCAA
TCGGGGGGATACAAATGGCGACAGCAATTGGTCCCATAATTTCATAATTTCCTTCTCC
AATCATTGCCGATCCAAACAGAAACGCCACCTTATTTACGGGACCGCCCATATCAAAT
GAGATCATCGCCCCTAAAATCAATGCCAGAAGGATCGAGCTCGACCCTTTCATCCCCG
CCAGCCAAACTGTTAAAGAGGCGAAAATTTGAGCTACAGGCGCGCCGATCAAAAACAC
AAACGCTAAACCTACAATCAGTGATGCAAACACCGGAATAATAATAATCGGCATAATC
```

bioRxiv preprint doi: https://doi.org/10.1101/510768; this version posted May 29, 2019. The copyright holder for this preprint (which was not certified by peer review) is the author/funder. All rights reserved. No reuse allowed without permission.
main — 2019/5/22 — 19:03 — page 59 — #59

GGCTGGATGGCTTTTGGAACTTTTAATTTTTTGATCCAAAGTGCCGCGTATCCGGCCA
AAAACCCGGCAATAATCCCCCCGAGGAATCCGGCGCCGCTTGCGCTGTCATAAAAACT
TCCAGTCGCCGCAATATAACCGCCGATCATACCTGGCACAAGCCCCGGTTTATCAGCG
ATGCTATAGGCGATATAGCCGGCTAAAATCGGAATCATAAATGAAAATGAAGCACTGC
CGATCTGTTCAATCGTTTTCCAGAAGGAATCATCCGGAATAACTAAGCCTTTAGGTGT
TTTCTCCCCTCCAAGCGTTAATGCAACCGCTATCAATAATCCGCCGACAACAATGAAA
GGAACCATAAATGAAACGCCGTTCATTAAATGACGGTAAATTGGATTTTGTTTCTTCT
CCTGATGATTACCGGATTCCGATTTTGTAGCGGAACGATAGACCGGTATATCCCCGTT
AAGAGCTTTTTGAATCAATTCTTCCGGTTTGCGGATACCGTCCTGTACCCCCACAGAC
AGCAGTTTTTTGCCTATAAACCGGTCTTTGTTTACCGAACGGTCTGCAGCAATAATGA
TTGCGTCCGCTTCGCGAATTTCCTCTTCGGTTAGCTTATTTTCAACACCAATCCCTCC
CTGGGTCTCAACTTTGATGCTAACGCCCAGTCTGTCAGCAGCTTTTTGCAGATTTTCT
GCTGCCATATACGTATGGGCGATTCCATTCGGACAAGATGTAATCGCTAACAGTTTCA
TAGGAAACCTCCTTTAAAGTGTGAATAATAAGATCTTGTCTCAACTGTATACCGAAAT
CAGCTCATTAAAATCGCTTTTTTTACCATAGGTTCCGGTAATAAAGGCATTTTTCCCA
TATGGCGATTAAGTTGGGTAACGCCAGGGTTTTCCCAGTCACGACGTTGTAAAACGAC
GGCCAGTGCAGATCTTCCGGATGGCTCGAGTTTTTCAGCAAGATATC”

misc_feature 2491..3562
/note=”Geneious type: Inserted sequence”
/standard_name=”kanR insertion”
primer_bind 2491..2514
/standard_name=”10404_kanR_fw”
CDS 2655..3449
/standard_name=”kanR”
primer_bind 2697..2757
/standard_name=”10430_LCR”
misc_feature complement(2707..2726)
/note=”Geneious type: primer_bind_reverse”
/standard_name=”10407_rv”
primer_bind 2727..2745
/standard_name=”10408_fw”
primer_bind 3002..3058
/standard_name=”10431_LCR”
misc_feature complement(3008..3026)
/note=”Geneious type: primer_bind_reverse”
/standard_name=”10409_rv”
primer_bind 3027..3046
/standard_name=”10410_fw”
misc_feature complement(3520..3539)
/note=”Geneious type: primer_bind_reverse”
/standard_name=”10433_kanR_OH_Rv”
primer_bind 3531..3584
/standard_name=”10432_LCR”
misc_feature 3563..4045
/note=”Geneious type: Inserted sequence”
/standard_name=”lacZ insertion”
primer_bind 3563..3580
/standard_name=”10185_lacZ_P1_fw”
misc_feature 3608..3729
/note=”Geneious type: promoter prokaryotic”
/standard_name=”lacZ promoter”
CDS 3730..4005
/standard_name=”lacZ’”
misc_feature complement(3806..3822)
/note=”Geneious type: primer_bind_reverse”
/standard_name=”10382_lacZ_Part1_rv”
misc_feature complement(3823..3902)
/note=”Geneious type: primer_bind_reverse”
/standard_name=”10388_lacZ_Part3_rv”
primer_bind 3823..3902

bioRxiv preprint doi: https://doi.org/10.1101/510768; this version posted May 29, 2019. The copyright holder for this preprint (which was not certified by peer review) is the author/funder. All rights reserved. No reuse allowed without permission.


```
/standard_name="10387_lacZ_Part2_fw"
primer_bind      3879..3925
/standard_name="10424_LCR"
primer_bind      3903..3922
/standard_name="10187_lacZ_P2_fw"
misc_feature     4046..4048
/note="Geneious type: Inserted sequence"
/standard_name="EcoRV restriction site (added by primer
overhang)"
misc_feature     4049..4083
/note="Geneious type: overhang"
/standard_name="pJET1.2/blunt overhang"
ORIGIN
1 agtgattttt ctctggtccc gccgcatcca taccgccagt tgtttaccct cacaacgttc
61 cagtaaccgg gcatgttcat catcagtaac ccgtatcgtg agcatcctct ctcgtttcat
121 cggtatcatt acccccatga acagaaatcc ccttacacgg gaggcatcag tgaccaaaca
181 ggaaaaaacc gcccttaaca tggcccgctt tatcagaagc cagacattaa cgcttctgga
241 gaaactcaac gagctggacg cggatgaaca ggcagacatc tgtgaatcgc ttcacgacca
301 cgctgatgag ctttaccgca gctgcctcgc gcgtttcggt gatgacggtg aaaacctctg
361 acacatgcag ctcccggaga cggtcacagc ttgtctgtaa gcggatgccg ggagcagaca
421 agcccgtcag ggcgcgtcag cgggtgttgg cgggtgtcgg ggcgcagcca tgacccagtc
481 acgtagcgat agcggagtgt atactggctt aactatgcgg catcagagca gattgtactg
541 agagtgcacc atatatgcgg tgtgaaatac cgcacagatg cgtaaggaga aaataccgca
601 tcaggcgctc ttccgcttcc tcgctcactg actcgctgcg ctcggtcgtt cggctgcggc
661 gagcggtatc agctcactca aaggcggtaa tacggttatc cacagaatca ggggataacg
721 caggaaagaa catgtgagca aaaggccagc aaaaggccag gaaccgtaaa aaggccgcgt
781 tgctggcgtt tttccatagg ctccgccccc ctgacgagca tcacaaaaat cgacgctcaa
841 gtcagaggtg gcgaaacccg acaggactat aaagatacca ggcgtttccc cctggaagct
901 ccctcgtgcg ctctcctgtt ccgaccctgc cgcttaccgg atacctgtcc gcctttctcc
961 cttcgggaag cgtggcgctt tctcatagct cacgctgtag gtatctcagt tcggtgtagg
1021 tcgttcgctc caagctgggc tgtgtgcacg aacccccccgt tcagcccgac cgctgcgcct
1081 tatccggtaa ctatcgtctt gagtccaacc cggtaagaca cgacttatcg ccactggcag
1141 cagccactgg taacaggatt agcagagcga ggtatgtagg cggtgctaca gagttcttga
1201 agtggtggcc taactacggc tacactagaa ggacagtatt tggtatctgc gctctgctga
1261 agccagttac cttcggaaaa agagttggta gctcttgatc cggcaaacaa accaccgctg
1321 gtagcggtgg ttttttgtt tgcaagcagc agattacgcg cagaaaaaaa ggatctcaag
1381 aagatccttt gatcttttct acggggttta aacgtgtttc caccattttt tcaatttttt
1441 tataattttt ttaatctgtt atttaaatag tttatagtta aatttacatt ttcattagtc
1501 cattcaatat tctctccaag ataactacga actgctaaca aaattctctc cctatgttct
1561 aatggagaag attcagccac tgcatttccc gcaatatctt ttggtatgat tttacccgtg
1621 tccatagtta aaatcatacg gcataaagtt aatatagagt tggtttcatc atcctgataa
1681 ttatctatta attcctctga cgaatccata atggctcttc tcacatcaga aaatggaata
1741 tcaggtagta attcctctaa gtcataattt ccgtatattc ttttatttt tcgttttgct
1801 tggtaaagca ttatggttaa atctgaattt aattccttct gaggaatgta tccttgttca
1861 taaagctctt gtaaccattc tccataaata aattcttgtt tgggaggatg attccacggt
1921 accatttctt gctgaataat aattgttaat tcaatatatc gtaagttgct tttatctcct
1981 attttttttg aaataggtct aatttttttgt ataagtattt ctttactttg atctgtcaat
2041 ggttcagata cgacgactaa aaagtcaaga tcactatttg gttttagtcc actctcaact
2101 cctgatccaa acatgtaagt accaataagg ttatttttta aatgtttccg aagtattttt
2161 ttcactttat taatttgttc gtatgtattc aaatatatcc tcctcactat tttgattagt
2221 acctatttta tatccatagt tgttaattaa ataaacttaa tttagtttat ttatagattt
2281 cattggcttc taaatttttt atctagataa taattatttt agttaatttt attctagatt
2341 atatatgata tgatctttca tttccataaa actaaagtaa gtgtaaacct attcattgtt
2401 ttaaaaatat ctcttgccag tcacgttacg ttattagtta tagttattat aacatgtatt
2461 cacgaacgaa aatcgccatt cgccaggggt gtcgatacta tgttatacgc caactttgaa
2521 aacaactttg aaaaagctgt tttctggtat ttaaggtttt agaatgcaag gaacagtgaa
2581 ttggagttcg tcttgttata attagcttct tggggtatct ttaaatactg tagaaaagag
2641 gaaggaaata ataaatggct aaaatgagaa tatcaccgga attgaaaaaa ctgatcgaaa
2701 aataccgctg cgtaaaagat acggaaggaa tgtctcctgc taaggtatat aagctggtgg
2761 gagaaaatga aaacctatat ttaaaaatga cggacagccg gtataaaggg accacctatg
```

bioRxiv preprint doi: https://doi.org/10.1101/510768; this version posted May 29, 2019. The copyright holder for this preprint (which was not certified by peer review) is the author/funder. All rights reserved. No reuse allowed without permission.


```
2821 atgtggaacg ggaaaaggac atgatgctat ggctggaagg aaagctgcct gttccaaagg
2881 tcctgcactt tgaacggcat gatggctgga gcaatctgct catgagtgag gccgatggcg
2941 tcctttgctc ggaagagtat gaagatgaac aaagccctga aaagattatc gagctgtatg
3001 cggagtgcat caggctcttt cactccatcg acatatcgga ttgtccctat acgaatagct
3061 tagacagccg cttagccgaa ttggattact tactgaataa cgatctggcc gatgtggatt
3121 gcgaaaactg ggaagaagac actccattta aagatccgcg cgagctgtat gatttttaa
3181 agacggaaaa gcccgaagag gaacttgtct tttcccacgg cgacctggga gacagcaaca
3241 tctttgtgaa agatggcaaa gtaagtggct ttattgatct tgggagaagc ggcagggcgg
3301 acaagtggta tgacattgcc ttctgcgtcc ggtcgatcag ggaggatatc ggggaagaac
3361 agtatgtcga gctatttttt gacttactgg ggatcaagcc tgattgggag aaaataaaat
3421 attatatttt actggatgaa ttgttttagt acctagattt agatgtctaa aaagcctgca
3481 gtcgcgaggc ctcgacggat ccccaaagca cttgcatagg ctaatgcctg gcttggtttt
3541 tcagctaaaa taaccgtact cacgctgcac cgtttcgaag agaccgccgg tggagagcgg
3601 gcagtgagcg caacgcaatt aatgtgagtt agctcactca ttaggcaccc caggctttac
3661 actttatgcc tccggctcgt atgttgtgtg gaattgtgag cggataacaa tttcacacag
3721 gaaacagcta tgaccatgat tacgccaagc gcgcaattaa ccctcactaa agggaacaaa
3781 agctggagga cctcgagggg gggcccggta cccaattcgc cctatagtga gtcgtattac
3841 gcgcgctcac tggccgtcgt tttacaacgt cgtgactggg aaaaccctgg cgttacccaa
3901 cttaatcgcc ttgcagcaca tccccctttc gccagctggc gtaatagcga agaggcccgc
3961 accgatcgcc cttcccaaca gttgcgcagc ctgaatggcg aatgggacgc gccctgtagc
4021 ggcgccggtc tcgatagcca ccactgatat ctttctagaa gatctcctac aatattctca
4081 gct
//
```

bioRxiv preprint doi: https://doi.org/10.1101/510768; this version posted May 29, 2019. The copyright holder for this preprint (which was not certified by peer review) is the author/funder. All rights reserved. No reuse allowed without permission.

Validation plasmid 2

```
LOCUS       ValidationPlasmid2          5246 bp    DNA     circular UNA 10-MAY-2019
DEFINITION  lacZ, pJOE8739.1 Backbone.
KEYWORDS    .
SOURCE
ORGANISM    .
FEATURES             Location/Qualifiers
     primer_bind     97..152
                     /standard_name="10425_BO"
     misc_feature    complement(103..122)
                     /note="Geneious type: primer_bind_reverse"
                     /standard_name="10383_lacZ_Part3_rv"
     primer_bind     123..144
                     /standard_name="10384_Rest+ori_Part1_fw"
     misc_feature    complement(163..182)
                     /note="Geneious type: primer_bind_reverse"
                     /standard_name="10420_Seq_rv"
     gene            170..361
                     /standard_name="ROP"
     CDS             170..361
                     /gene="rop"
                     /standard_name="rop CDS"
     rep_origin      complement(541..1394)
     primer_bind     1162..1180
                     /standard_name="11253_Seq_fw"
     primer_bind     1182..1236
                     /standard_name="10426_BO"
     misc_feature    complement(1186..1208)
                     /note="Geneious type: primer_bind_reverse"
                     /standard_name=11313
     primer_bind     1209..1232
                     /standard_name=11315
     CDS             complement(1440..2192)
                     /gene="SpcR"
                     /standard_name="specR"
     primer_bind     1531..1590
                     /standard_name="10427_BO"
     misc_feature    complement(1539..1565)
                     /note="Geneious type: primer_bind_reverse"
                     /standard_name=11308
     primer_bind     1566..1588
                     /standard_name="10385_specR_Part2_fw"
     primer_bind     2035..2101
                     /standard_name="10428_BO"
     misc_feature    complement(2045..2067)
                     /note="Geneious type: primer_bind_reverse"
                     /standard_name="10389_specR_rv"
     primer_bind     2068..2092
                     /standard_name="10381_specR_fw"
     CDS             complement(2553..4505)
                     /gene="manP"
                     /product="manP"
                     /standard_name="manP"
     repeat_region   4624..4686
                     /standard_name="Repeat 1"
     primer_bind     4632..4649
                     /standard_name="10186_lacZ_P1_rv"
     misc_feature    4688..4722
                     /note="Geneious type: overhang"
                     /standard_name="pJET1.2/blunt; overhang"
```

bioRxiv preprint doi: https://doi.org/10.1101/510768; this version posted May 29, 2019. The copyright holder for this preprint (which was not certified by peer review) is the author/funder. All rights reserved. No reuse allowed without permission.


```
primer_bind      4697..4747
/standard_name="10422_BO"
misc_feature     complement(4702..4725)
/note="Geneious type: primer_bind_reverse"
/standard_name="10386_specR_Part3_rv"
misc_feature     complement(4702..4722)
/note="Geneious type: primer_bind_reverse"
/standard_name="pJET-A1k1Int-loxURA-ARE1-Leu2Min-TurboGFP
- 23043_pJetFor"
misc_feature     4723..4725
/note="Geneious type: Inserted sequence"
/standard_name="EcoRV restriction site (added by primer
overhang)"
misc_feature     4726..5208
/note="Geneious type: Inserted sequence"
/standard_name="lacZ insertion"
primer_bind      4726..4743
/standard_name="10185_lacZ_P1_fw"
misc_feature     4771..4892
/note="Geneious type: promoter prokaryotic"
/standard_name="lacZ promoter"
CDS              4893..5168
/standard_name="lacZ'"
primer_bind      4966..5011
/standard_name="10423_BO"
misc_feature     complement(4969..4985)
/note="Geneious type: primer_bind_reverse"
/standard_name="10382_lacZ_Part1_rv"
misc_feature     complement(4986..5065)
/note="Geneious type: primer_bind_reverse"
/standard_name="10388_lacZ_Part3_rv"
primer_bind      4986..5065
/standard_name="10387_lacZ_Part2_fw"
repeat_region    complement(5011..5073)
/standard_name="Repeat 1"
primer_bind      5042..5088
/standard_name="10424_BO"
primer_bind      5066..5085
/standard_name="10187_lacZ_P2_fw"
misc_feature     5209..5211
/note="Geneious type: Inserted sequence"
/standard_name="EcoRV restriction site (added by primer
overhang)"
primer_bind      5212..5230
/note="Geneious type: overhang"
/standard_name="pJET1.2/blunt; overhang"
misc_feature     5231..4687
/note="Geneious type: Vector"
/standard_name="pJOE8739.1"
ORIGIN
1 agtgattttt ctctggtccc gccgcatcca taccgccagt tgtttaccct cacaacgttc
61 cagtaaccgg gcatgttcat catcagtaac ccgtatcgtg agcatcctct ctcgtttcat
121 cggtatcatt acccccatga acagaaatcc cccttacacg gaggcatcag tgaccaaaca
181 ggaaaaaacc gcccttaaca tggcccgctt tatcagaagc cagacattaa cgcttctgga
241 gaaactcaac gagctggacg cggatgaaca ggcagacatc tgtgaatcgc ttcacgacca
301 cgctgatgag ctttaccgca gctgcctcgc gcgtttcggt gatgacggtg aaaacctctg
361 acacatgcag ctcccggaga cggtcacagc ttgtctgtaa gcggatgccg ggagcagaca
421 agcccgtcag ggcgcgtcag cgggtgttgg cgggtgtcgg ggcgcagcca tgacccagtc
481 acgtagcgat agcggagtgt atactggctt aactatgcgg catcagagca gattgtactg
541 agagtgcacc atatatgcgg tgtgaaatac cgcacagatg cgtaaggaga aaataccgca
```

bioRxiv preprint doi: https://doi.org/10.1101/510768; this version posted May 29, 2019. The copyright holder for this preprint (which was not certified by peer review) is the author/funder. All rights reserved. No reuse allowed without permission.

601 tcaggcgctc ttccgcttcc tcgctcactg actcgctgcg ctcggtcgtt cggctgcggc
661 gagcggtatc agctcactca aaggcggtaa tacggttatc cacagaatca ggggataacg
721 caggaaagaa catgtgagca aaaggccagc aaaaggccag gaaccgtaaa aaggccgcgt
781 tgctggcgtt tttccatagg ctccgccccc ctgacgagca tcacaaaaat cgacgctcaa
841 gtcagaggtg gcgaaacccg acaggactat aaagatacca ggcgtttccc cctggaagct
901 ccctcgtgcg ctctcctgtt ccgaccctgc cgcttaccgg atacctgtcc gcctttctcc
961 cttcgggaag cgtggcgctt tctcatagct cacgctgtag gtatctcagt tcggtgtagg
1021 tcgttcgctc caagctgggc tgtgtgcacg aacccccgt tcagcccgac cgctgcgcct
1081 tatccggtaa ctatcgtctt gagtccaacc cggtaagaca cgacttatcg ccactggcag
1141 cagccactgg taacaggatt agcagagcga ggtatgtagg cggtgctaca gagttcttga
1201 agtggtggcc taactacggc tacactagaa ggacagtatt tggtatctgc gctctgctga
1261 agccagttac cttcggaaaa agagttggta gctcttgatc cggcaaacaa accaccgctg
1321 gtagcggtgg ttttttgtt tgcaagcagc agattacgcg cagaaaaaaa ggatctcaag
1381 aagatccttt gatcttttct acggggttta aacgtgtttc caccattttt tcaatttttt
1441 tataattttt ttaatctgtt atttaaatag tttatagtta aatttacatt ttcattagtc
1501 cattcaatat tctctccaag ataactacga actgctaaca aaattctctc cctatgttct
1561 aatggagaag attcagccac tgcatttccc gcaatatctt ttggtatgat tttacccgtg
1621 tccatagtta aaatcatacg gcataaagtt aatatagagt tggtttcatc atcctgataa
1681 ttatctatta attcctctga cgaatccata atggctcttc tcacatcaga aaatggaata
1741 tcaggtagta attcctctaa gtcataattt ccgtatattc ttttatttt tcgttttgct
1801 tggtaaagca ttatggttaa atctgaattt aattccttct gaggaatgta tccttgttca
1861 taaagctctt gtaaccattc tccataaata aattcttgtt tgggaggatg attccacggt
1921 accatttctt gctgaataat aattgttaat tcaatatatc gtaagttgct tttatctcct
1981 attttttttg aaataggtct aatttttttgt ataagtattt ctttactttg atctgtcaat
2041 ggttcagata cgacgactaa aaagtcaaga tcactatttg gttttagtcc actctcaact
2101 cctgatccaa acatgtaagt accaataagg ttatttttta aatgtttccg aagtattttt
2161 ttcactttat taatttgttc gtatgtattc aaatatatcc tcctcactat tttgattagt
2221 acctatttta tatccatagt tgttaattaa ataaacttaa tttagtttat ttatagattt
2281 cattggcttc taaatttttt atctagataa taattatttt agttaatttt attctagatt
2341 atatatgata tgatctttca tttccataaa actaaagtaa gtgtaaacct attcattgtt
2401 ttaaaaatat ctcttgccag tcacgttacg ttattagtta tagttattat aacatgtatt
2461 cacgaacgaa aatcgccatt cgccaggggt ttaattgcgt cgagacccct gtgggtctcg
2521 ttttttggat caccggtatg gcgccatatg ctttattcga tttcttctag cagcttgtat
2581 gcttcttctg ttgtttgcac ggagagcagc cgctccctat aattgtcatc cattagcttt
2641 cgagatagca tctgcagtat tttgagatgc tggtttcccc cgctctcttt cggtacagca
2701 atcataaaga ttaatttagc ttctgatcca tccaggctat tccaatcaac gcctgatcgt
2761 ttgatcccaa aggcaacact cggctccctg accgcctcag actttccgtg cggaatcgcg
2821 atattcatgc caatcgccgt tgttccctgt tgttcacgat tcaaaatggc ttgtttaaac
2881 ccgctctctg aaagcagcgc acctcttcgt gacaatttct gaatcaattc atctatgatg
2941 tcatcactcg tttcccccga taaatttggt tcaattaatt ccgggctgat aatgtctgtc
3001 agttttttaa attccgacat ctcagctttt tggctttgaa ttggctgctt tatttcattt
3061 gctgccgcag cttcacttgg cgcggaggtc ggtgcagttt cactgagcac aggagacgcc
3121 gtaatatcct tttttagtac attgacgaac agagcagtga caagagatcc tgcaatcaca
3181 gcaataaaaa acatcaagac atgatcaact gcgccaagca ctgcaacgat aggtccgccg
3241 tgcgccactc tgtctcccac attgccaatc atggctatca cagaacctgt cattgagcct
3301 gccataatac ttggaataac gcgcagaggg tcctgcgccg caaatggaat cgctccttca
3361 gtaatgccga agagccccat cgtaaatgcc gctttcccca tttctctttg agatgcctcg
3421 aattttcttt ttcctaaaaa cgtcgcaatg ccaaggccaa tcgggggggat acaaatggcg
3481 acagcaattg gtcccataat ttcataattt ccttctccaa tcattgccga tccaaacaga
3541 aacgccacct tatttacggg accgcccata tcaaatgaga tcatcgcccc taaaatcaat
3601 gccagaagga tcgagctcga ccctttcatc cccgccagcc aaactgttaa agaggcgaaa
3661 atttgagcta caggcgcgcc gatcaaaaac acaaacgcta aacctacaat cagtgatgca
3721 aacaccggaa taataataat cggcataatc ggctggatgg cttttggaac ttttaatttt
3781 ttgatccaaa gtgccgcgta tccggccaaa aacccggcaa taatcccccc gaggaatccg
3841 gcgccgcttg cgctgtcata aaaacttcca gtcgccgcaa tataaccgcc gatcatacct
3901 ggcacaagcc ccggtttatc agcgatgcta taggcgatat agccggctaa aatcggaatc
3961 ataaatgaaa atgaagcact gccgatctgt tcaatcgttt tccagaagga atcatccgga
4021 ataactaagc ctttaggtgt tttctccccct ccaagcgtta atgcaaccgc tatcaataat
4081 ccgccgacaa caatgaaagg aaccataaat gaaacgccgt tcattaaatg acggtaaatt
4141 ggattttgtt tcttctcctg atgattaccg gattccgatt ttgtagcgga acgatagacc

bioRxiv preprint doi: https://doi.org/10.1101/510768; this version posted May 29, 2019. The copyright holder for this preprint (which was not certified by peer review) is the author/funder. All rights reserved. No reuse allowed without permission.


```
4201 ggtatatccc cgttaagagc ttttt gaatc aattcttccg gtttgcggat accgtcctgt
4261 acccccacag acagcagttt tttgcctata aaccggtctt tgtttaccga acggtctgca
4321 gcaataatga ttgcgtccgc ttcgcgaatt tcctcttcgg ttagcttatt ttcaacacca
4381 atccctccct gggtctcaac tttgatgcta acgcccagtc tgtcagcagc ttttt gcaga
4441 ttttctgctg ccatatacgt atgggcgatt ccattcggac aagatgtaat cgctaacagt
4501 ttcataggaa acctccttta aagtgtgaat aataagatct tgtctcaact gtataccgaa
4561 atcagctcat taaaatcgct ttttttacca taggttccgg taataaaggc attttt ccca
4621 tatggcgatt aagttgggta acgccagggt tttcccagtc acgacgttgt aaaacgacgg
4681 ccagtgcaga tcttccggat ggctcgagtt tttcagcaag atatccgctg caccgtttcg
4741 aagagaccgc cggtggagag cgggcagtga gcgcaacgca attaatgtga gttagctcac
4801 tcattaggca ccccaggctt tacactttat gcctccggct cgtatgttgt gtggaattgt
4861 gagcggataa caatttcaca caggaaacag ctatgaccat gattacgcca agcgcgcaat
4921 taaccctcac taaagggaac aaaagctgga ggacctcgag gggggcccg gtacccaatt
4981 cgccctatag tgagtcgtat tacgcgcgct cactggccgt cgttttacaa cgtcgtgact
5041 gggaaaaccc tggcgttacc caacttaatc gccttgcagc acatcccccc ttcgccagct
5101 ggcgtaatag cgaagaggcc cgcaccgatc gcccttccca acagttgcgc agcctgaatg
5161 gcgaatggga cgcgccctgt agcggcgccg gtctcgatag ccaccactga tatctttcta
5221 gaagatctcc tacaatattc tcagct
//
```